Universidade do Porto
Faculdade de Engenharia
FEUP

Development and Application of Statistical Methods to Support Air Quality Policy Decisions

José Carlos Magalhães Pires

Graduated in Chemical Engineering
by the Faculty of Engineering of the University of Porto

Dissertation submitted to obtain the degree of
Doctor of Philosophy in Environmental Engineering

Porto, July 2009

Universidade do Porto

Faculdade de Engenharia

FEUP

Development and Application of Statistical Methods to Support Air Quality Policy Decisions

José Carlos Magalhães Pires

Supervision

Fernando Gomes Martins (PhD) and Maria do Carmo da Silva Pereira (PhD)
Department of Chemical Engineering, Faculty of Engineering, University of Porto

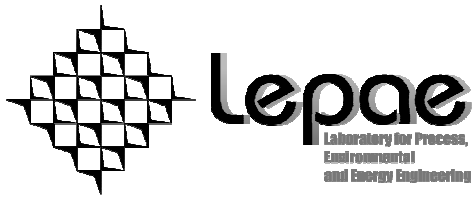

Porto, July 2009

Abstract

It is well known the health effects associated with air pollution. Several studies were published, showing an increasing awareness among the scientific community and policy makers about public health problems due to exposure to air pollution. Policy makers require more detailed air quality information to take measures to reduce the effects on health and to improve the air quality management. This thesis aims to develop procedures using statistical methods to support a broad range of policy decisions concerning this subject.

The first aim was the application of statistical methods, such as principal component analysis and cluster analysis, to characterize the air pollution behaviours in an urban area allowing the identification of monitoring sites with redundant air quality measurements. These measurements represent a loss of profitability of the air quality monitoring network resources. Accordingly, the application of these statistical methods let the following policy decisions: (i) remove the redundant monitoring sites, reducing the costs of the equipment maintenance; or (ii) move the redundant monitoring sites to other places increasing the area of monitored region. The air pollutant concentrations at the removed sites can be estimated with statistical models using the concentrations measured at the remaining sites. Moreover, the air pollution behaviours are related with the location of emission sources. The possible location of important sources of air pollutants was also determined through the analysis of variation of their concentrations with the wind direction. Concerning the characterization of the air pollution behaviours, the actual distribution of monitoring sites in the air quality monitoring network of Oporto Metropolitan Area presented several redundant measurements. The number of monitoring sites could be reduced at about 50% in some of the analysed air pollutants. Several air pollution sources were identified with the analysis of the variation of the air pollutant concentrations with the wind

direction. The most important source was located at E-SE direction sector affecting all monitoring sites during the analysed period.

The second aim of this thesis was the development of statistical models to predict the concentrations of air pollutants (O_3 and PM_{10}) of the next day. Several models were applied, including linear and non-linear ones. As far as the author knows, independent component regression, partial least squares regression, stepwise artificial neural networks, threshold regression and genetic programming were applied for the first time in this field. Besides prediction of the air pollutant concentrations, these models selected the important variables (environmental and meteorological) that influence these values, which is an useful information for the air quality management. The linear models had an advantage of taking less computational time than the other models. Taking into account the performance of these models, quantile regression presented better results in the training period, as it tries to model the entire distribution of the dependent variable. However, this model presented worse performance in the test period. The linear model with best predictive performance was the partial least squares regression. Despite having longer computation time, the non-linear models predicted better than the linear ones, specially the models using the evolutionary procedure for their determination. Threshold regression using genetic algorithms and genetic programming for O_3 and multi-gene genetic programming for PM_{10} were the models with better predictive performance.

Keywords: air quality management, statistical methods, air quality modelling, linear models, artificial neural networks, genetic programming.

Resumo

Os efeitos negativos associados à poluição do ar são bem conhecidos. Muitos estudos foram publicados, apresentando uma crescente preocupação da comunidade científica e dos decisores políticos relativamente aos problemas de saúde pública causados pela poluição do ar. Os decisores políticos necessitam de informação mais detalhada sobre a qualidade do ar de modo a tomar medidas de redução dos seus efeitos na saúde e melhorar a gestão da qualidade do ar. Este trabalho tem como principal objectivo o desenvolvimento de procedimentos usando métodos estatísticos para apoio de decisões políticas relacionadas com este tema.

A aplicação de métodos estatísticos, tais como a análise de componentes principais e análise de agrupamentos, permitiu a caracterização da variação da concentração dos poluentes atmosféricos numa região urbana e, ao mesmo tempo, a identificação de locais de monitorização com medições redundantes. Estas medições representam uma perda de rentabilidade dos recursos das redes de monitorização da qualidade do ar. Deste modo, a aplicação dos referidos métodos estatísticos pode suportar as seguintes decisões: (i) eliminar as estações de monitorização com medições redundantes, reduzindo os custos relativos à manutenção do respectivo equipamento; ou (ii) deslocalizar as referidas estações para outros locais, aumentando a área da região monitorizada. As concentrações de poluentes nos locais em que se pode desactivar as estações podem ser estimadas com modelos estatísticos usando os valores medidos nas restantes estações de monitorização. A variação das concentrações dos poluentes atmosféricos está relacionada com a localização relativa de fontes de emissão dos respectivos poluentes. A possível localização de importantes fontes de emissão foi determinada através da análise da variação da concentração de poluentes com a direcção do vento. Caracterizando as variações observadas pelas concentrações dos poluentes analisados, verificou-se que a distribuição das estações na rede de

monitorização da Área Metropolitana do Porto apresentava várias medições redundantes. O número de locais de monitorização pode, para alguns poluentes, ser reduzido para metade. Várias fontes de emissão foram identificadas com a análise da variação da concentração de poluentes com a direcção do vento. A mais importante esteve localizada fora da região definida pela rede de monitorização na direcção E-SE, afectando todas as estações durante o período analisado.

Vários modelos estatísticos (lineares e não lineares) foram desenvolvidos para prever as concentrações dos poluentes atmosféricos (O_3 e PM_{10}). Tanto quanto se sabe, a regressão por componentes independentes, a regressão por mínimos quadrados parciais, as redes neuronais artificiais desenvolvidas passo a passo, a regressão com limiares e a programação genética foram técnicas de modelização aplicadas pela primeira vez nesta área. Além de prever as concentrações de poluentes atmosféricos, estes modelos seleccionam variáveis importantes (concentrações de outros poluentes ou variáveis meteorológicas) que influenciam esses valores, sendo uma informação útil para a gestão da qualidade do ar. Os modelos lineares têm a vantagem de necessitar de menos tempo de computação do que os modelos não lineares. Tendo em conta os desempenhos destes modelos, a regressão por percentis teve melhores resultados no período de treino, uma vez que o modelo tenta descrever toda a distribuição da variável dependente. No entanto, este modelo teve pior desempenho na etapa de previsão. O modelo linear com melhor desempenho na previsão foi a regressão por mínimos quadrados parciais. Apesar de ter maior tempo de computação, os modelos não lineares prevêem melhor que os modelos lineares, especialmente quando usam o procedimento evolucionário na sua determinação. Assim, os modelos com limiares usando algoritmos genéticos e programação genética para o O_3 e programação genética com múltiplos genes para PM_{10} foram os que apresentaram os melhores desempenhos.

Palavras-chave: qualidade do ar, métodos estatísticos, modelização da qualidade do ar, modelos lineares, redes neuronais artificiais, programação genética.

Résumé

Les effets négatifs associés à la pollution de l'air sont bien connus. Plusieurs études ont été publiées montrant la préoccupation croissante de la communauté scientifique et des décideurs politiques concernant les problèmes de santé publique causés par la pollution de l'air. Les décideurs politiques ont la nécessité d'avoir une information plus détaillée de la qualité de l'air afin de pouvoir prendre des mesures de réduction de ces effets sur la santé et améliorer la gestion de la qualité de l'air. Ce travail a pour principal objectif le développement de procédures utilisant des méthodes statistiques de forme a soutenir les décisions politiques liées à ce sujet.

L'application de méthodes statistiques, telles que l'analyse en composantes principales et l'analyse de grappes, a permis la caractérisation de la variation de la concentration des polluants atmosphériques dans une zones urbaines ainsi que l'identification de sites de surveillance avec des mesures redondantes. Ces mesures représentent une perte de rentabilité des ressources des réseaux de surveillance de la qualité de l'air. Ainsi, l'application de ces methodes statistiques peuvent appuyer les decisions politiques suivantes: (i) éliminer les sations de surveillance avec des mesures redondantes, reduisant le coût d'entretien des equipements; ou (ii) déplacer ces stations à d'autres endroits, augmentant l'aire de la region controlée. Les concentrations de polluants dans les endroits oú l'on peut désactiver les sations peuvent être estimés à l'aide de modèles statistiques utilisant les valeurs moyennes mesurées dans les autres sations de surveillance. La variation des concentrations des polluants atmosphériques est liée à la localisation relative des sources d'émission des polluents respectifs. Le possible emplacement de sources importantes de polluants a également éte déterminé par l'analyse de la variation de leurs concentrations avec la direction du vent. À travers la caractérisation des variations observées par les concentrations de polluants analysés, il a été constaté que la distribution des sites dans les réseau de surveillance de la zone

métropolitaine de Porto présentait plusieurs mesures redondantes. Le nombre de sites de surveillance peut, pour certains polluants, être réduit de moitié. Plusieurs sources d'émissions ont été identifiés à travers l'analyse de la variation de la concentraction de polluants avec la direction du vent. La plus importante était située à l'extérieur de la region définie par le réseau de surveillance dans la direction E-SE, affectant l'ensemble des stations au cours de la période analysée.

Plusieurs modèles statistiques, linéaires et non linéaires, ont été développés afin de prévoir les concentrations de polluants atmosphériques (O_3 e PM_{10}). Pour autant qu'il se sache, la régression par composants indépendants, la régression des moindres carrés partiels, les réseaux neuronaux artificiels développés pas à pas, la régression avec des seuils et la programmation génétique ont été des techniques de modélisation appliquées pour la première fois dans ce domaine. En plus de pévoir les concentrations de polluants atmosphériques, ces modèles sélectionnent des variables importantes qui influent sur ces valeurs, étant ainsi une information utile pour la gestion de la qualité de l'air. Les modèles linéaires ont l'avantage d'exiger moins de temps de calcul que les modèles non linéaires. Compte tenu de la performance de ces modèles, la régression quantile a présenté de meilleurs résultats au cours de la période d'essai, une fois que le modèle tente de décrire l'ensemble de la distribution de la variable dépendante. Toutefois, ce modèles présente une pire performance prédictive. Le modèle linéaire ayant la meilleure performance en matière de prévision est la régression des moindres carrés partiels. Bien qu'ayant un temps de calcul superieur, les modèles non linéaires prédisent mieux que les modéles linéaires, en particulier ceux utilisant le processus d'évolution dans sa détermination. Ainsi, les modèles avec des seuils utilisant des algorithmes génétiques et la programmation génétique pour le O_3 et la programmation génétiques avec multiples genes pour PM_{10} ont été ceux présentant les meilleures performances.

Mots-clés: qualité de l'air, méthodes statistiques, modélisation de la qualité de l'air, modèles linéaires, réseaux de neurones artificiels, programmation génétique.

Acknowledgements

I am grateful to my supervisors Fernando Gomes Martins (PhD) and Maria do Carmo da Silva Pereira (PhD), for introducing me this research topic and then providing me the necessary support. I also wish to thank Maria da Conceição Machado Alvim Ferraz (PhD) for her advice, suggestions and for sharing her knowledge in air quality with me. I can not forget the important suggestions and contributions of Joana, Sofia and Elodie in the preparation of this manuscript.

I also acknowledge: (i) the *Faculdade de Engenharia da Universidade do Porto,* the *Departamento de Engenharia Química* and *Laboratório de Engenharia de Processos, Ambiente e Energia* for providing all the necessary facilities to perform my studies; (ii) the *Fundação para a Ciência e a Tecnologia* for the fellowship SFRH/BD/23302/2005; and (iii) the *Comissão de Coordenação e Desenvolvimento Regional do Norte* and the *Instituto Geofísico da Universidade do Porto* for kindly providing the air quality and meteorological data.

At the end, I want to thank my family, Nádia and my friends for the support, patience and encouragement during this period.

To my family

To Nádia

To my friends

Table of Contents

Part II. Prediction of Air Pollutant Concentrations

Figure Index

Table Index

List of Abbreviations

AIC	Akaike Information Criterion
AN	Antas
ANN	Artificial neural network
AOT40	Accumulated exposure over a threshold of 40 ppb
$AOT40_v$	Averaged exposure Over a Threshold of 40 ppb
AQMN	Air quality monitoring network
BG	Baguim
BV	Boavista
CA	Cluster analysis
CL	Cluster
CS	Custóias
E	East
EC	European Council
ER	Ermesinde
EU	European Union
GA	Genetic algorithm
GP	Genetic programming
HOL	Hidden-to-output layer
IC	Independent component
ICA	Independent component analysis
ICi	Independent component i
ICR	Independent component regression
IHL	Input-to-hidden layer
k-NN	*k*-nearest neighbours
LB	Leça do Balio
MAE	Mean absolute error
MBE	Mean bias error

MGP	Multi-gene genetic programming
MLR	Multiple linear regression
MT	Matosinhos
N	North
NE	Northeast
NW	Northwest
ODV_{90}	90% of the original data variance
Oporto-MA	Oporto Metropolitan Area
OV	Original variable
PAD	Percentage of available data
PC	Principal component
PCA	Principal component analysis
PCi	i^{th} principal component
PCR	Principal component regression
PLSR	Partial least squares regression
PM	Particulate matter
PR	Perafita
Q_i	i^{th} annual quarter
QR	Quantile regression
RH	Relative humidity
RMSE	Root mean squared error
S	South
SE	Southeast
SH	Senhora da Hora
sig	Sigmoid function
sin	Sine function
SR	Solar radiation
SSE	Sum of the squared errors
SW	Southwest

SWANN	Stepwise artificial neural network
T	Air temperature
tgh	Hyperbolic tangent function
TR	Threshold regression
USEPA	United States Environmental Protection Agency
UV	Ultraviolet
VC	Vila do Conde
VOC	Volatile Organic Compounds
VR	Vermoim
VT	Vila Nova da Telha
W	West
WBG	World Bank Group
WHO	World Health Organization
WS	Wind speed

Notation

α	Significance level
$\hat{\alpha}_i$	Regression parameters
$\hat{\beta}_i$	Regression parameters
$\hat{v}_i$	Regression parameters
ε	Error associated with the regression
λ	Eigenvalue
θ	Bias
$\hat{\sigma}$	Standard deviation
σ^2	Variance
τ	Percentile
$(\mathbf{X})^{-1}$	Inverse of the matrix **X**
$(\mathbf{X})^{\mathbf{T}}$	Transpose of the matrix **X**
$\lvert\mathbf{X}\rvert$	Determinant of the matrix **X**
B	Regression parameters matrix
b	Regression parameters vector
b_{jp}	Loading of the original variable *j* in the principal component *p*
$\mathbf{B_{PLS}}$	Regression parameters of partial least squares regression
c	**y** weight vector
C	**y** weights matrix
Cov	Covariance matrix
CO	Carbon monoxide
d	Index of threshold variable
d_2	Index of agreement of second order
F()	Cumulative probability density function

$f()$	Activation function
$\mathbf{I}$	Identity matrix
k	Number of parameters
n	Number of data points
NO	Nitrogen oxide
NO_2	Nitrogen dioxide
NO_x	Nitrogen oxides
O_3	Tropospheric ozone
$O_{3\|t+24h}$	Next day hourly average ozone concentrations
$\mathbf{P}$	**X** loadings matrix
$\mathbf{p}$	**X** loadings vector
PM_{10}	Particulate matter with aerodynamic diameter smaller than 10 μm
$PM_{2.5}$	Particulate matter with aerodynamic diameter smaller than 2.5 μm
R	Pearson correlation coefficient
r	Threshold value
SO_2	Sulphur dioxide
Sxx_i	Sum of squares related to x_i
t	Student t distribution
$\mathbf{T}$	**X** score matrix
$\mathbf{t}$	**X** score vector
$\mathbf{U}$	**y** score matrix
$\mathbf{u}$	**y** score vector
$\mathbf{W}$	**X** weight matrix
$\mathbf{w}$	**X** weight vector
w_i	Weight value
$\mathbf{X}$	Matrix of the explanatory variables
$\mathbf{X_0}$	**X** standardized matrix
x_d	Threshold variable
x_i	Input value

Y_i	Output value
$\hat{Y}_i$	Model output
$\overline{Y_i}$	Average of the output variable
y	Output value
$\mathbf{y}$	Vector of the dependent variable
$\mathbf{y_0}$	**y** standardized vector

Chapter 1

Introduction

This chapter describes the project associated with this thesis. The importance of this study is also demonstrated. At the end, there is a description of the structure of the thesis.

1.1. Scientific relevance

Clean air is considered to be a basic requirement of human health. The quality of the air is the result of a complex interaction of many factors that involve the chemistry and motions of the atmosphere, as well as the emissions of a variety of pollutants from sources that are both natural and anthropogenic.

Before the increase of large cities and industries, the nature was able to keep the air fairly clean. Wind mixed and dispersed the gases, rain washed the dust and other easily dissolved substances to the ground and plants absorbed carbon dioxide and replaced it by oxygen. With urbanisation and industrialisation, humans started to release more wastes into the atmosphere than nature could manage with. Thus, these concentrated gases exceed safe limits and became a pollution problem.

Air pollution can not be considered a local problem. The air pollutants released in one country can be transported by the wind, causing several negative impacts (in human health, vegetation, ecosystems, climate and materials) elsewhere. Thus, air pollution should be considered as a transboundary concern.

European Union established several directives related with air quality. These directives established limit values for air pollutant concentrations concerning the protection of the human health, vegetation and ecosystems. They also indicate the number of monitoring sites that should operate according to population size and pollution levels. However, the number and location of the monitoring sites should be optimized for the different regions. In other words, the redundant measurements should be avoided due to the high cost of the monitoring equipment maintenance.

One of the most important air pollutant usually associated with poor air quality is tropospheric ozone (O_3). O_3 is naturally present in the atmosphere, but in elevated amounts it is damaging to the living tissue of plants and animals. However, the most relevant pollutant for air quality is particulate matter (PM). An important target of this thesis is the prediction of concentrations of O_3 and PM_{10} (particulate matter with aerodynamic diameter smaller than 10 μm) with a day in advance. Thus, the persons belonging to risk groups (with respiratory problems, children and elderly) can be advised for high concentrations episodes. Other components important in air quality include carbon monoxide, sulphur dioxide, NO_x and VOC (O_3 precursors), and air toxics such as benzene, mercury and other hazardous air pollutants.

The need for improved understanding of the science of air quality remains a priority for the wider scientific and user communities. Despite improvements in technology, users still require new, robust management and assessment tools to formulate effective control policies and strategies for reducing the health impact of air pollution. Accordingly, this thesis presents statistical methods useful for policy makers seeking to improve air quality management in their cities.

1.2. Thesis structure

The project associated with this document, entitled *Development and Application of Statistical Methods to Support Air Quality Policy Decisions*, was performed at

Departamento de Engenharia Química of *Faculdade de Engenharia da Universidade do Porto* from 2006 to 2009.

The thesis was divided in two parts: (i) management of air quality monitoring networks (Part I); and (ii) prediction of air pollutant concentrations (Part II). Part I contains the Chapters 2 to 4, while Part II contains the Chapters 5 to 10.

Chapter 2 describes the air pollutants whose monitoring is of particular interest for the characterization of the air quality. Their sources, effects and legislation related with their concentrations are the main topics focused. Additionally, this chapter: (i) characterizes the region where the air quality was measured; (ii) refers the equipment used for each air pollutant monitoring; and (iii) determines for a specific period the number of exceedances to the limits established by the EU for protection of human health, vegetation and ecosystems.

Chapter 3 shows how principal component analysis and cluster analysis can be applied to define the number of monitoring sites that should operate in an air quality monitoring network (AQMN). Additionally, the location of the main emission sources was identified based on the influence of wind direction on the increase of the air pollutant concentrations.

In Chapter 4, principal component analysis was applied using another criterion to select the number of principal components. This number, corresponding to the minimum number of monitoring sites that should operate, was then compared with the value presented by the European legislation. At the end of this chapter, the air pollutant concentrations at the removed monitoring sites were estimated using the values of the selected monitoring sites.

Chapter 5 presents several previous studies about prediction of O_3 and PM_{10} concentrations through statistical models.

Chapter 6 shows the comparison of the performance of five linear models in the prediction of O_3 and PM_{10} concentrations.

Chapter 7 presents two step-by-step methodologies to define artificial neural network models. These models were applied to predict the concentrations of the same air pollutants.

Chapter 8 shows how to apply genetic algorithms to define threshold regression models for prediction of O_3 concentrations.

In Chapter 9, genetic programming was applied to predict O_3 concentrations.

In Chapter 10, multi-gene genetic programming was applied to predict PM_{10} concentrations.

Finally, Chapter 11 presented the main conclusions of this thesis and some suggestions for future work.

Part I

(from www.qualar.org)

Management of Air Quality Monitoring Networks

Chapter 2

Air Quality Evaluation in Oporto Metropolitan Area

This chapter describes the air pollutants whose monitoring is of particular interest for the characterization of the air quality. Their sources, effects and the legislation related with their concentrations are the main topics of this chapter. Additionally, the aims are: (i) characterize the region where the air quality was measured; (ii) refer to the equipment used for each air pollutant monitoring; and (iii) determine for this period the number of exceedances to the limits established by the European Union for protection of human health, vegetation and ecosystems.

The contents of this chapter were adapted from: (i) Pires, J.C.M., Sousa, S.I.V., Pereira, M.C., Alvim-Ferraz, M.C.M., Martins, F.G., **2008**. Management of Air Quality Monitoring using Principal Component and Cluster Analysis – Part I: SO_2 and PM_{10}. *Atmospheric Environment* 42 (6), 1249-1260; and (ii) Pires, J.C.M., Sousa, S.I.V., Pereira, M.C., Alvim-Ferraz, M.C.M., Martins, F.G., **2008**. Management of Air Quality Monitoring using Principal Component and Cluster Analysis – Part II: CO, NO_2 and O_3. *Atmospheric Environment* 42 (6), 1261-1274.

2.1. Sulphur dioxide

Sulphur dioxide (SO_2) is one of the most important pollutants, as it results from the combustion of sulphur compounds. Volcanoes and oceans are the major natural sources of SO_2 (Carmichael et al., 2002; Garg et al., 2006; Reddy and Venkataraman, 2002; World Health Organization - WHO, 2000). Anthropogenic emissions of SO_2 come from the combustion of fossil fuels (mainly coal and heavy oils), biomass burning and the smelting of sulphur containing ores.

Many efforts have been done to reduce SO_2 emissions; consequently, in the last 20 years the atmospheric levels of SO_2 have been continuously decreasing in most

Western industrialized countries (Nunnari et al., 2004). SO_2 and its oxidation by-products are removed from the atmosphere by wet and dry deposition (acid precipitation). Besides these transformation and removal processes, SO_2 can be carried out over large distances, causing transboundary pollution (ApSimon and Warren, 1996).

SO_2 is an irritant gas when inhaled and at high concentrations may cause breathing difficulties in people directly exposed to it. Absorption of SO_2 in the nose mucous membranes and in the upper respiratory tract results from its solubility in water (WHO, 2000). The effects of SO_2 inhalation appear in only a few minutes and people suffering from asthma and chronic lung disease may be especially susceptible to its adverse effects. This pollutant also affects plants and depending on its concentration levels, can produce: chlorophyll degradation; reduction of photosynthesis; raise of respiration rates; and changes in protein metabolism (Carlson, 1979; Lee et al., 1997). Nevertheless, sulphur is an important nutrient for plants due to the fact that, by instance, atmospheric sulphur may be taken up by leaves of some species, contributing to the plant vitality in soils with low sulphur concentrations such as calcareous soils. SO_2 (combined with other air pollutants and under specific conditions of relative humidity, temperature and precipitation) is responsible for the deterioration of materials, such as metals and stones. In many parts of Europe, some monuments which resisted deterioration for hundreds or even thousands of years have shown an accelerated degradation of their surface in the last decades.

The European Union (EU) established limit values for SO_2 concentrations: (i) the hourly limit for the protection of human health (350 $\mu g\ m^{-3}$, not to be exceeded more than 24 times per year); (ii) the daily limit for the protection of human health (125 $\mu g\ m^{-3}$, not to be exceeded more than 3 times per year); and (iii) the annual limit for protection of ecosystems (20 $\mu g\ m^{-3}$) (EC Directive, 1999).

2.2. Particulate matter

Particulate matter (PM) is the designation of solid and liquid particles suspended in the atmosphere. They are emitted by both, natural (volcanic eruptions, seismic activity and forest fires) and anthropogenic sources (all types of man-made combustion and some industrial processes).

PM is one of the most important air pollutants that adversely influence human health in Europe (Koelemeijer et al., 2006). In the last decade, several studies were published about the impact of PM on human health (Alvim-Ferraz et al., 2005; Brunekreef and Holgate, 2002; Dockery and Pope, 1994; Hoek et al., 2002). Long exposure to PM_{10} and to $PM_{2.5}$ (particles with an aerodynamic diameter smaller than 10 and 2.5 μm, respectively) has been associated with respiratory and cardiovascular diseases. Recent research seems to indicate that PM_{10} are associated with childhood morbidity and mortality (Kappos et al., 2004).

Aiming the protection of human health, the EU established two limits for PM_{10}, which should be enforced on two different periods of time; the first beginning in 2005 and the last one in 2010. The limits to be enforced from 2005 until 2010 are: (i) the daily limit of 50 μg m^{-3}, not to be exceeded more than 35 times per year; and (ii) the annual limit of 40 μg m^{-3}. The limits to be enforced from 2010 are: (i) the daily limit of 50 μg m^{-3}, not to be exceeded more than 7 times per year; and (ii) the annual limit of 20 μg m^{-3} (EC Directive, 1999).

2.3. Carbon monoxide

Carbon monoxide (CO) is a colourless, practically odourless, tasteless and no irritating gas which is the result of the incomplete oxidation of carbon in combustion (Raub, 1999; Raub et al., 2000). The main sources are the combustion of fuel (that occurs when the ratio air-to-fuel presents low values), industrial emissions and other combustion sources (as coal, gas, wood and kerosene). Natural sources, such as volcanoes, natural gases in coal mines and forest fires, have also an important contribution. The emissions of CO increase significantly

during the cold weather. In these conditions, the engines need more fuel to work and some emission control devices, such as oxygen sensors and catalytic converters, operate less efficiently when they are cold (Raub et al., 2000; United States Environmental Protection Agency - USEPA, 2004).

The effects in the human health associated to the presence of CO depend on its concentration and the duration of exposure. At low concentrations, CO causes fatigue in healthy people and chest pain in people with heart disease. At high concentrations, it causes headaches, confusion and nausea. When inhaled, CO is absorbed from the lungs to the bloodstream, where it forms a complex with haemoglobin known carboxyhaemoglobin. The presence of this complex reduces the oxygen carrying capacity, causing hypoxia (low oxygen level available to the body tissues) (Raub, 1999; Raub et al., 2000; USEPA, 2000; USEPA, 2004; WHO, 2000). CO is one of the contaminants found normally in the atmosphere that requires prevention and control measures to ensure adequate protection of the human health.

EU established 10 mg m^{-3} as a limit value for the protection of human health (EC Directive, 2000) based in the maximum daily 8-hour average concentration.

2.4. Nitrogen oxides

Nitrogen oxides (NO_x) are a group of highly reactive gases. These gases contain atoms of nitrogen and oxygen in different proportions. Nitrogen oxide (NO) and nitrogen dioxide (NO_2) are the most important gases of this group and they are considered significant pollutants in the troposphere (USEPA, 1998; World Bank Group - WBG, 1998). Anthropogenic emissions of NO_x result from the combustion processes, including motor vehicles, electric utilities, and other industrial, commercial and residential sources that burn fossil fuels. Natural events, such as anaerobic biological processes in soil and water, volcanic activity and photochemical destruction of nitrogen compounds in the upper atmosphere, have also a high contribution for NO_x emissions (USEPA, 1998; WBG, 1998).

Nitrogen oxides have diverse negative effects (Hashim et al., 2004; Kalabokas et al., 2002; USEPA, 1998; WBG, 1998; WHO, 2000), such as: (i) formation of acid rain – they react with other substances in the air to form acids which fall to earth as rain, fog, snow, or dry particles; (ii) deterioration of the water quality - increased nitrogen loading in water bodies, particularly coastal estuaries, upsets the chemical balance of nutrients used by aquatic plants and animals; (iii) formation of toxic chemicals – NO_x reacts with common organic chemicals to form a wide variety of toxic products, such as nitrate radicals, nitroarenes and nitrosamines; (iv) reduction of the visibility – nitrogen dioxide can block the transmission of light; (v) contribution to the increase of the earth's temperature – one of the nitrogen oxides, nitrous oxide, is a greenhouse gas; and (vi) formation of ground-level ozone – in the presence of hydrocarbons and sunlight, NO_x contribute to the formation of tropospheric ozone, which can cause serious respiratory problems.

EU established limit values for NO_2 and NO_x (EC Directive, 1999). Concerning hourly average concentrations, NO_2 limit for the protection of human health is 200 $\mu g\ m^{-3}$ and may not be exceed more than 18 times in the year (limit value to be met till January of 2010). Concerning annual average concentrations, NO_2 limit for the protection of human health is 40 $\mu g\ m^{-3}$ (limit value to be met till January of 2010) and NO_x limit for protection of the vegetation is 30 $\mu g\ m^{-3}$.

2.5. Ozone

Ozone (O_3) is a strong photochemical oxidant found in the troposphere and in other layers of the atmosphere. While ozone has an important role in the stratosphere (protection from the ultraviolet radiation), in the troposphere this irritating and reactive molecule has negative impacts on human health, climate, vegetation and materials (Alvim-Ferraz et al., 2006; Chan et al., 1998). Concerning human health effects, the most important are: (i) damage to respiratory tract tissues; (ii) death of lung cells and increased rates of cell replication

(hyperplasia); (iii) inflammation of airways; and (iv) increase of the respiratory symptoms, such as cough, chest soreness, difficulty in taking a deep breath and, in some cases, headaches or nausea (Kley et al., 1999; Leeuw, 2000). Concerning climate, a temperature increase is expected to be related to the tropospheric ozone increase, because it is a greenhouse gas and influences the atmospheric residence time of other greenhouse gases (Bytnerowicz et al., 2006). In vegetation, it causes leaf injury, growth and yield reduction, and changes in the sensitivity to biotic and abiotic stresses (Alvim-Ferraz et al., 2006; Leeuw, 2000). Concerning materials, ozone in combination with other atmosphere pollutants contributes to the increase of the corrosion on building materials like steel, zinc, copper, aluminium and bronze (Leeuw, 2000).

The presence of ozone in the troposphere is a result of three basic processes: (i) photochemical production by the interaction of hydrocarbons and nitrogen oxides (emitted by gasoline vapours, fossil fuel power plants, refineries, and other industries) under the action of suitable ambient meteorological conditions (Guerra et al., 2004; Strand and Hov, 1996; Zolghadri et al., 2004); (ii) tropospheric/stratospheric exchange that causes the transport of stratospheric air, rich in ozone, into the troposphere (Dueñas et al., 2002); and (iii) horizontal transport due to the wind that brings ozone produced in other regions.

EU established limit values for ozone in the ambient air (EC Directive, 2002). The information threshold (considered to carry health risks for short-time exposure of groups particularly sensible) is 180 $\mu g\ m^{-3}$ for hourly average concentration, and the alert threshold (considered to carry health risks for short-time exposure of the population in general) is 240 $\mu g\ m^{-3}$. The O_3 target value for the protection of the human health is 120 $\mu g\ m^{-3}$ concerning maximum daily 8-hour average concentrations and may not be exceeded more than 25 days per calendar year averaged over three years (limit value to be met till 2010). Concerning the cumulative ozone exposure index (AOT40 – Accumulated exposure Over a Threshold of 40 ppb or 80 $\mu g\ m^{-3}$) calculated from 1 h values from May to July,

the O_3 target value for the protection of the vegetation is 18000 μg m^{-3} h^{-1} averaged over five years (limit value to be met till 2010). The long-term objectives for O_3 in Europe are: (i) maximum daily 8-hour average of 120 μg m^{-3} for the protection of the human health; and (ii) AOT40 calculated from 1 h values from May to July of 6000 μg m^{-3} h^{-1}.

2.6. Air quality data

Oporto is the second largest city of Portugal, located at North. The important air pollution sources in Oporto Metropolitan Area (Oporto-MA) are vehicle traffic, an oil refinery, a petrochemical complex, a thermoelectric plant (planned for working with natural gas), an incineration unit and an international shipping port (Pereira et al., 2007).

The air quality data was collected from the monitoring sites integrated in the air quality monitoring network (AQMN) of Oporto-MA, managed by the Regional Commission of Coordination and Development of Northern Portugal (*Comissão de Coordenação e Desenvolvimento Regional do Norte*), under the responsibility of the Ministry of Environment. The AQMN of Oporto-MA is currently composed of 14 monitoring sites that regularly monitor the air levels of SO_2, PM_{10}, CO, NO, NO_2, NO_x and O_3. $PM_{2.5}$, benzene, toluene and xylene are also measured in some monitoring sites of the network.

SO_2 concentrations were obtained by the ultraviolet fluorescence method, according to the EC Directive 1999/30/EC (EC Directive, 1999) using the AF21M equipment from Environment SA (Pereira et al., 2007). PM_{10} concentrations were obtained through the beta radiation attenuation method, considered equivalent to the method advised by the EU Directive 1999/30/EC (EC Directive, 1999), using the MPSI 100 I et E equipment from Environment SA (Pereira et al., 2005). Nondispersive infrared spectrometric method was applied to measure the CO concentrations (Sousa et al., 2006), according to the EU Directive 2000/69/EC (EC Directive, 2000). NO_2 and NO_x were obtained through the chemiluminescence

method (Sousa et al., 2006), according to EU Directive 1999/30/EC (EC Directive, 1999). Ozone measurements, according to EU Directive 2002/3/EC (EC Directive, 2002), were performed through UV-absorption photometry using the equipment 41 M UV Photometric Ozone Analyser from Environment S.A. (Pereira et al., 2005). This equipment was submitted to a rigid maintenance program, being calibrated each 4 weeks. Measurements were continuously registered and hourly average concentrations (in $\mu g\ m^{-3}$) were recorded.

2.7. Exceedances to EU limits

The exceedances to the limits established by the EU were evaluated for the period between 2003 and 2005. Two of the fourteen monitoring sites that constitute the AQMN of Oporto-MA showed high percentage of missing data during the analysed period. The exceedances to EU limits were not evaluated in these monitoring sites. The monitoring sites selected for this study were: *Antas* (AN), *Baguim* (BG), *Boavista* (BV), *Custóias* (CS), *Ermesinde* (ER), *Leça do Balio* (LB), *Matosinhos* (MT), *Perafita* (PR), *Senhora da Hora* (SH), *Vermoim* (VR), *Vila do Conde* (VC) and *Vila Nova da Telha* (VT). Table 2.1 shows the main AQMN monitoring site characteristics, including the type and the main pollution sources associated to them (QualAr, 2006). Figure 2.1 presents the map of Oporto-MA with the locations of these monitoring sites. Table 2.2 shows, from the five air pollutants described above, the ones whose concentrations are measured at each monitoring site. The ER site presented high percentage of missing PM_{10} data. Thus, the exceedances to EU limits for PM_{10} were not evaluated at ER site.

The analysis of SO_2 data showed that their concentrations were in compliance at all sites with the legislation established by the EU for the protection of human health (EC Directive, 1999). The hourly limit was exceeded in four monitoring sites: (i) CS (once in 2004); (ii) MT (4, 3 and 2 times in 2003, 2004 and 2005, respectively); (iii) PR (15 times in 2003); and (iv) VT (once in 2004).

Table 2.1 Site characteristics of the air quality monitoring network of Oporto Metropolitan Area

Site	Type	Main pollution source
AN	Urban	Traffic
BG	Urban	Traffic
BV	Urban	Traffic
CS	Suburban	Industrial
ER	Urban	(Background)
LB	Suburban	(Background)
MT	Urban	Traffic
PR	Suburban	Industrial
SH	Urban	Traffic
VR	Urban	Traffic
VC	Suburban	Traffic
VT	Suburban	(Background)

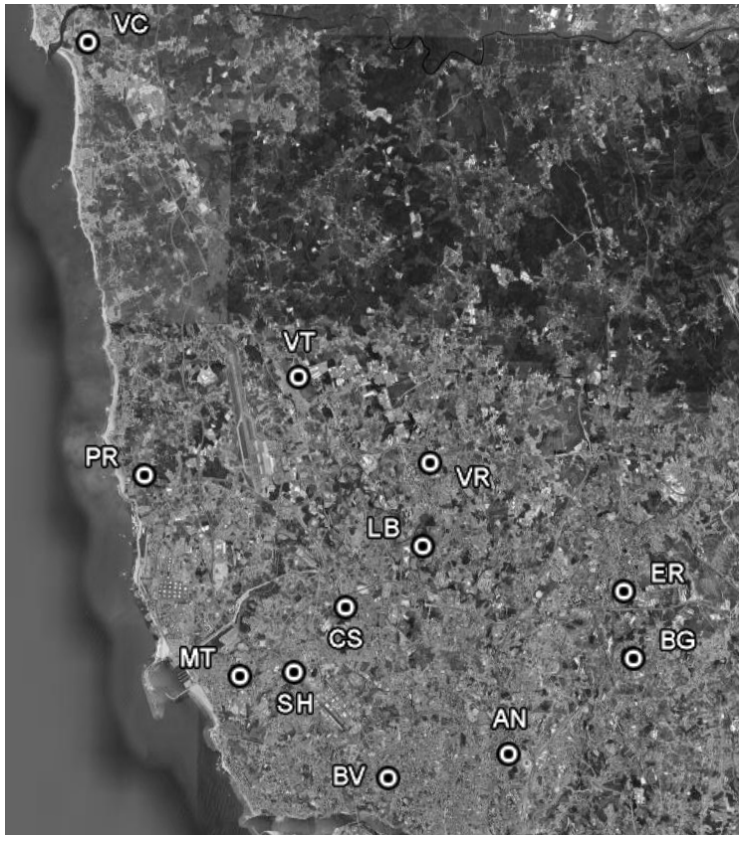

Figure 2.1 Location of the monitoring sites in the map of Oporto-MA (from Google Earth)**.**

Table 2.2 Air pollutants whose concentrations are measured at each monitoring site

Site	SO_2	PM_{10}	CO	NO_2	O_3
AN		×	×	×	×
BG			×	×	×
BV	×	×	×	×	×
CS	×	×	×	×	×
ER	×	×		×	×
LB	×	×	×	×	×
MT	×	×	×	×	×
PR	×	×	×	×	×
SH	×	×	×	×	
VR	×	×	×	×	×
VC	×	×	×	×	×
VT	×	×	×	×	×

According to the referred legislation, the SO_2 hourly average concentrations limit of 350 μg m^{-3} cannot be exceeded more than 24 times a year (~0.3% of the total number of hours) in order to be in compliance with the norm (EC Directive, 1999). The PR and MT sites showed the larger number of exceedances during the analysed period. It is noted that all of the exceedances for the PR site occurred in 2003, which represent ~0.2% of the available hourly average concentrations and that the correspondent percentages for MT site were even lower (~0.05%). The daily average concentrations of SO_2 were calculated when more than 75% of the hourly average concentrations were available. The daily limit of SO_2 concentrations is 125 μg m^{-3} and cannot be exceeded more than 3 times a year (~0.8% of the total number of days) to be in compliance with the norm (EC Directive, 1999). The daily limit was exceeded only once at the PR site, representing ~0.3% of the available daily average concentrations. To determine these exceedances (to hourly and daily limits), the minimum for the percentage of available data (PAD) was 73%.

Table 2.3 shows the annual averages of SO_2 concentrations calculated at each monitoring site for the years 2003, 2004 and 2005 as well as the correspondent PAD. It is observed that those annual averages did not change considerably during the analysed period. MT site showed the highest annual average values

Table 2.3 Annual averages of SO_2 concentrations at each site (it should not exceed 20 μg m^{-3} for ecosystem protection) and the correspondent PAD (in brackets)

Year	BV	CS	ER	LB	MT	PR	SH	VR	VC	VT
2003	6.5 (97)	5.8 (91)	4.5 (97)	6.0 (99)	11.1 (98)	6.9 (96)	6.4 (97)	4.6 (96)	2.5 (98)	5.0 (85)
2004	5.5 (98)	6.8 (99)	5.3 (100)	6.6 (100)	10.3 (100)	5.1 (95)	8.9 (99)	4.3 (99)	2.7 (99)	3.9 (98)
2005	5.7 (100)	7.5 (99)	5.8 (73)	5.7 (90)	9.5 (100)	4.9 (99)	9.5 (100)	5.5 (91)	3.1 (99)	2.8 (100)

due to the proximity of one emission source; nevertheless, even there, the annual average concentrations were about half of the 20 μg m^{-3} limit established for ecosystem protection by the EC Directive (1999).

Table 2.4 presents the number of exceedances of the limit of 50 μg m^{-3} established by the EU for the protection of human health and the correspondent PAD, regarding the daily average concentrations of PM_{10}. In order to be in compliance, the limit cannot be exceeded more than 35 times a year which corresponds to ~10% of the total number of available days (EC Directive, 1999). The number of exceedances allowed by the EU was surpassed at all monitoring sites during the analysed years. VC site showed the highest number of exceedances, representing about approximately half of the available data. Table 2.5 shows the annual averages of PM_{10} concentrations at each monitoring site and the correspondent PAD. During the entire studied period, only the VT monitoring site was in compliance of the annual limit of 40 μg m^{-3} implemented by the EC Directive (1999) for the protection of human health. Besides the traffic and industrial emissions of PM_{10}, the regional transport played an important role in the pollutant concentration. The research made by Pereira et al. (2005) showed that even at rural sites (absence of direct influence of emission sources) exceedances were observed due to intra-regional pollutant transport.

Table 2.4 Number of exceedances of the limit established by the European Union for the protection of human health regarding daily averages of PM_{10} concentrations and the correspondent PAD (in brackets)

Year	AN	BV	CS	LB	MT	PR	SH	VR	VC	VT
2003	127 (93)	111 (98)	86 (88)	114 (82)	92 (92)	123 (97)	121 (85)	107 (89)	167 (95)	62 (73)
2004	92 (90)	135 (95)	107 (96)	82 (98)	104 (98)	78 (95)	79 (98)	59 (72)	160 (89)	72 (98)
2005	86 (95)	115 (100)	134 (92)	67 (83)	122 (99)	80 (96)	104 (94)	88 (85)	161 (99)	86 (100)

Table 2.5 Annual averages of PM_{10} concentrations at each site (it should not exceed 40 μg m^{-3} for the protection of human health) and the correspondent PAD (in brackets)

Year	AN	BV	CS	LB	MT	PR	SH	VR	VC	VT
2003	46.2 (95)	43.2 (98)	36.4 (90)	45.6 (84)	40.0 (93)	45.2 (97)	47.0 (87)	41.6 (92)	53.2 (96)	37.1 (74)
2004	40.9 (92)	50.2 (94)	40.5 (98)	34.9 (98)	41.9 (98)	39.5 (96)	37.3 (99)	36.3 (75)	52.7 (90)	35.7 (98)
2005	40.9 (95)	44.4 (99)	48.2 (93)	35.2 (84)	44.9 (98)	38.3 (97)	42.4 (95)	40.7 (87)	51.2 (98)	38.8 (99)

During the analysed period, the maximum daily 8-hour average concentrations of CO did not exceed the limits established by the EU for the protection of human health (10 mg m^{-3}) (EC Directive, 2000) at any monitoring site.

According to the legislation established by EU for the protection of human health, the hourly average concentration of NO_2 may not be exceed 200 μg m^{-3} more than 18 times a year (EC Directive, 1999). The LB site presented the highest number of exceedances (20 hourly average concentrations) that occurred only in 2005. This means that the number of exceedances allowed by the EU (18 exceedances in a year) was surpassed at this site. As the annual average NO_2 concentration at this site was not usually high, these exceedances were probably due to industrial emissions. The exceedances of hourly limit occurred also 13 times at MT site

(2005), 6 times at VR site (2004), 4 times at AN and BV sites (2005) and twice at BG site (2005). To determine these exceedances, the minimum for the percentage of available data (PAD) was 63%. Table 2.6 shows the annual average of NO_2 concentrations calculated at each monitoring site for the years of 2003, 2004 and 2005 as well as the correspondent PAD. AN, BV and MT were the sites that presented annual average concentrations above the limit established by the EU for the protection of human health (40 μg m^{-3}) (EC Directive, 1999). Besides the influence of industrial sources, these sites are strongly influenced by the traffic emissions. Table 2.7 shows the annual average of NO_x concentrations calculated at each monitoring site and the correspondent PAD. The annual limit for the protection of vegetation (30 μg m^{-3}) was exceeded at all sites with exception

Table 2.6 Annual average NO_2 concentrations at each site (it should not exceed 40 μg m^{-3} for the protection of human health) and the correspondent PAD (in brackets)

Year	AN	BG	BV	CS	ER	LB	MT	PR	SH	VR	VC	VT
2003	43.4 (94)	34.9 (95)	48.9 (90)	27.3 (86)	28.6 (96)	27.8 (97)	43.8 (99)	21.6 (93)	32.8 (93)	31.4 (93)	29.3 (98)	21.4 (95)
2004	45.4 (93)	30.5 (93)	39.7 (63)	27.6 (96)	30.0 (100)	26.1 (99)	41.3 (99)	18.4 (98)	36.4 (99)	32.5 (96)	23.8 (81)	18.5 (98)
2005	48.3 (94)	31.6 (100)	42.6 (98)	29.0 (99)	29.8 (94)	27.5 (86)	41.0 (95)	19.9 (95)	35.5 (99)	32.3 (89)	22.3 (80)	17.9 (95)

Table 2.7 Annual average NO_x concentrations at each site (it should not exceed 30 μg m^{-3} for the protection of vegetation) and the correspondent PAD (in brackets)

Year	AN	BG	BV	CS	ER	LB	MT	PR	SH	VR	VC	VT
2003	96.4 (94)	68.5 (95)	114.5 (90)	44.1 (86)	49.2 (96)	52.1 (98)	98.3 (99)	31.3 (93)	67.0 (93)	58.4 (93)	70.1 (98)	21.4 (95)
2004	110.5 (93)	63.1 (93)	101.6 (63)	46.9 (96)	49.5 (100)	52.9 (99)	91.1 (99)	30.3 (98)	63.3 (99)	58.3 (96)	63.7 (81)	28.7 (98)
2005	104.5 (94)	62.8 (100)	86.4 (98)	48.3 (99)	45.8 (94)	49.4 (86)	84.2 (95)	28.9 (95)	61.0 (99)	55.4 (89)	61.7 (80)	26.3 (95)

of VT site (during the entire period) and PR site (in 2005) (EC Directive, 1999). As it happened with NO_2, AN, BV and MT sites presented the highest annual average concentrations of NO_x. For both pollutants, there was not a significant variation of their annual average concentration during the analysed period.

Table 2.8 presents the exceedances of the O_3 thresholds for public information (180 μg m^{-3}) established by the EU and the correspondent PAD (EC Directive, 2002). The AN, BG, ER, LB, VR and VT sites presented the highest numbers of exceedances during the entire analysed period. The threshold for public alert (240 μg m^{-3}) was exceeded once at BG, VR and VT sites in 2003. Table 2.9 presents the exceedances of the standard value established by the EU for the protection of human health and the correspondent PAD, regarding maximum daily 8-hour average of O_3 concentration (120 μg m^{-3}, that may not be exceeded more than 25 times a year averaged over three years). During the entire analysed period (three years), ER site presented the highest number of exceedances; nevertheless, even there, the maximum number of exceedances allowed by the EU was obeyed. Concerning the protection of vegetation, the value of AOT40 is calculated by the sum of the difference between hourly average concentrations greater than 80 μg m^{-3} (equal to 40 parts per billion) and 80 μg m^{-3} over a given period using only the 1 hour values measured between 8 and 20 hours (Central European Time) each day. At all sites, all possible measured data was not available. Therefore, the calculated value of AOT40 was divided by the measured hourly values ($AOT40_v$ – Averaged exposure Over a Threshold of 40 ppb or 80 μg m^{-3}) and compared to the ratio between AOT40 limit and the total possible number of hours (16.3 μg m^{-3} h^{-2} averaged over five years). Table 2.10 shows the values of $AOT40_v$ calculated at each monitoring site and the correspondent PAD. During the entire period, the O_3 limit $AOT40_v$ (16.3 μg m^{-3} h^{-2} averaged over five years) for the protection of the vegetation was obeyed at all sites.

Table 2.8 Exceedances of the O_3 thresholds for public information (180 μg m^{-3}) established by the European Union and the correspondent PAD (in brackets)

Year	AN	BG	BV	CS	ER	LB	MT	PR	VR	VC	VT
2003	6 (86)	5 (93)	2 (95)	0 (92)	4 (97)	0 (47)	0 (100)	0 (99)	5 (96)	0 (98)	7 (95)
2004	2 (97)	1 (100)	0 (99)	3 (100)	4 (99)	1 (94)	0 (100)	5 (98)	3 (99)	1 (99)	4 (98)
2005	10 (99)	7 (100)	0 (100)	2 (53)	17 (100)	27 (69)	0 (90)	1 (100)	8 (91)	0 (98)	12 (100)

Table 2.9 Exceedances of the standard value established by the European Union for human health protection, regarding maximum daily 8-hour average of O_3 concentration and the correspondent PAD (in brackets)

Year	AN	BG	BV	CS	ER	LB	MT	PR	VR	VC	VT
2003	7 (87)	9 (94)	1 (96)	5 (94)	11 (98)	0 (47)	1 (100)	3 (100)	10 (98)	5 (98)	12 (97)
2004	4 (98)	3 (100)	1 (99)	7 (100)	11 (100)	3 (95)	2 (100)	11 (100)	9 (100)	2 (100)	6 (99)
2005	7 (100)	9 (100)	3 (100)	1 (53)	23 (100)	19 (70)	6 (91)	13 (100)	17 (92)	9 (99)	17 (100)

Table 2.10 Values of $AOT40_v$ at each site (it should not exceed 16.3 μg m^{-3} h^{-2} averaged over five years, for the protection of vegetation) and the correspondent PAD (in brackets)

Year	AN	BG	BV	CS	ER	LB	MT	PR	VR	VC	VT
2003	3.5 (95)	4.0 (99)	1.8 (100)	5.2 (96)	7.7 (98)	-	1.7 (99)	4.5 (99)	6.2 (88)	4.7 (100)	7.6 (95)
2004	3.4 (90)	5.4 (100)	1.4 (96)	7.9 (99)	8.0 (99)	3.5 (82)	2.5 (99)	9.2 (99)	4.6 (100)	4.3 (99)	5.8 (98)
2005	3.4 (100)	5.9 (99)	1.4 (99)	5.0 (75)	8.5 (100)	14.5 (75)	2.8 (69)	6.2 (98)	11.9 (99)	5.2 (99)	8.2 (100)

2.8. Conclusions

The analysis to the exceedances to EU limits showed that Oporto-MA presents lower levels of CO and SO_2 concentrations. As it is a region strongly influenced by traffic, the concentrations of NO_x and PM_{10} surpassed the limits at almost all

monitoring sites. For NO_2, the concerning monitoring sites were AN, BV, LB and MT. With higher levels of NO_x, the equilibrium chemical reaction evolving NO_x and O_3 limits the concentrations of the last one. Despite this fact, the limits relative to O_3 concentrations regarding the protection of human health were surpassed at all sites.

Chapter 3

Characterization of Air Pollution Behaviours

The air quality monitoring of air pollutant levels should be adequately managed in any air quality monitoring network. The number of monitoring sites that constitute the network should be optimized helping to reduce expenses; but at the same time guarantying the adequate characterization of the regional air quality. This means that only one monitoring site should operate in an area characterized by specific air pollution behaviour. This chapter shows how principal component and cluster analyses can be applied to define the minimum number of monitoring sites that should operate in an air quality monitoring network. Additionally, the location of main emission sources was identified based on the wind direction.

The contents of this chapter were adapted from: (i) Pires, J.C.M., Sousa, S.I.V., Pereira, M.C., Alvim-Ferraz, M.C.M., Martins, F.G., **2008**. Management of Air Quality Monitoring using Principal Component and Cluster Analysis – Part I: SO_2 and PM_{10}. *Atmospheric Environment* 42 (6), 1249-1260; and (ii) Pires, J.C.M., Sousa, S.I.V., Pereira, M.C., Alvim-Ferraz, M.C.M., Martins, F.G., **2008**. Management of Air Quality Monitoring using Principal Component and Cluster Analysis – Part II: CO, NO_2 and O_3. *Atmospheric Environment* 42 (6), 1261-1274.

3.1. Introduction

Principal component analysis (PCA) is a statistical technique that creates new variables, called principal components (PCs) that are orthogonal and uncorrelated to each other. These PCs are linear combinations of the original variables and are obtained in such a way that the first PC explains the largest fraction of the original data variability; the second PC explains a lesser fraction of the data variance than the first PC and so forth (Abdul-Wahab et al., 2005; Sousa et al., 2007; Wang and Xiao, 2004). To better clarify the influence of each original variable in the PCs, a

rotational algorithm such as varimax rotation is generally applied to obtain the rotated factor loadings that represent the contribution of each variable to a specific PC. PCA procedure is described in more detail in Chapter 6. Although PCA is mostly used for reducing the multiple dimensions associated to multivariate analyses, it was applied in this study as a method of classification, in order to group the monitoring sites into classes (PCs) having the similar air pollution behaviour.

Cluster analysis (CA) is a classification method used to divide the data in classes or clusters. Its main aim is to establish a set of clusters such that objects in the same cluster (CL) are similar to each other and different from objects located in another clusters (Manly, 1994). The ideal number of clusters may be determined graphically through a dendrogram, a tree diagram commonly used in CA (Manly, 1994; McKenna, 2003). This classification method can also be useful for data reduction.

PCA and CA have been used in many studies aiming the management of water monitoring networks (Kannel et al., 2007; Mendiguchía et al., 2004; Shrestha and Kazama, 2007; Singh et al., 2004; Singh et al., 2005). Nevertheless, as far as it is known by the author, only the research made by Gramsch et al. (2006) has applied CA for the analysis of air quality management. Their study determined the seasonal trends and spatial distribution of PM_{10} and O_3 for Santiago de Chile, concluding that the city had four large sectors with dissimilar air pollution behaviours.

The global aim of this chapter was to evaluate the performance of PCA and CA for the management of air pollutant concentrations monitoring with the following specific objectives: (i) to identify city areas with similar air pollution behaviour; and (ii) to locate main emission sources.

3.2. Air quality data

PCA and CA were applied to the analysis of the air pollutant (SO_2, PM_{10}, CO, NO_2 and O_3) concentrations collected in the AQMN of Oporto-MA, from January 2003 to December 2005. To be able to apply these statistical methods, hourly concentrations need to be available at all sites in the same time period. For SO_2, the number of available hourly data at each monitoring site were 5281, 7761 and 5355 for the 2003, 2004 and 2005 years, respectively; for PM_{10}, the number of available hourly data at each monitoring site were 4490, 4369 and 5548; for CO, the number of available hourly data at each monitoring site were 2681, 3478 and 2565; for NO_2, the number of available hourly data at each monitoring site were 4277, 3482 and 4675; and for O_3, the number of available hourly data at each site were 1967, 7390 and 1943. Concentration values were Z standardized to have zero mean and unit standard deviation.

3.3. Results and discussion

PCA was applied as a non-parametric method of classification in order to group the monitoring sites into classes having similar air pollution behaviours and differing from those in other classes. Table 3.1 shows the main results of the PCA application for both pollutants at all sites. Considering eigenvalues greater than 1 (Kaiser criterion; Yidana et al., 2008), only the first four PCs that explain 63.8% of the original data variance need to be taken into account for analyzing the SO_2 concentrations. However, in order to consider a cumulative variance greater than 75%, the PC5 and PC6 components were selected (having eigenvalues of 0.91 and 0.81, respectively), in which case 81.0% of the data variance was explained. Considering the same criterion, two PCs could be selected for CO concentrations, explaining 71.6% of variance of the original data. One more PC with eigeinvalue close to 1 (0.71) could be selected to achieve at least 75% of the original data variance, resulting in 78.1% of the total variance. On the other hand, for PM_{10}, NO_2 and O_3 concentrations, two PCs were selected for each pollutant and

Table 3.1 Main results of the PCA application for the analysed pollutants at all sites

Site		PC1	PC2	PC3	PC4	PC5	PC6		PC1	PC2
AN									**-0.807**	-0.207
BV		**-0.848**	-0.020	-0.009	-0.066	-0.054	0.026		**-0.757**	-0.117
CS		-0.226	-0.074	0.022	**-0.776**	-0.076	0.062		**-0.846**	-0.154
ER		-0.054	-0.058	-0.024	**-0.820**	-0.028	0.038			
LB		-0.040	**-0.886**	0.004	-0.073	-0.030	-0.013		-0.190	**-0.931**
MT	SO_2	**-0.877**	-0.044	-0.023	-0.026	-0.004	0.029	PM_{10}	**-0.889**	-0.115
PR		0.024	0.009	**0.996**	0.005	0.001	0.080		**-0.784**	-0.133
SH		**-0.731**	-0.016	0.005	-0.372	0.009	-0.002		**-0.874**	-0.233
VR		-0.024	**-0.885**	-0.014	-0.057	-0.049	0.036		-0.162	**-0.937**
VC		-0.040	-0.020	0.081	-0.089	-0.031	**0.991**		**-0.698**	-0.155
VT		-0.038	-0.072	-0.001	-0.089	**-0.991**	0.031		**-0.857**	-0.147
Eigenvalue		2.55	1.58	1.21	1.04	0.91	0.81		5.87	1.48
Variance (%)		25.5	15.8	12.1	10.4	9.1	8.1		58.7	14.8
Cumulative variance (%)		25.5	41.3	53.4	63.8	72.9	81.0		58.7	73.5

Site		PC1	PC2	PC3		PC1	PC2		PC1	PC2
AN		**-0.745**	-0.175	0.306		**-0.852**	-0.137		**-0.895**	-0.214
BG		**-0.751**	-0.254	0.351		**-0.830**	-0.163		**-0.903**	-0.250
BV		**-0.794**	-0.162	0.196		**-0.830**	-0.150		**-0.906**	-0.190
CS		**-0.843**	-0.226	0.294		**-0.898**	-0.200		**-0.926**	-0.240
ER						**-0.845**	-0.205		**-0.903**	-0.258
LB	CO	-0.198	**-0.931**	0.019	NO_2	-0.202	**-0.936**	O_3	-0.226	**-0.957**
MT		-0.611	-0.132	**0.654**		**-0.844**	-0.111		**-0.892**	-0.179
PR		**-0.747**	-0.098	0.120		**-0.740**	-0.156		**-0.851**	-0.219
SH		**-0.784**	-0.190	0.383		**-0.879**	-0.100			
VR		-0.192	**-0.912**	0.174		-0.152	**-0.943**		-0.258	**-0.947**
VC		-0.286	-0.094	**0.900**		**-0.755**	-0.171		**-0.847**	-0.273
VT		**-0.819**	-0.139	0.159		**-0.813**	-0.201		**-0.873**	-0.243
Eigenvalue		6.48	1.40	0.71		7.46	1.53		8.13	1.39
Variance (%)		58.9	12.7	6.5		62.1	12.7		73.9	12.7
Cumulative variance (%)		58.9	71.6	78.1		62.1	74.9		73.9	86.5

Values in bold indicate the variables that mostly influence the correspondent principal component.

explained 73.5%, 74.9% and 86.5% of the original variance, respectively. The rotated factor loadings in bold indicate the variables that mostly influence the correspondent PC. For SO_2 concentrations, the first PC (PC1) had important contributions from BV, MT and SH sites, while PC2 was heavily loaded by the contributions from LB and VR sites. PC4 had important contributions from CS

and ER monitoring sites; while PR, VT and VC sites were significantly associated with PC3, PC5 and PC6 components, respectively. For CO concentrations, PC1 had important contributions of sites AN, BG, BV, CS, PR, SH and VT, PC2 was heavily loaded by LB and VR sites, and the sites MT and VC were considered important in PC3. Besides the inclusion of MT site in PC3, it has also an important contribution in PC1 (factor loading of 0.611). For PM_{10}, NO_2 and O_3 concentrations, PC2 had significant contributions from LB and VR sites, while PC1 was heavily loaded by the remaining monitoring sites.

CA was also used to group monitoring sites based on the similarity of the pollutant standardized concentration values. Euclidean distance was used to compute the distance among monitoring sites and the clustering procedure used was the average linkage method (Manly, 1994). This procedure is based on the average distance between all pairs of objects - that is monitoring sites - considering that the two objects must belong to different clusters. The two objects with the lowest average distance are linked to form a new cluster. The complete procedure is presented as follows: step 1: determination of the distances between all objects; step 2: linkage of the two objects that correspond to the lowest distance to conform a new cluster or group of objects; step 3: compare the two objects that form part of the newly formed group with the remaining objects. In this stage of the analysis, each object not yet classified will be associated then with two distances. Finally, the ascribed distance to the unclassified object will be the average of both distances; step 4: repeat step 3 until all objects belong to one cluster.

Figure 3.1 shows the dendrograms (a) to (e) resulting from the application of CA to the SO_2, PM_{10}, CO, NO_2 and O_3 concentrations, respectively. For SO_2 concentrations, the results obtained showed that the ten monitoring sites (measuring SO_2 concentrations) of the AQMN can be grouped into six clusters: cluster I (CL1) - BV, MT and SH sites; cluster II (CL2) - CS and ER sites; cluster III (CL3) - LB and VR sites; cluster IV (CL4) - VT site; cluster V (CL5) - PR site; cluster VI (CL6) - VC site. Similar results were achieved with the application of

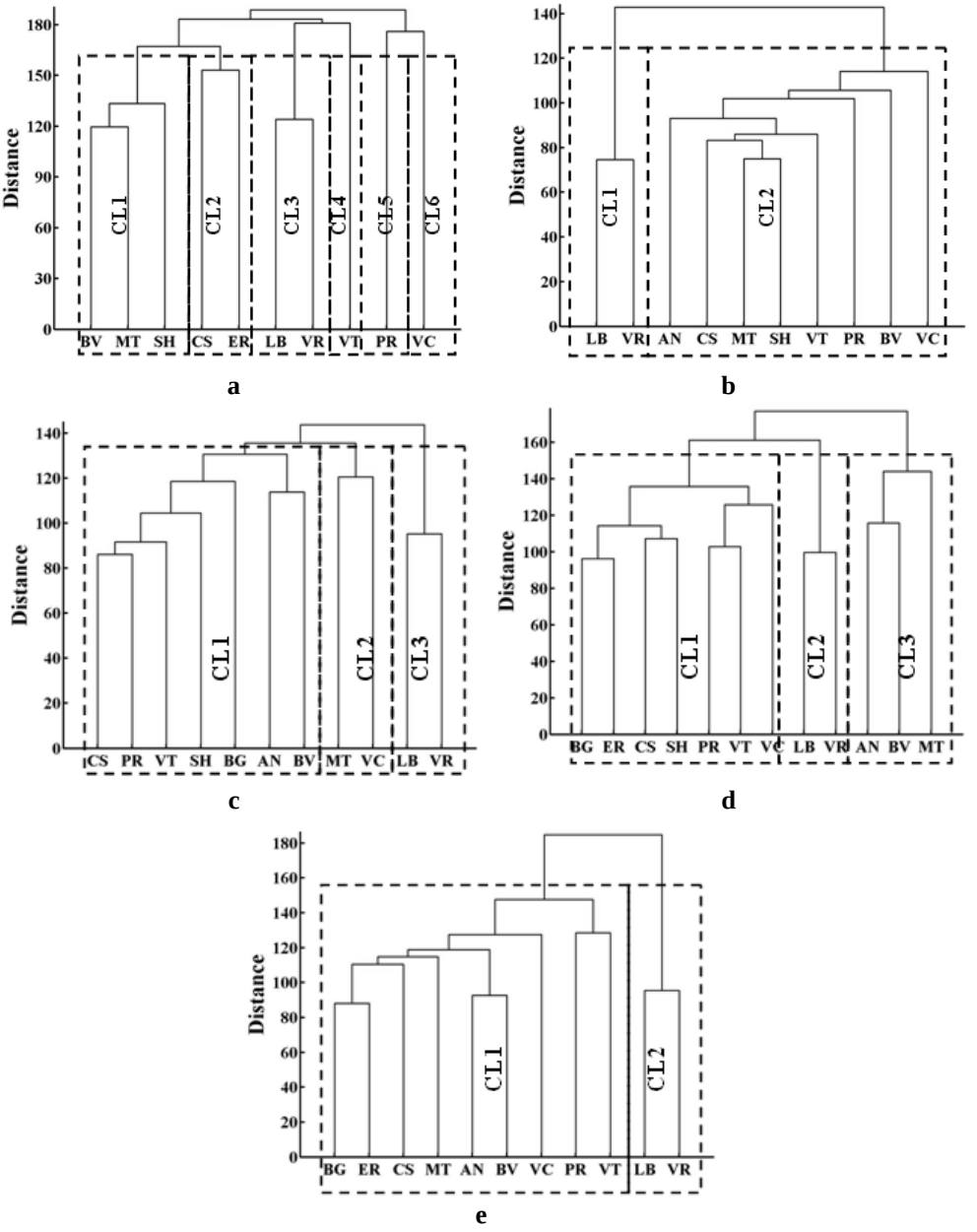

Figure 3.1 Dendrograms resulting from the application of CA to the (a) SO_2, (b) PM_{10}, (c) CO, (d) NO_2 and (e) O_3 concentrations.

PCA, where the PC1, PC2, PC3, PC4, PC5 and PC6 principal components corresponded exactly to the CL1, CL3, CL5, CL2, CL4 and CL6 clusters of the

CA, respectively. For the PM_{10} concentrations, similar results were achieved with PCA, with the PC1 and PC2 principal components of the PCA corresponding exactly to the CL2 and CL1 clusters of the CA, respectively. For CO concentrations, the results obtained showed that the eleven monitoring sites of the AQMN could be coupled into three clusters: cluster I (CL1) – AN, BG, BV, CS, PR, SH and VT sites; cluster II (CL2) – MT and VC sites; cluster III (CL3) – LB and VR sites. Similar results were achieved with PCA, where PC1, PC2 and PC3 corresponded to CL1, CL3 and CL2, respectively. For NO_2 concentrations, the twelve sites could be also coupled into three clusters: cluster I (CL1) – sites BG, CS, ER, PR, SH, VC and VT; cluster II (CL2) –sites LB and VR; cluster III (CL3) –sites AN, BV and MT. For this pollutant, PCA and CA did not achieve the same results. PC2 corresponded to CL2, but the sites coupled in PC1 were divided into CL1 and CL3. Furthermore, for O_3 concentrations, PCA and CA also achieved similar results, with PC1 and PC2 corresponding to CL1 and CL2, respectively. Therefore, it was possible to conclude that the O_3 concentrations monitored at the eleven sites could be coupled in no more than two groups.

Figure 3.2 (from a to f) shows the average daily profile of the hourly average SO_2 concentrations at the monitoring sites grouped by the correspondent PC/CL category. Similar behaviours of SO_2 pollution can be observed in sites belonging to the same PC/CL category. Figure 3.3 (from a to b) shows the daily profile of the hourly average PM_{10} concentrations grouped by the correspondent PC/CL category. For the second group (PC2/CL1 category), the monitoring sites had similar pollution profile. Nevertheless, and for the first group (PC1/CL2), the sites had the same profile until 17 hours, but between 17 and 22 hours VC site showed a peak of PM_{10} concentration. The inclusion of VC site in this group by the PCA is related to the low proportion of the original data variance explained by the first two PCs (communality of 0.51). In CA, this is explained by the correspondent Euclidean distance of the VC site, which was greater than in other sites belonging

to the CL2 category. This means that VC site exhibited more dissimilar air pollution behaviour than the other monitoring sites classified into this group.

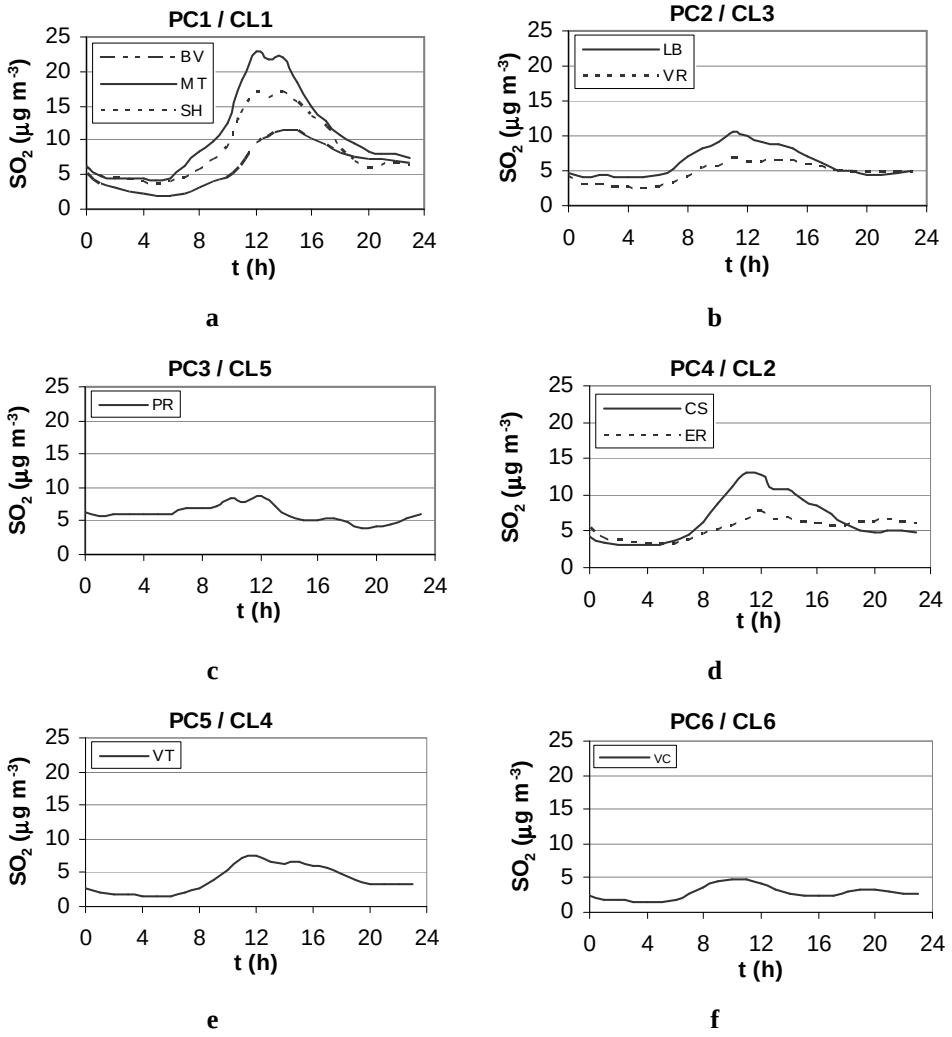

Figure 3.2 Average daily profile of the hourly average SO_2 concentrations at the monitoring sites grouped by the correspondent PC/CL category: (a) PC1/CL1, (b) PC2/CL3, (c) PC3/CL5, (d) PC4/CL2, (e) PC5/CL4 and (f) PC6/CL6.

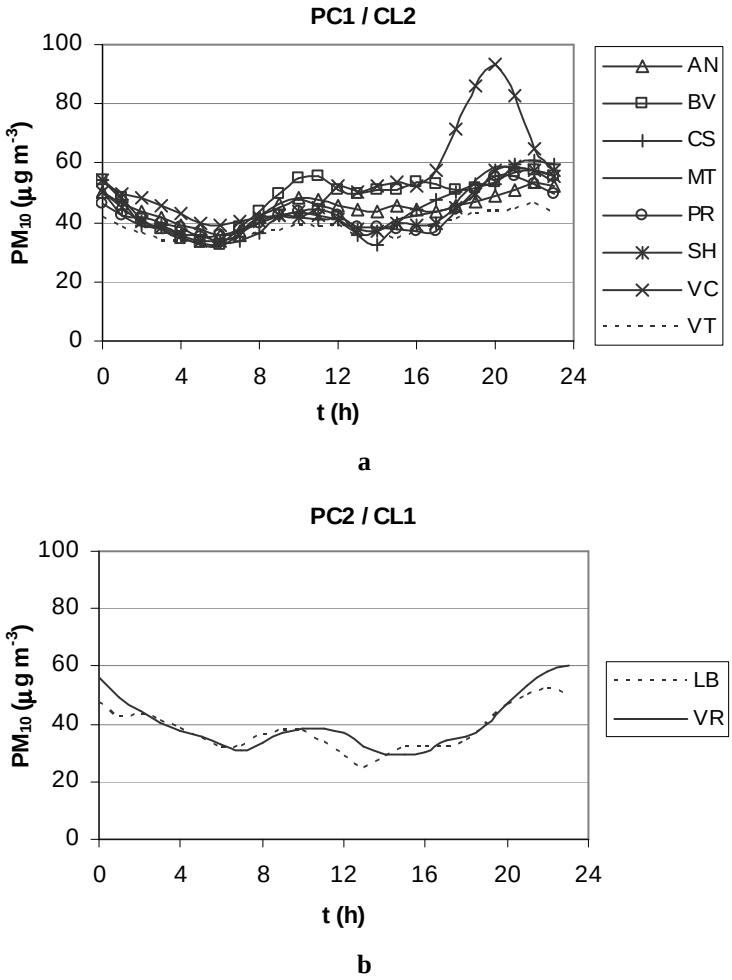

Figure 3.3 Average daily profile of the hourly average PM_{10} concentrations for the monitoring sites grouped by the correspondent PC/CL category: (a) PC1/CL2 and (b) PC2/CL1.

Figure 3.4 (from a to c) shows the average daily profile of hourly average CO concentrations at the monitoring sites grouped by the correspondent PC/CL category. Similar profiles of CO can be observed at the sites belonging to the same PC/CL. Figure 3.5 (from a to c) shows the average daily profile of hourly average NO_2 concentrations grouped by the correspondent PC/CL category.

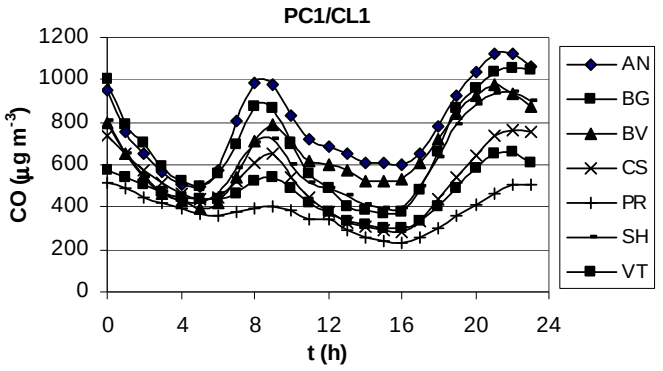

a

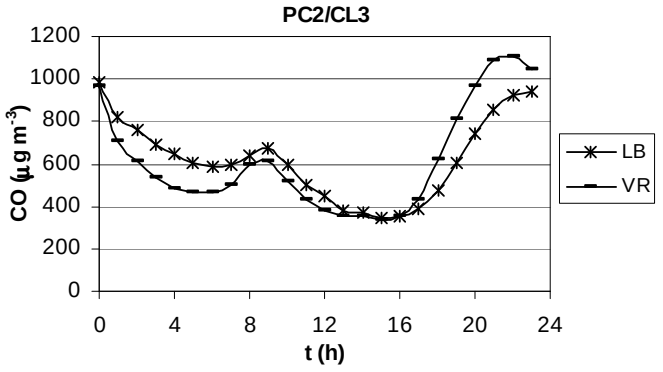

b

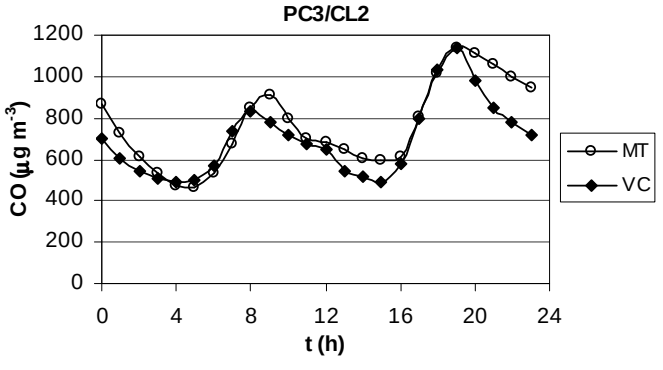

c

Figure 3.4 Average daily profile of the hourly mean CO concentrations for the monitoring sites grouped by the correspondent PC/CL category: (a) PC1/CL1, (b) PC2/CL3, and (c) PC3/CL2.

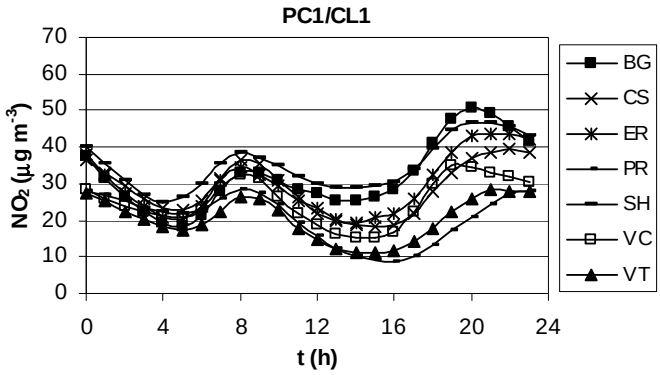

a

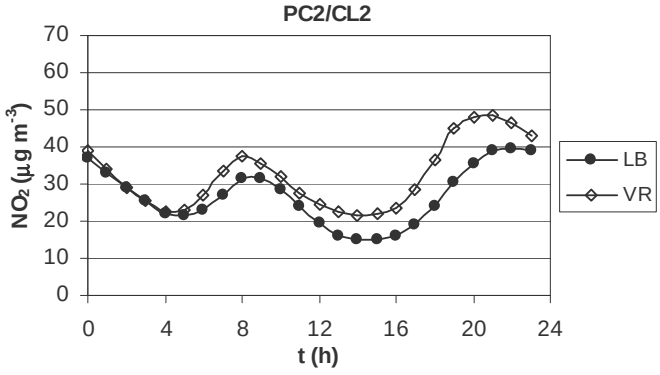

b

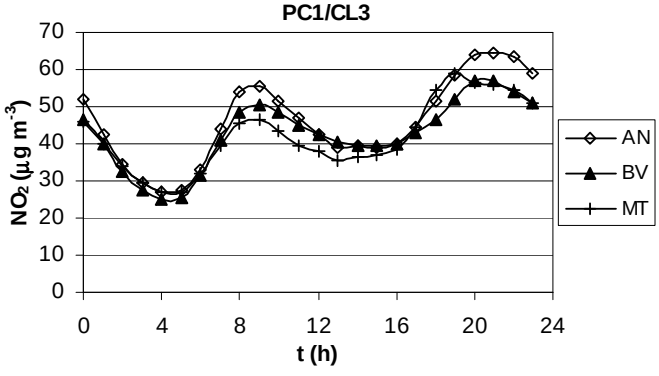

c

Figure 3.5 Average daily profile of the hourly average NO_2 concentrations for the monitoring sites grouped by the correspondent PC/CL category: (a) PC1/CL1, (b) PC2/CL2, and (c) PC1/CL3.

Comparing the two statistical methods, CA created one more group of sites. This group was composed by the sites with strong influence of traffic (AN, BV and MT). Figure 3.6 (a and b) shows the average daily profile of hourly average O_3 concentrations, grouped by the correspondent PC/CL category. Similar profile was observed in the grouped sites.

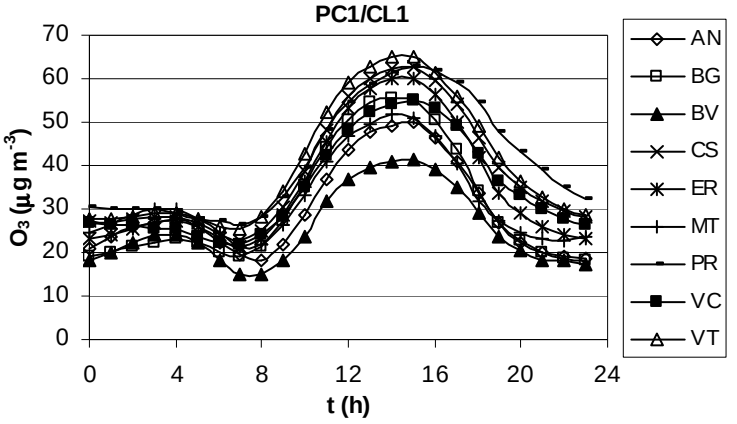

a

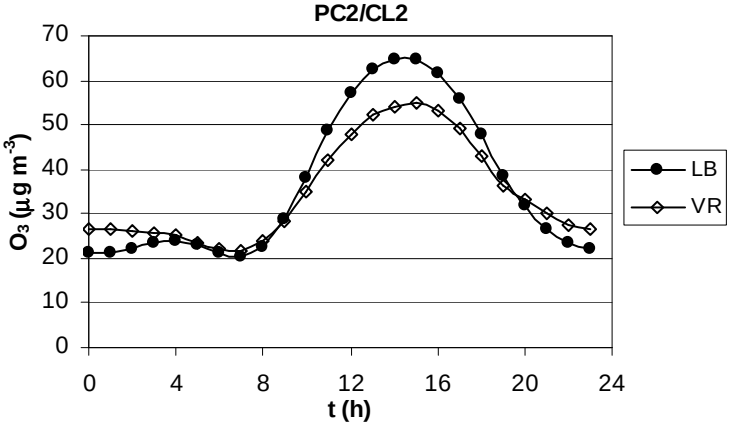

b

Figure 3.6 Average daily profile of the hourly average O_3 concentrations for the monitoring sites grouped by the correspondent PC/CL category: (a) PC1/CL1 and (b) PC2/CL2.

The existence of different air pollution behaviours in the monitoring network can be explained by the geographical location of the main pollutant sources and by the variability of wind directions across the region. This last fact was evaluated by analysing the influence of the wind direction on the increase of the pollutant concentrations. Figure 3.7 presents the relative frequency of the direction from which the wind was blowing when hourly average concentrations of SO_2 above 125 $\mu g\ m^{-3}$ were collected (VC site did not present any SO_2 concentration above this value). The selected value for reference that only aimed the comparison was under EU limit value because SO_2 concentrations were almost always under that limit. Because the BV, MT and SH monitoring sites were classified in the same group, they should be affected by the same SO_2 source or sources at the same time. These sources are probably located in the W-NW direction sector as it is observed from those sites. On the other hand, the highest SO_2 concentrations at PR site, located at north of the MT monitoring site (see Figure 2.1) were measured when wind blew predominantly from the S-SW wind direction sector. Thus, the main emission source of SO_2 was located between the PR and MT sites. SO_2 concentrations higher than 125 $\mu g\ m^{-3}$ emitted from this source were also detected at the CS and ER sites (both included in the PC4/CL2 group) when the wind came predominantly from the W-NW direction sector. The number of site groups with similar air pollution behaviour was influenced by the geographic location of the emission sources. As the main emission source was located inside the region covered by the AQMN, for each wind direction, the daily evolution of SO_2 concentrations was not the same at all monitoring sites; this means that the sites can be grouped according to this specific behaviour. Results showed that six monitoring sites were needed to characterize the SO_2 concentrations.

The influence of the wind direction sector on the increasing of PM_{10} concentrations was analysed in order to check for the existence of significant emission sources for this pollutant. Figure 3.8 presents the relative frequency of the direction from which the wind was blowing when hourly average PM_{10}

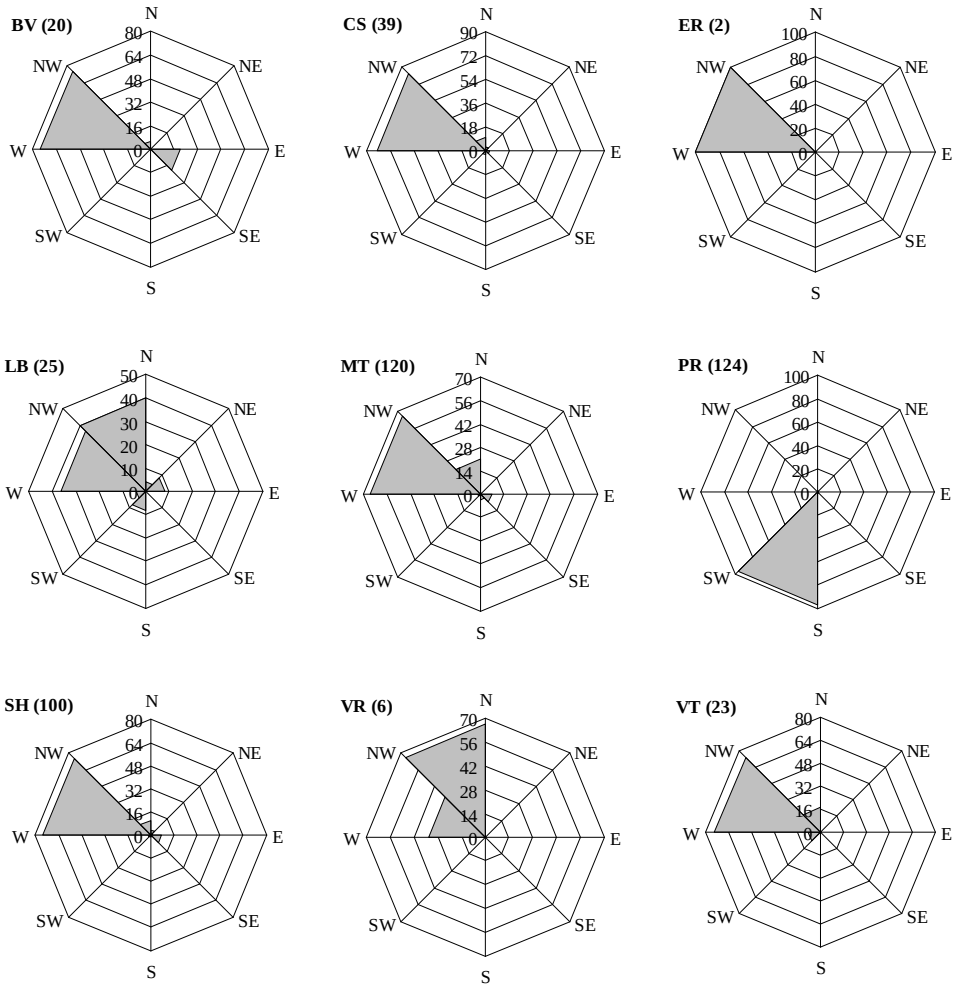

Figure 3.7 Relative frequency (%) of the direction from which the wind was blowing when hourly average concentrations of SO_2 above 125 μg m^{-3} were collected (number of occurrences in brackets).

concentration increased at least 50 μg m^{-3} during the period that lasted from 17 to the 22 hours (period when highest PM_{10} concentrations were observed for all sites). Main results indicated that the additional emission source or sources that affected VC site were located along the NW-N and W-NW wind direction sectors. These sources had a strong influence on that site in 2003 and 2004, but their impact notably diminished in 2005. Furthermore, it was observed that these

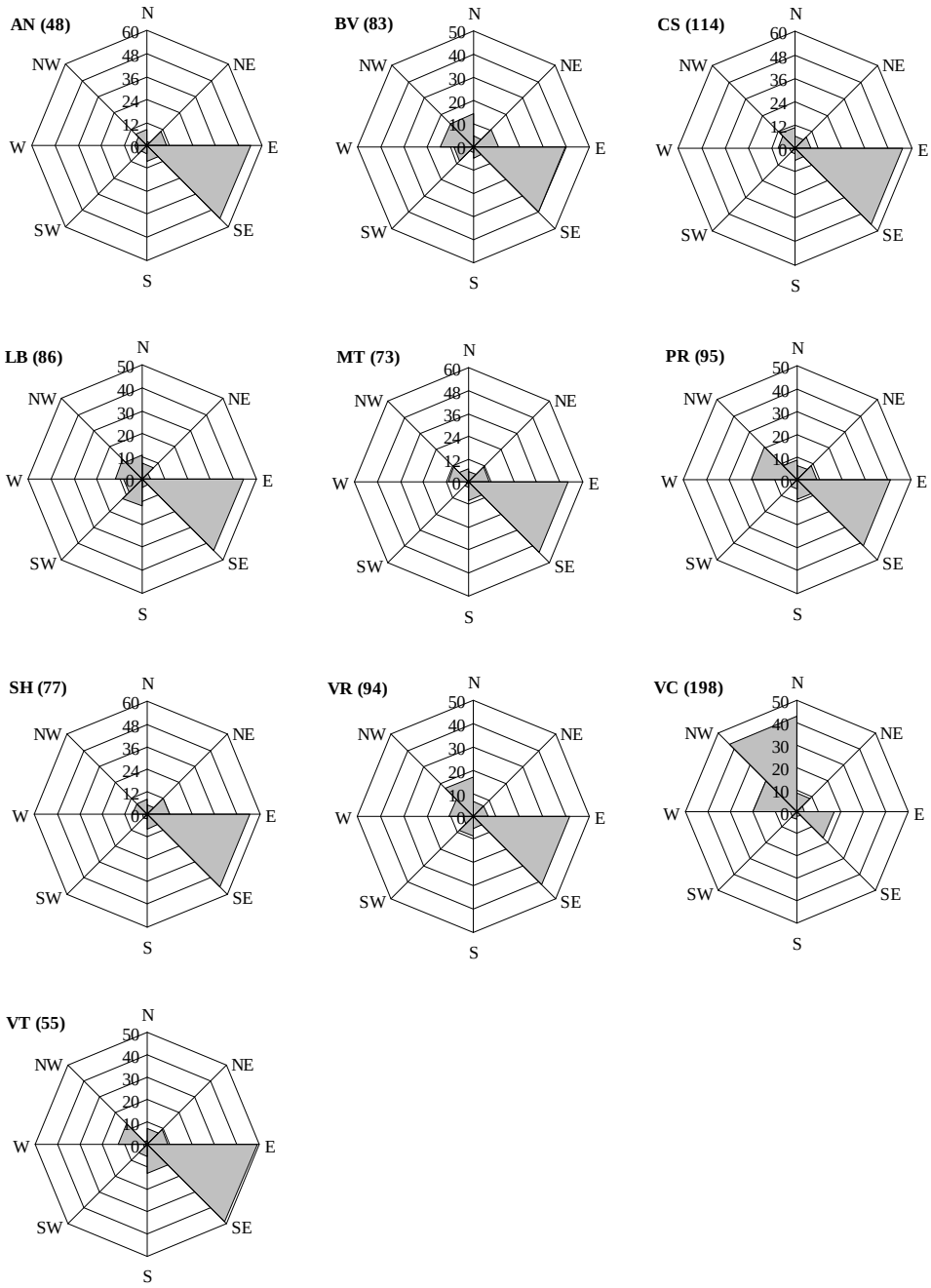

Figure 3.8 Relative frequency (%) of the direction from which the wind was blowing when hourly average concentrations of PM_{10} increased at least 50 μg m^{-3} during the period that lasted from 17 to the 22 hours (number of occurrences in brackets).

emission sources was responsible for the peak of PM_{10} concentration referred above as the major difference of the pollution behaviour presented by VC site in the PC1/CL2 class. During 2003 and 2004, VC site presented different pollution behaviour only in the period of day between 17 and 22 hours (when the wind blew from NW-N and W-NW direction). With the decrease of the impact of this emission source in 2005, the pollution behaviour of VC site became more similar to the others belonging to PC1/CL2 class. Additionally, during the entire analysed period all monitoring sites were highly influenced by PM_{10} emissions coming from the E-SE direction sector, which implies the existence of an emission source located outside the region defined by the AQMN and along that wind direction sector. High concentrations of CO and NO_2 were also measured with this wind direction. Therefore, this emission source had anthropogenic origin.

The two PM_{10} emission sources described in the above paragraph did not explain very well, however, the existence of the PC/CL class conformed by the LB and VR sites. The emission source located to the NW-N and the W-NW direction sectors significantly affected the PM_{10} concentrations measured at VC site, but not enough to avoid the inclusion of this site in the PC1/CL2 category of the PM_{10} pollutant. The second emission source, located along the E-SE direction sector, significantly affected the PM_{10} concentrations measured at all sites, including the LB and VR sites. Figure 3.9 shows, as example, the profile of the hourly average PM_{10} concentrations for January the 11^{th}, 2004 when the wind blew more frequently from the S-SW direction sector. The LB and VR monitoring sites showed the highest PM_{10} concentrations and presented profiles different from the other sites (reason to be grouped in a different PC/CL class). Thus, a PM_{10} emission source was located at the vicinity of these sites.

Figure 3.10 presents the relative frequency of the direction from which the wind was blowing when hourly average concentrations of CO above 4 mg m^{-3} was collected (LB, VC and VT sites did not present any CO concentration above this value). CO concentrations above 4 mg m^{-3} were detected at all sites when the wind

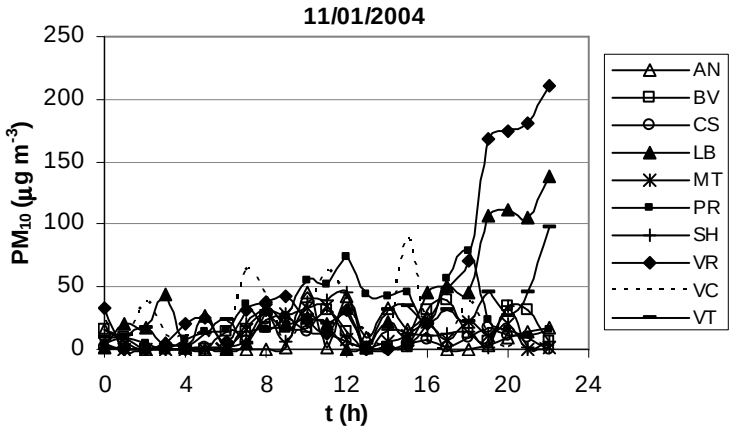

Figure 3.9 Example of the profile of the hourly average PM_{10} concentrations when the wind blew predominantly from S-SW direction sector.

came from E-SE direction sector. Thus one important emission source was located outside the region defined by AQMN of Oporto-MA. The AN, MT and SH sites also measured high concentrations when the wind blew from NW-N direction sector. Thus one emission source of CO was located at NW-N of these sites. If different sites located inside AQMN had different air pollution behaviour, the emission sources responsible for these differences were inside of the monitoring area. These two main emission sources did not explain the existence of the three groups characterized by different air pollution behaviours. Figure 3.11 (a and b) shows, as example, the profiles of the hourly average CO concentrations: (a) for December 24th and 25th, 2003 when the wind blew more frequently from the NE-E direction sector; and (b) for April 1st, 2003 when the wind blew more frequently from the NW-N direction sector. In the first example (Figure 3.11a), the LB and VR sites recorded the highest CO concentrations and presented profiles different from the other sites (reason to be grouped in different PC/CL). In the second example (Figure 3.11b), the MT and VC sites had the highest concentrations. Even not showing the same profiles, they were different from those presented by the other sites. Because MT site had similar contributions in PC1 and PC3, the difference in the profiles of CO concentrations collected at MT and VC sites

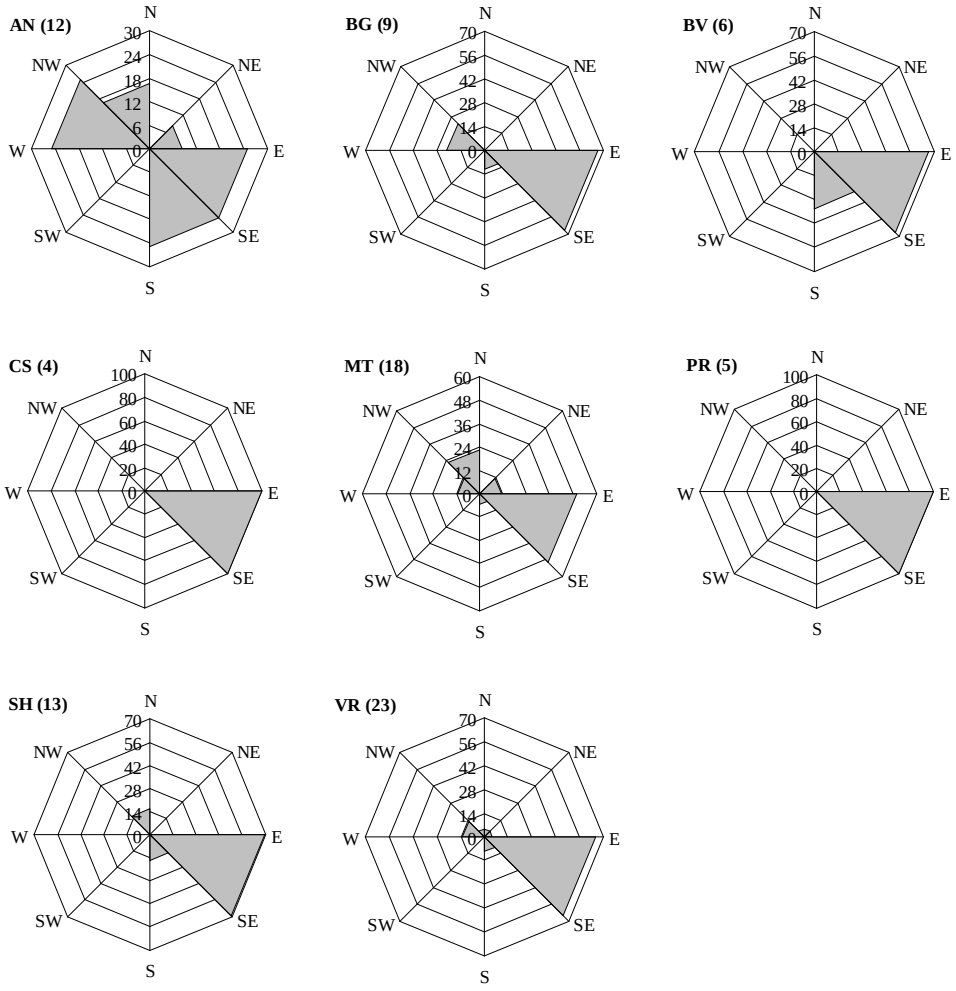

Figure 3.10 Relative frequency (%) of the direction from which the wind was blowing when hourly average CO concentration above 4 mg m^{-3} was collected (number of occurrences in brackets).

(grouped in the same PC/CL category) should be expected. As AN and SH sites presented different profiles from the MT site, it was concluded that there was an additional emission source located at NW-N wind direction sector affecting significantly the CO concentrations recorded at MT and VC sites.

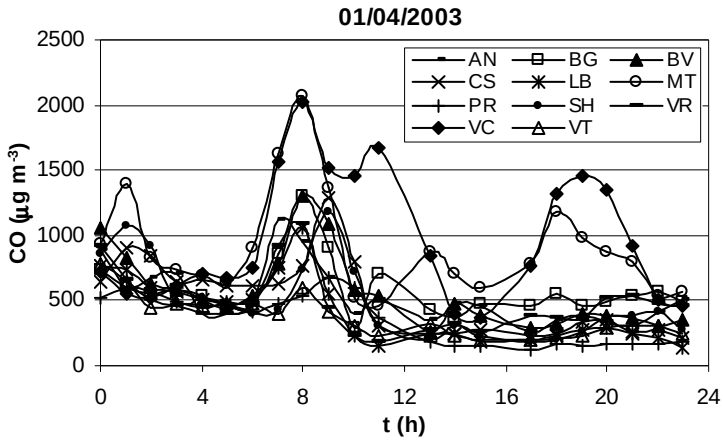

Figure 3.11 Examples of the daily profiles of CO concentrations when the wind blew predominantly from: (a) NE-E, and (b) NW-N direction sectors.

Figure 3.12 presents the relative frequency of the direction from which the wind was blowing when hourly average NO_2 concentration above 100 µg m^{-3} was collected. Three wind direction sectors were considered important. NO_2 transported by the wind that came from E-SE direction sector affected all sites. This important emission source was located outside the region defined by AQMN. The AN, BG, BV, ER, LB, MT, SH and VR sites were also affected by NO_2 transported by the wind that came from W-NW and NW-N direction sectors. Thus,

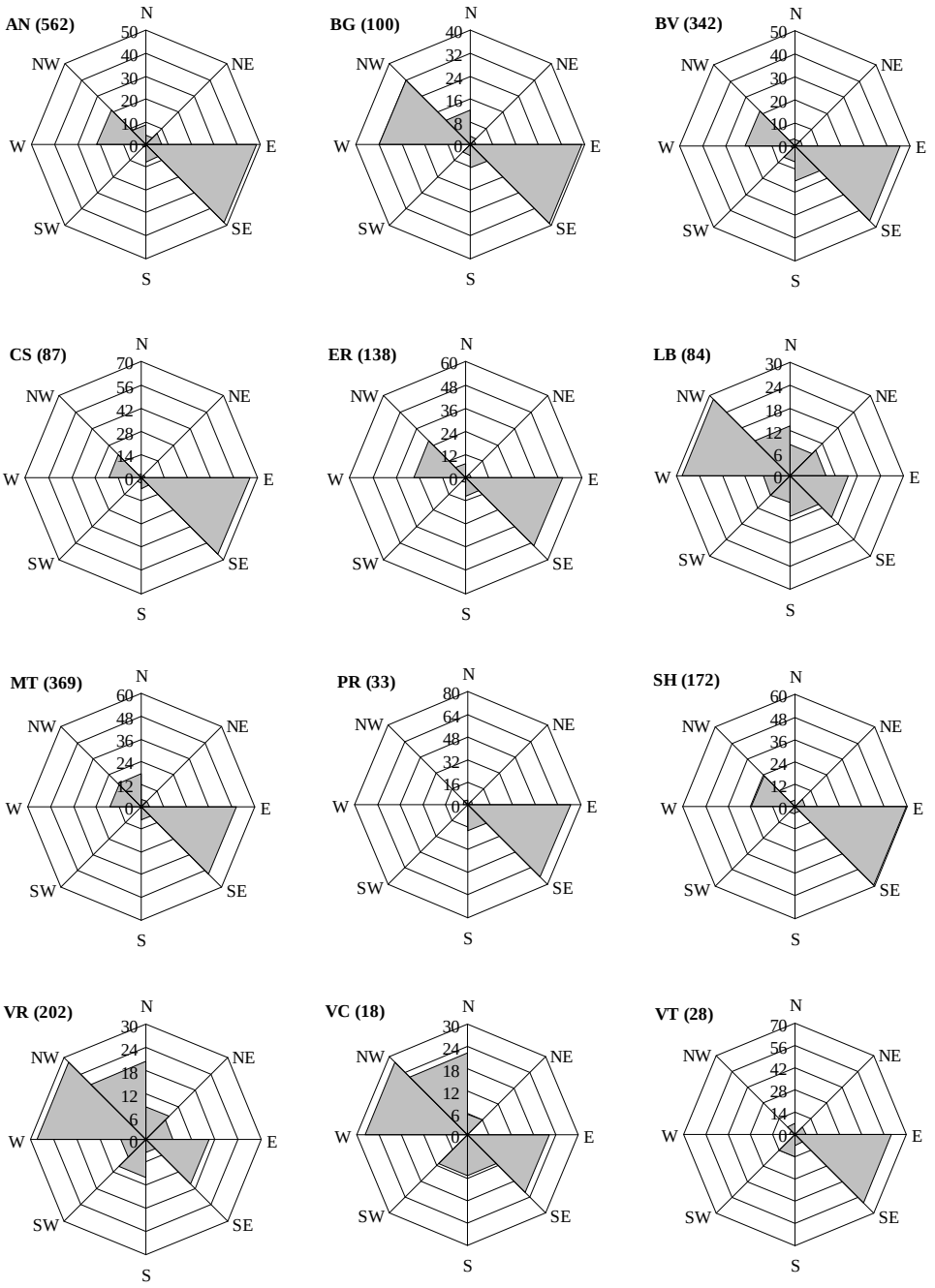

Figure 3.12 Relative frequency (%) of the direction from which the wind was blowing when hourly average NO_2 concentration above 100 μg m^{-3} was collected (number of occurrences in brackets).

knowing the geographical location of these sites, three main emission sources of NO_2 were located affecting three different groups of monitoring sites: (i) AN, BV, MT and SH; (ii) LB and VR; and (iii) BG and ER. The main emission source associated to LB and VR sites was the only one that significantly affected their air pollution behaviour to include them in a different group (PC/CL). Figure 3.13 shows, as example, the profiles of the hourly average NO_2 concentrations for September 7th, 2005 when the wind came from NW-N direction sector. The LB and VR sites had the highest NO_2 concentrations and presented profiles different from the other sites (reason to be grouped in different PC/CL). The sites AN, BV and MT were included in another group due to the strong influence of traffic in the NO_2 concentrations.

O_3 is a secondary pollutant (it is not directly emitted), resulting from the photochemical interaction between emitted pollutants (nitrogen oxides and volatile organic compounds) (Alvim-Ferraz et al., 2006). Therefore, the analysis of wind direction influence on the increase of O_3 concentrations was done not to locate main emission sources, but to detect places with high O_3 concentrations that could be transported by the wind. Figure 3.14 presents the relative frequency of the direction from which the wind was blowing when hourly average O_3

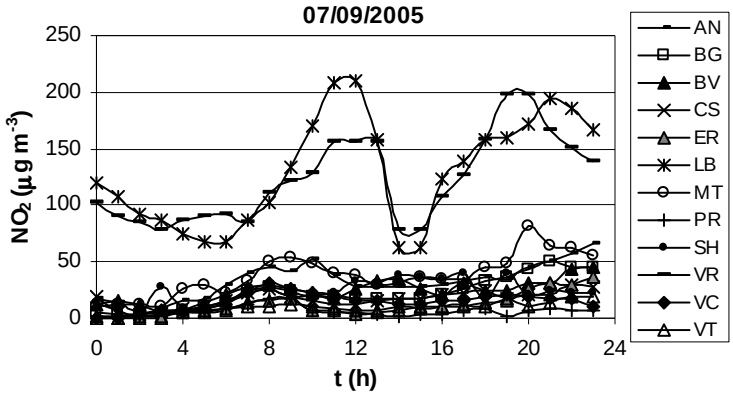

Figure 3.13 Example of the daily profile of NO_2 concentrations when the wind blew predominantly from NW-N direction sector.

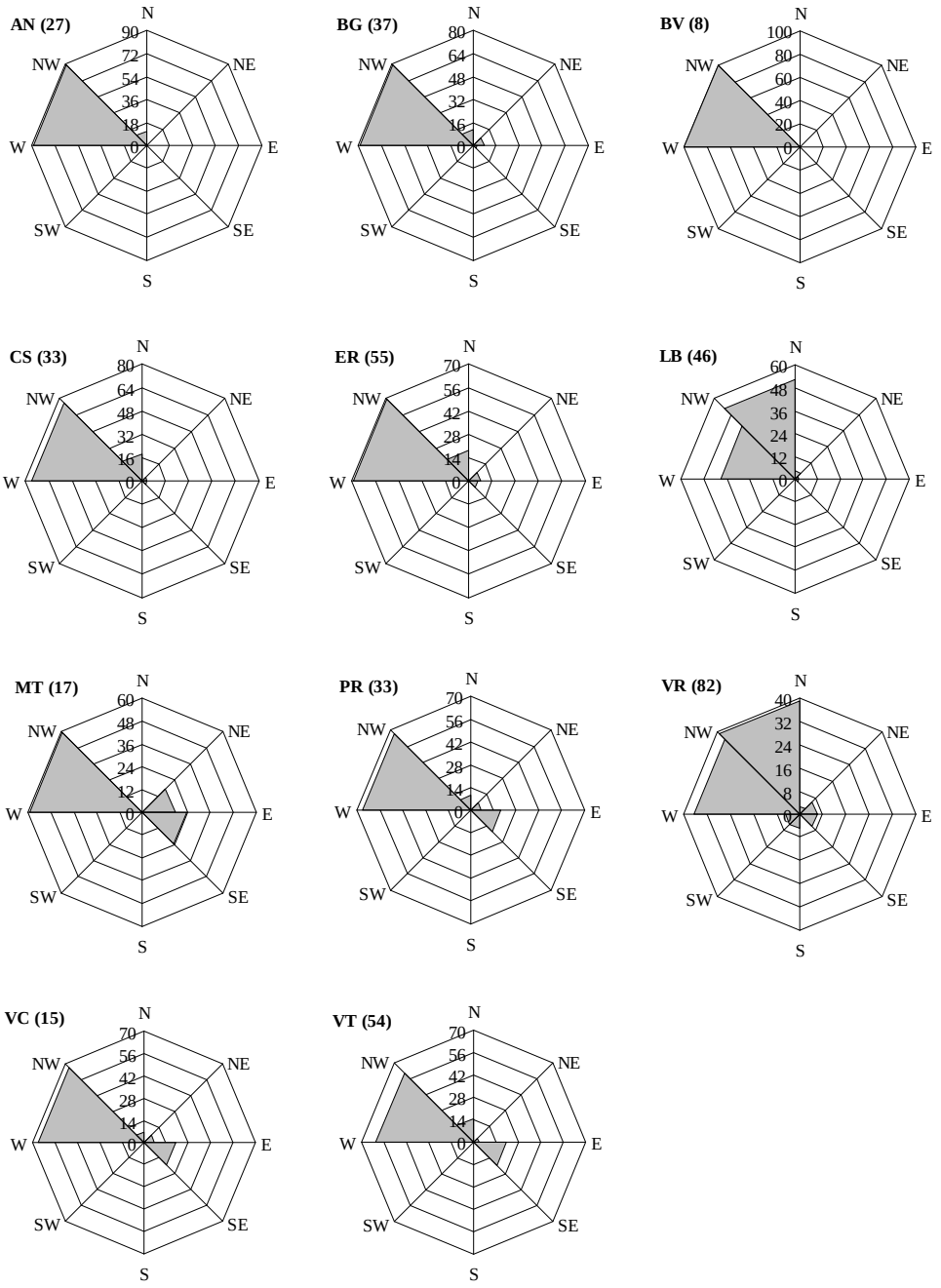

Figure 3.14 Relative frequency (%) of the direction from which the wind was blowing when hourly average O_3 concentration above 120 μg m^{-3} was collected (number of occurrences in brackets).

concentration above 120 μg m^{-3} was collected. The wind coming from NW-N direction sector was associated with the increase of O_3 concentrations at LB and VR sites, while the wind blowing from W-NW direction sector affected the concentration of this pollutant at all sites. This means that O_3 transported by the wind from the sea had a great contribution in the observed daily peaks of this pollutant concentration. This phenomenon was studied by many authors (Barros et al., 2003; Guerra et al., 2004; Jorba et al., 2003; Millán et al., 1996). According to the authors, a significant contribution in the O_3 concentration was the transport from the sea by the wind. The marine inversions or recirculation of air flows along the sea caused by the land-sea interface trapped pollutants enabling O_3 formation and accumulation (Jorba et al., 2003; Millán et al., 1996). The O_3 was accumulated in stratified layers (stacked up to 2-3 km high, along the coast) that act as reservoirs and retained this pollutant from one day to the following days. The LB and VR sites were included in a different group of sites due to the different air pollution behaviour presented in the period analysed. Figure 3.15 shows, as example, the profiles of the hourly average O_3 concentrations when the wind blew predominantly from W-NW direction sector. The LB and VR sites recorded the

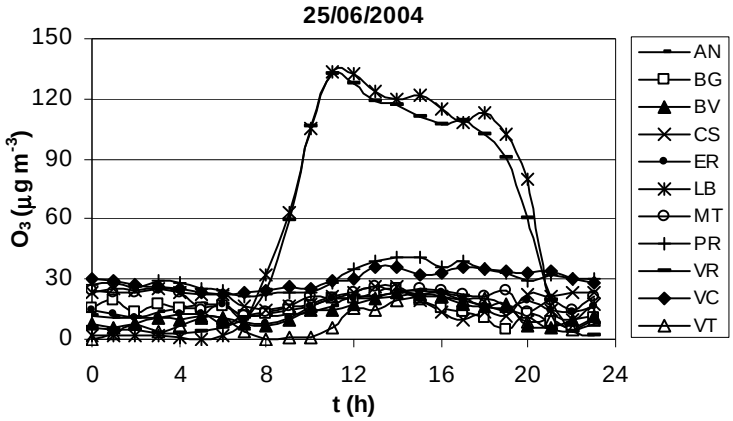

Figure 3.15 Example of the daily profile of O_3 concentrations when the wind blew predominantly from W-NW direction sector.

highest O_3 concentrations and presented profiles different from the other sites (reason to be grouped in different PC/CL).

For all pollutants considered in this study, the LB and VR sites were always differentiated by their air pollution behaviour. The location of main emission sources is one of the possible reasons, justifying the highest pollutant concentrations recorded at these sites comparing to the other sites. However, after a detailed analysis, the LB and VR sites presented daily profiles with low pollutant concentrations. Figure 3.16 shows, as example, the profile of the hourly average NO_2 concentrations for March 10th, 2005. It can be observed that LB and VR sites had profiles different from the others, presenting also lower concentrations, which means that the topography of the sites is also important for this study. These monitoring sites are located in a region between two important valleys, one from Leça River located at south and other from Almorode River located at east. These two valleys create a local atmosphere with specific air pollution behaviour different from the ones observed in other regions of Oporto-MA.

The application of PCA and CA to the air quality data, monitored at one air quality monitoring network, showed that there were city areas having the same air

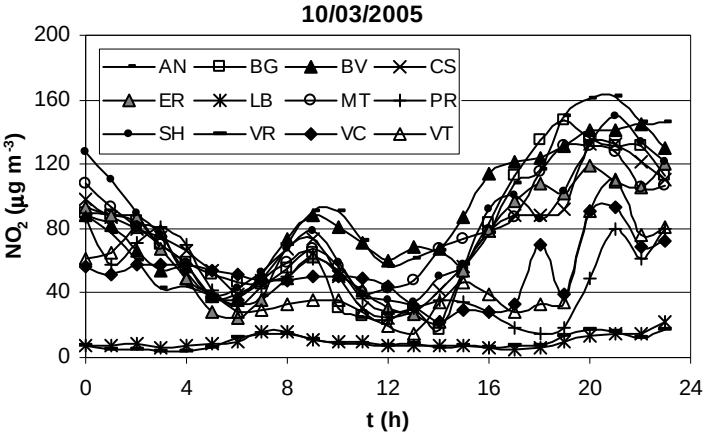

Figure 3.16 Example of the daily profile of NO_2 concentrations.

pollution behaviour covered by too many monitoring sites; suggesting that monitoring network can be better managed. This means that PCA and CA have a great potential for the management of air quality monitoring systems, helping the identification of redundant equipment that might be transferred to other sites allowing an enlargement of the monitored area.

3.4. Conclusions

Aiming the identification of city areas with similar air pollution behaviours in Oporto-MA, two statistical methods, PCA and CA, were applied. Different results were obtained for each pollutant. PCA and CA divided the sites in: (i) six different groups for SO_2; (ii) three groups for CO and for NO_2; and (iii) two groups for PM_{10} and O_3.

The number of site groups with similar pollution behaviour was affected by the geographic location of the emission sources. Approximate source locations were found through the analysis of the information contained in the wind direction sectors associated to the presence of high concentrations of the analysed air pollutants. Only one main source of SO_2 was identified, being located inside the region covered by the AQMN. For each wind direction, the daily evolution of SO_2 concentrations was not the same at all monitoring sites; this means that the sites can be grouped according to this specific behaviour. Results showed that six monitoring sites were needed to characterize SO_2 concentrations. Three main emission sources of PM_{10} were located: (i) one inside the region defined by the AQMN (significantly affected only two sites) and (ii) two outside that region (affecting all monitoring sites). One emission source located outside the region affected significantly only one monitoring site in a short period of the day. This emission source decreased its impact in 2005. Therefore, only two monitoring sites are needed to characterize PM_{10} concentrations. Additionally, four main emission sources of CO and NO_2 were located. Additionally, it was observed that sea wind

had an important contribution in the increase of the O_3 concentration due to the O_3 accumulation above the sea.

Two monitoring sites presented different air pollution behaviour for all pollutants during the analysed period. This difference was related with the location of main emission sources and also with the topography of the region where these sites are located.

Chapter 4

Identification of redundant air quality measurements

This chapter shows the results obtained by principal component analysis in the identification of redundant measurements using two different criteria for selection of the number of principal components. For each air pollutant, the minimum number of monitoring sites evaluated by this analysis was compared to what was established by the European Union legislation. To validate the results, the statistical models were determined to estimate air pollutant concentrations at removed monitoring sites using the concentrations measured at the remaining monitoring sites. These models were tested in a year's data.

The contents of this chapter were adapted from: (i) Pires, J.C.M., Pereira, M.C., Alvim-Ferraz, M.C.M., Martins, F.G., **2009**. Identification of redundant air quality measurements through the use of principal component analysis. *Atmospheric Environment* 43, 3837-3842.

4.1. Introduction

The concerns about the negative effects of air pollution led to increased efforts to prevent and control this phenomenon. The location of sampling points for the measurement of air pollutant concentrations was defined by the European Union directive 2008/50/EC (EC Directive, 2008). According to this directive, monitoring sites should be placed to provide data: (i) in areas within zones and agglomerations, where the population is likely to be directly or indirectly exposed to high concentrations (limit and target values were established as references); (ii) in other areas within zones and agglomerations which are representative of the general population exposure. The same directive defined the number of monitoring sites that should operate according to population size and pollution levels. In

Oporto Metropolitan Area (Oporto-MA) with population of about 1.7 millions and a population density of 540 inhabitants per square kilometre, NO_2 and PM_{10} concentrations exceeded many times the limits established by the legislation (see Chapter 2). Five monitoring sites should operate (including at least an urban background site and a traffic site) to measure NO_2 and PM_{10} concentrations and three monitoring sites should measure the O_3 concentrations (at least 50% of the monitoring sites should be placed in suburban areas).

In Chapter 3, PCA and CA were applied to identify the monitoring sites with similar air pollution behaviour and to locate emission sources of SO_2, PM_{10}, CO, NO_2 and O_3. However, this study was performed using all period of study, not considering the annual variations of the air pollutant behaviours due to the different meteorological conditions. In this study, PCA was applied to the data divided into annual quarters. Moreover, an additional criterion for selection of the number of PCs was applied, aiming to select PCs containing more information about the original data than the criterion usually applied (Kaiser criterion) and the number of monitoring sites was compared with what was established by the legislation. Finally, after the selection of the monitoring sites that should operate, the air pollutant concentrations measured in these locations were used to predict the concentrations at the removed monitoring sites.

4.2. Air quality data

The monitoring sites considered in this study were *Antas* (AN), *Boavista* (BV), *Custóias* (CS), *Leça do Balio* (LB), *Matosinhos* (MT), *Perafita* (PR), *Vermoim* (VR), *Vila do Conde* (VC) and *Vila Nova da Telha* (VT). Their location, type and main characteristics are presented in Chapter 2. Oporto monitoring network includes other monitoring sites that were not considered in this study: some did not measure all the considered air pollutants (*Baguim* and *Senhora da Hora*) and others presented a high percentage of missing data during the analysed period (*Ermesinde* and *Espinho*). The pollutants considered were NO_2, PM_{10} and O_3,

since CO and SO_2 did not present a significant number of exceedances to the limits established by the European Union for the protection of human health during the analysed period (Pires et al., 2008a, 2008b).

The analysed period was from January 2003 to December 2005. PCA was applied to the data corresponding to the first two years that were divided in eight annual quarters (Q_i). The division into annual quarters had the objective of analyse the persistence of the PCA results during the year. The annual analysis can hide seasonal changes, i.e., variability of the meteorological conditions. The last year was used to validate the results of PCA. After the selection of the monitoring sites that should be removed or replaced, the air pollutant concentrations at these places were estimated using the values measured at the remaining monitoring sites. The data were organized in such a way that each column had the hourly average concentrations of a specific air pollutant at a specific monitoring site. To be possible to apply the PCA, the air pollutant concentrations must be available at the same time in all monitoring sites. The data available for the analysis in 2003, 2004 and 2005 were, respectively: (i) 4897, 3532 and 4755 for NO_2; (ii) 4737, 4408 and 5869 for O_3; and (iii) 2534, 7492 and 1951 for PM_{10}. Concentrations were Z standardized to have zero mean and unit standard deviation.

4.3. Results and discussion

PCA was applied as a classification method to group monitoring sites with redundant measurements of air pollutant concentrations during the analysed period. The first step of PCA is the selection of the number of PCs. Kaiser criterion, which selects PCs with eigenvalues greater than 1, is commonly used for this purpose (Yidana et al., 2008); as this criterion does not usually achieve 90% of the original data variance (Mendiguchía et al., 2004; Pires et al., 2008a, 2008b), in this study, a different criterion was also used, aiming to select PCs representing at least 90% of the original data variance (ODV_{90}); this procedure allowed to

obtain more information about original variables contained in the selected PCs and to increase the confidence in the PCA results.

Table 4.1 shows, as an example, the main results of the PCA application for O_3 at all monitoring sites, during the third quarter of 2004. Considering eigenvalues greater than 1, only two PCs were selected, explaining 87.3% of the original data variance. The rotated factor loadings (achieved by varimax rotation algorithm) indicate the influence of each variable on the PCs. Liu et al. (2003) classified the influence of the original variables on each PC as strong, moderate and weak for absolute loading values >0.75, 0.5-0.75 and 0.3-0.5, respectively. However, this study uses a different classification for rotated factor loadings. Values in bold correspond to the greatest contributions of the variables on the PCs. Original variables with factor loadings in italic, corresponding to absolute values greater than 0.4, were also considered as having significant contributions. Therefore, PC1 had important contributions of AN, BV, CS, MT, PR, VC and VT sites; PC2 was heavily loaded by the contributions of LB and VR sites. Considering the ODV_{90} criterion, three PCs were selected. PC1 had important contributions of AN, BV,

Table 4.1 Main results of the PCA application for O_3 at all monitoring sites during the third quarter of 2004

	Kaiser criterion		**ODV_{90} criterion**		
Site	**PC1**	**PC2**	**PC1**	**PC2**	**PC3**
AN	**-0.875**	-0.252	*-0.403*	-0.240	**-0.840**
BV	**-0.911**	-0.183	*-0.455*	-0.169	**-0.836**
CS	**-0.934**	-0.219	*-0.628*	-0.205	**-0.698**
LB	-0.220	**-0.961**	-0.170	**-0.958**	-0.162
MT	**-0.874**	-0.160	**-0.758**	-0.146	*-0.481*
PR	**-0.898**	-0.220	**-0.819**	-0.206	*-0.455*
VR	-0.226	**-0.959**	-0.168	**-0.956**	-0.173
VC	**-0.881**	-0.254	**-0.836**	-0.239	*-0.415*
VT	**-0.882**	-0.188	*-0.549*	-0.175	**-0.703**
Eigenvalue	6.41	1.44	6.41	1.44	0.38
Variance (%)	71.2	16.1	71.2	16.1	4.2
Cumulative variance (%)	71.2	87.3	71.2	87.3	92.4

Values in bold correspond to the greatest contributions of the variables in the PCs; factor loadings with absolute values greater than 0.4 are presented in italic.

CS, MT, PR, VC and VT sites; PC2 was heavily loaded by the contributions of LB and VR sites; PC3 had important contributions of CS, MT, PR, VC and VT sites. This distribution is explained by the relative geographical location of the main emission sources to the monitoring sites and the topography of the region (Pires et al., 2008a, 2008b). The last one has a great impact on the air quality in LB and VR sites. As these monitoring sites are located in a region between two important valleys, they presented different pollution behaviour when compared to other regions in Oporto-MA.

Table 4.2 shows the number of PCs selected for each analysed period applying both criteria. Using Kaiser criterion, two PCs were considered in five (for O_3 and PM_{10}) and six (for NO_2) of the eight analysed periods. In all periods where two PCs were selected, the PC2 had important contributions of LB and VR sites, while PC1 was heavily loaded by the remaining sites. The percentage of the original data variance contained in the selected PCs using this criterion was always below 90%. Thus, the results obtained using ODV_{90} were considered with more confidence. The monitoring sites that had different air pollution behaviours in at least one of the analysed periods can not be removed. Thus, the number of monitoring sites that should be maintained corresponds to the maximum number of PCs achieved in all analysed periods using ODV_{90} criterion. Accordingly, using Kaiser criterion only two monitoring sites should be maintained for all air pollutants. Using ODV_{90}

Table 4.2 Number of PCs selected for each analysed period using the two criteria: Kaiser (left) and ODV_{90} criterion (right)

	Year	**Q_1**	**Q_2**	**Q_3**	**Q_4**
NO_2	2003	2 | 4	2 | 5	1 | 4	1 | 4
	2004	2 | 4	2 | 5[a]	2 | 5	2 | 4
O_3	2003	1 | 2	1 | 2	1 | 2[b]	2 | 3
	2004	2 | 3	2 | 3	2 | 3	2 | 3
PM_{10}	2003	1 | 5	1 | 6	1 | 6	2 | 5
	2004	2 | 5	2 | 7	2 | 6	2 | 6

(a) BV site was removed due to missing values; (b) LB site was removed due to missing values.

criterion, the number of monitoring sites needed to characterize the region was: (i) five for NO_2; (ii) three for O_3; and (iii) seven for PM_{10}. Using the last criterion, the number of monitoring sites for NO_2 and O_3 was in agreement with what was established by the legislation. However, for PM_{10}, Oporto-MA needed two more monitoring sites.

The sites to be maintained should be selected according to the following criteria: (i) sites should be representative, namely for monitoring of the highest pollutant concentrations; (ii) the number of pollutants being monitored at each site should be maximized; and (iii) the distribution should maximize distances between monitoring sites. Table 4.3 shows the relative frequency (in percentage) of each pair of monitoring sites that had important contributions in the same PC during the eight analysed periods (training period) using Kaiser (upper triangular matrix) and ODV_{90} criteria (lower triangular matrix). High frequencies (values in bold) means that the correspondent pair of monitoring sites often presented redundant measurements. Based on this information, the monitoring sites that presented high redundancy in the data were identified. The selection of the monitoring sites to be maintained or removed was performed considering the frequencies presented in Table 4.3 and the criteria referred above. Accordingly, considering Kaiser criterion, only two monitoring sites should be maintained for all analysed air pollutants. The selected monitoring sites were BV and LB. Considering ODV_{90} criterion, the sites that should be removed are: CS and VR for PM_{10}; CS, VR, AN and VT for NO_2; and CS, VR, AN, VT, MT and PR for O_3.

To validate the PCA results, air pollutant concentrations at the removed monitoring sites were estimated through statistical models using the values measured at other places in Oporto-MA. The performance of these models was evaluated using the data of the last year of the study period. Multiple linear regression (MLR) was applied with this aim and the input variables were selected according to Table 4.3. For example, NO_2 concentrations at CS site can be estimated using the NO_2 concentrations measured at BV if Kaiser criterion was

Table 4.3 Relative frequency (in percentage) of each pair of monitoring sites with important contributions in the same PC during the first two years of study (eight periods) using Kaiser criterion (upper triangular matrix) and ODV_{90} criterion (lower triangular matrix)

	AN	**BV**	**CS**	**LB**	**MT**	**PR**	**VR**	**VC**	**VT**
NO_2									
AN	-	**100**	**100**	50	**100**	**75**	50	**100**	**75**
BV	**88**	-	**100**	57	**100**	**86**	57	**100**	**86**
CS	**100**	**86**	-	50	**100**	**100**	50	**100**	**100**
LB	38	29	38	-	50	50	**100**	50	50
MT	**88**	**71**	**88**	38	-	**88**	50	**100**	**88**
PR	0	14	**100**	25	0	-	50	**88**	**100**
VR	38	43	38	**100**	38	13	-	50	50
VC	25	14	38	0	63	13	0	-	**88**
VT	**75**	**71**	**100**	38	63	**88**	38	25	-
O_3									
AN	-	**100**	**100**	29	**100**	**100**	38	**100**	**100**
BV	**100**	-	**100**	29	**100**	**100**	38	**100**	**100**
CS	**88**	**88**	-	29	**100**	**100**	38	**100**	**100**
LB	29	29	29	-	29	29	**100**	29	29
MT	**88**	**100**	**100**	29	-	**100**	38	**100**	**100**
PR	**88**	**75**	**100**	29	**100**	-	38	**100**	**100**
VR	38	38	38	**100**	38	38	-	38	38
VC	**88**	**88**	**100**	29	**100**	**100**	38	-	**100**
VT	**88**	**100**	**100**	29	**100**	**100**	38	**100**	-
PM_{10}									
AN	-	**100**	**100**	38	**100**	**100**	38	**100**	**100**
BV	63	-	**100**	38	**100**	**100**	38	**100**	**100**
CS	50	38	-	38	**100**	**100**	38	**100**	**100**
LB	0	13	38	-	38	38	**100**	38	38
MT	63	63	**88**	25	-	**100**	38	**100**	**100**
PR	13	13	13	0	25	-	38	**100**	**100**
VR	0	0	25	**100**	25	0	-	38	38
VC	0	0	0	0	13	13	0	-	**100**
VT	50	50	**100**	38	**75**	38	25	0	-

Values in bold correspond to relative frequencies greater or equal to 75%

considered or at BV, MT and PR sites if ODV_{90} criterion was considered. MLR models were determined with the data corresponding to the first two years of study (training period). Table 4.4 and 4.5 show all developed MLR models to estimate the air pollutant concentrations at all removed monitoring sites (with Z standardized input variables) attending to Kaiser and ODV_{90} criteria, respectively.

Table 4.4 MLR models used to estimate the air pollutant concentrations at all removed monitoring sites using the values measured at other sites in Oporto-MA for the Kaiser criterion

	Sites	MLR models
NO_2	AN	L1: AN = 45.9 + 19.8 × BV
	CS	L2: CS = 29.3 + 15.7 × BV
	MT	L3: MT = 47.7 + 15.7 × BV
	PR	L4: PR = 22.2 + 10.1 × BV
	VR	L5: VR = 33.6 + 18.2 × LB
	VC	L6: VC = 28.5 + 10.4 × BV
	VT	L7: VT = 22.7 + 13.2 × BV
O_3	AN	L8: AN = 29.1 + 21.5 × BV
	CS	L9: CS = 38.3 + 24.0 × BV
	MT	L10: MT = 32.0 + 20.2 × BV
	PR	L11: PR = 39.9 + 21.2 × BV
	VR	L12: VR = 35.3 + 25.5 × LB
	VC	L13: VC = 35.2 + 19.3 × BV
	VT	L14: VT = 38.5 + 21.5 × BV
PM_{10}	AN	L15: AN = 45.9 + 20.0 × BV
	CS	L16: CS = 40.3 + 21.7 × BV
	MT	L17: MT = 42.1 + 19.0 × BV
	PR	L18: PR = 43.9 + 16.0 × BV
	VR	L19: VR = 40.7 + 30.1 × LB
	VC	L20: VC = 54.8 + 17.1 × BV
	VT	L21: VT = 36.6 + 15.3 × BV

Table 4.5 MLR models used to estimate the air pollutant concentrations at all removed monitoring sites using the values measured at other sites in Oporto-MA for ODV_{90} criterion

	Sites	MLR models
NO_2	AN	M1: AN = 45.9 + 13.5 × BV + 10.5 × MT
	CS	M2: CS = 29.3 + 6.1 × BV + 8.0 × MT + 9.6 × PR
	VR	M3: VR = 33.6 + 18.2 × LB
	VT	M4: VT = 22.7 + 15.9 × PR
O_3	AN	M5: AN = 29.1 + 17.1 × BV + 5.8 × VC
	CS	M6: CS = 38.3 + 14.0 × BV + 13.1 × VC
	MT	M7: MT = 32.0 +10.5 × BV + 12.7 × VC
	PR	M8: PR = 39.9 + 22.8 × VC
	VR	M9: VR = 35.3 + 25.5 × LB
	VT	M10: VT = 38.5 + 12.3 × BV + 12.0 × VC
PM_{10}	CS	M11: CS = 40.3 + 16.9 × MT + 14.2 × VT
	VR	M12: VR = 40.7 + 30.1 × LB

The data corresponding to the last year of study were used to evaluate the performance of MLR models. The performance indexes used in this study were the Pearson correlation coefficient (R) and the index of agreement of second order (d_2). Figure 4.1 and 4.2 show the performance indexes of all MLR models in the (a) training and (b) test periods for Kaiser and ODV_{90} criteria, respectively. The models achieved with ODV_{90} criterion presented better performances. Considering this criterion, all models achieved good performances, which mean that the monitoring sites proposed by PCA were enough to infer the air pollutant concentrations at all monitored region. The air pollutant analysers corresponding to the redundant measurements can be installed in non-monitored regions, allowing the enlargement of the air quality monitoring network.

4.4. Conclusions

This study aims to apply PCA to evaluate redundant measurements in the air quality monitoring network of Oporto-MA. PCA was used to group the monitoring sites with redundant measurements. Two different criteria were used for selection of the number of PCs. ODV_{90} criterion had always more information about the original variables when compared with Kaiser criterion. According to the PCA results with ODV_{90} criterion, only five monitoring sites for NO_2, three for O_3 and seven for PM_{10} were needed to characterize the region. The number of monitoring sites for NO_2 and O_3 was in agreement with what was established by the legislation. However, for PM_{10}, Oporto-MA needed two more monitoring sites. To validate PCA results, MLR models were determined to estimate air pollutant concentrations at removed monitoring sites using the concentrations measured in the remaining monitoring sites. These models were applied to a year's data. The good performance obtained by the models showed that the monitoring sites selected by the procedure presented in this study were enough to infer the air pollutant concentrations in the region defined by the initial monitoring sites.

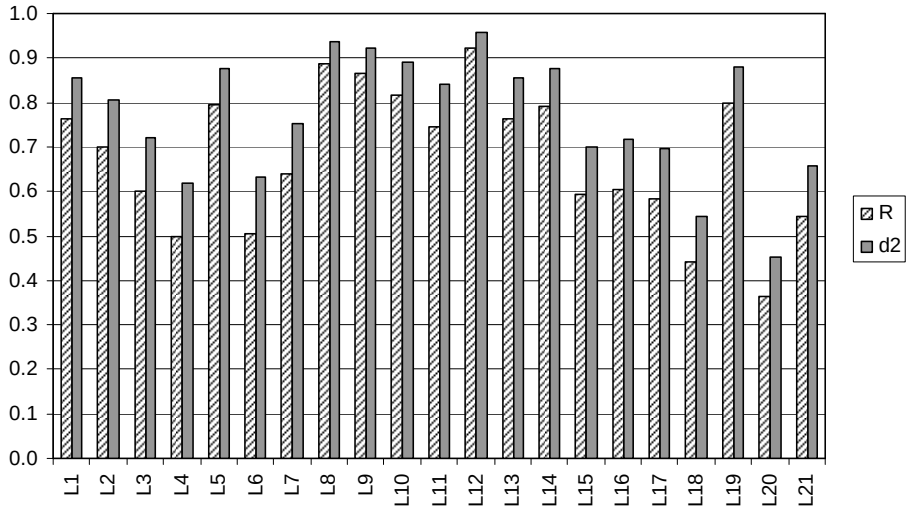

a

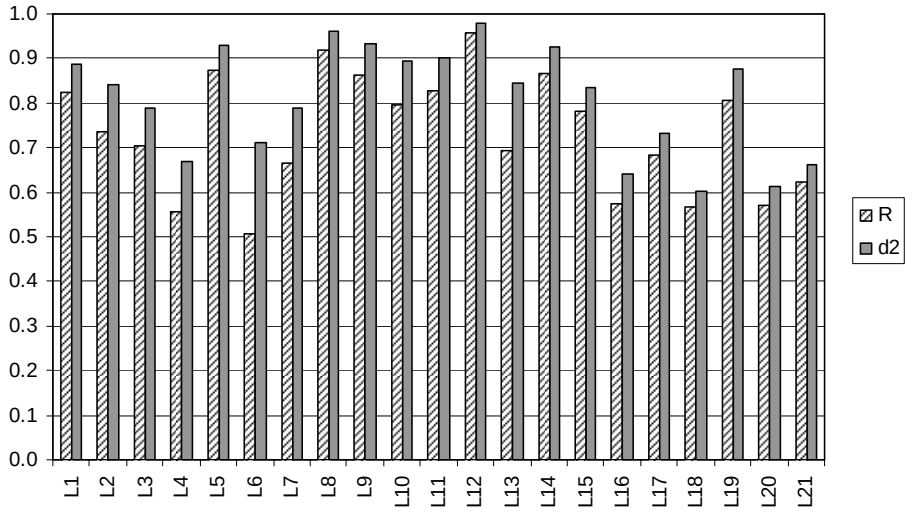

b

Figure 4.1 Performance indexes of all MLR models in the (a) training and (b) test periods for the Kaiser criterion.

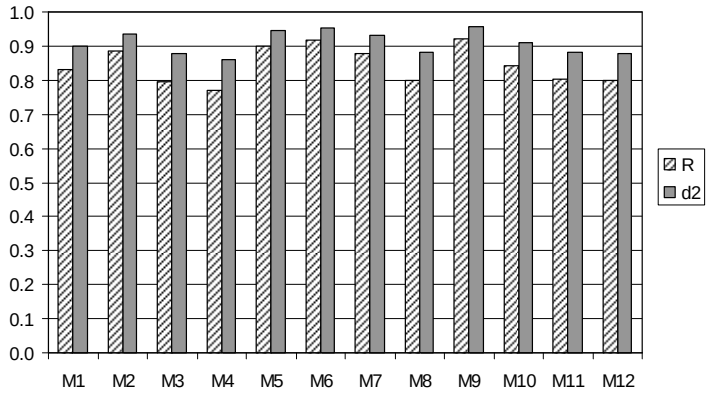

a

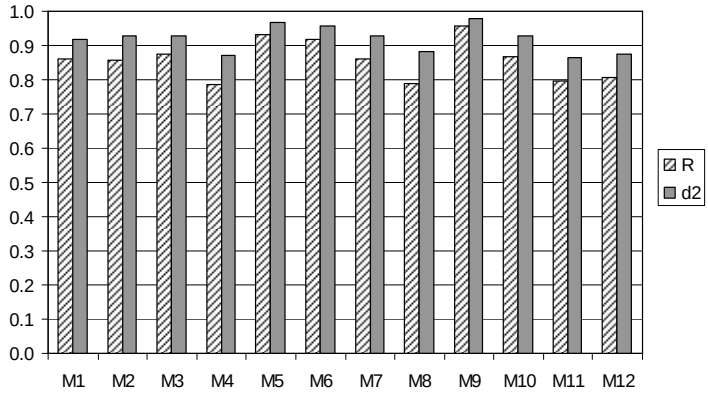

b

Figure 4.2 Performance indexes of all MLR models in the (a) training and (b) test periods for the ODV_{90} criterion.

Concluding, the air pollutant analysers corresponding to the redundant measurements can be installed in non-monitored regions, allowing the enlargement of the air quality monitoring network.

Part II

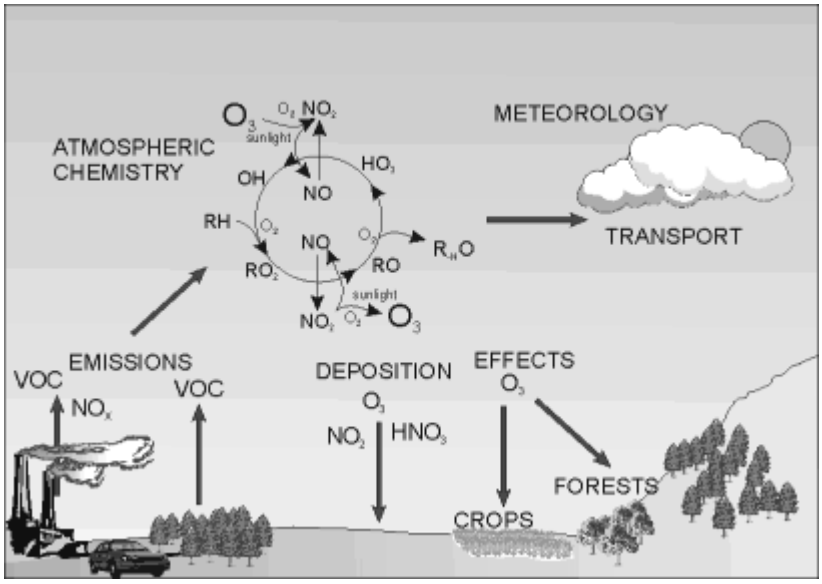

(from http://www.york.ac.uk/depts/eeem/gsp/esm/issues/ozone.htm)

Prediction of Air Pollutant Concentrations

Chapter 5

Prediction using statistical models

In last years, several statistical models were tested aiming the prediction of O_3 and PM_{10} concentrations. This chapter describes some of these studies. Additionally, the models applied in this thesis were briefly presented.

5.1. State of the art

Several studies can be found in literature aiming the prediction of O_3 and PM_{10} concentrations through statistical models. Prybutok et al. (2000) predicted the daily maximum O_3 concentrations using artificial neural networks (ANNs), multiple linear regression and autoregressive integrated moving average (ARIMA) models. The ANN model presented better performance.

Schlink et al. (2003) applied 15 different statistical techniques for ozone forecasting using ten data sets. This study was the only one found in the literature that applied artificial neural network quantile regression to the environmental field. However, the artificial neural network was determined using only the median regression and not taken into account all potentialities of the quantile regression.

Wang et al. (2003) developed an ANN model, which combines the adaptive radial basis function network with statistical characteristics of O_3 in selected specific areas, and is used to predict the daily maximum O_3 concentrations. The model was capable to predict successfully the daily maximum concentrations.

Baur et al. (2004) applied the linear quatile regression (QR) for the interpretation of nonlinear relationships between daily maximum hourly average ozone concentrations and meteorological variables. This study showed that the contributions of the explanatory variables in the O_3 concentrations vary significantly at different O_3 regimes. Additionally, linear QR model (with five quantiles) was compared with ordinary least-squares regression models in the prediction of O_3 concentrations presenting better performance indexes.

Heo and Kim (2004) tried to predict daily maximum O_3 concentrations at four monitoring sites using a fuzzy expert and ANN models. The developed models were able to correct themselves and presented reduced forecasting errors.

Dueñas et al. (2005) developed stochastic models, such as ARIMA, for urban and rural areas that turned out to be site specific. In both sampling points, predictions of hourly ozone concentrations agree reasonably well with measured values.

Sousa et al. (2006) compared the performances of multiple linear regression (MLR), feedforward ANN and time series in the prediction of the daily average O_3 concentrations. These models were also applied to urban and rural sites. MLR models showed good performance in the training step, but ANN presented better predictive performance.

Sousa et al. (2007) predicted next day hourly average O_3 concentrations through a new methodology based on feedforward ANNs using principal components as inputs. The performance of this model was compared with other approach on neural networks and with a linear model. The results showed that ANNs predict better than linear models.

Sousa et al. (2009) also compared MLR and QR approach for the prediction of the next day hourly average O_3 concentrations. Three different periods were applied: daylight, night time and all day. QR allowed more efficient previsions of extreme values which are very useful once the forecasting of higher concentrations is fundamental to develop strategies for protecting the public health.

Concerning the prediction of PM_{10} concentrations, Fuller et al. (2002) used an empirical model to forecast the concentrations of PM_{10} at background and roadside locations. The method was based on the regression analysis between PM_{10} and NO_x. The model accurately predicted daily mean PM_{10} concentrations but presented some limitations. For example, it depended of the existence of a consistent relationship between PM_{10} and NO_x emissions. As a conclusion of these studies, it was noted that the comparisons between linear and nonlinear models did not find significant differences in the results obtained by the different methodologies.

Perez and Reyes (2002) developed a neural network (nonlinear approach) to predict the maximum of the 24 h moving average of PM_{10} concentration on the next day. This method was compared with linear perceptron (linear approach) and presented slightly better performance.

Kukkonen et al. (2003) applied five ANN models, a linear statistical model and a deterministic modelling system for the prediction of urban NO_2 and PM_{10} concentrations. For both pollutants, ANN models presented better results than the other models.

Corani (2005) tried to predict this pollutant using feedforward ANNs, pruned neural networks (nonlinear approaches) and lazy learning (local linear modelling approach). Comparing these three methodologies, lazy learning presents slightly better results than the other methods.

Slini et al. (2006) applied classification and regression trees and ANN to forecast PM_{10} concentrations trends. Both methods presented good results, having the first one the best performance indexes.

Grivas and Chaloulakou (2006) applied ANN models to predict hourly average PM_{10} concentrations. The input variables were selected using a genetic algorithm procedure. The performance of these models was better than the one presented by MLR.

5.2. Models applied in this thesis

This thesis presented the development and application of some statistical models (linear and nonlinear) to predict the next day hourly average O_3 concentrations and the daily average PM_{10} concentrations in urban areas. The linear models applied with this aim were: (i) MLR; (ii) principal component regression (PCR); (iii) independent component regression (ICR); (iv) partial least squares regression (PLSR); and (v) QR. As far as it is known, no study had applied ICR for the prediction of O_3 or PM_{10} concentrations. Moreover, a method was presented to estimate the percentile of the predicted variable in QR. Considering the artificial neural networks, two step-by-step methodologies were applied to define these models, taking into account some limitations of these models. The last models are related to evolutionary algorithms. Genetic algorithms were applied to define threshold regression models to predict O_3 concentrations. Finally, genetic programming and multi-gene genetic programming were applied to predict O_3 and PM_{10} concentrations, respectively.

Chapter 6

Linear models

This chapter has the objective of evaluate the performance of five linear regression models in the prediction of the next day hourly average O_3 concentrations and the daily average PM_{10} concentrations. The selected models were: (i) multiple linear regression; (ii) principal component regression; (iii) independent component regression; (iv) partial least squares regression; and (v) quantile regression. The predictors were meteorological data (hourly/daily averages of temperature, relative humidity and wind speed) and environmental data (hourly/daily average concentrations of SO_2, CO, NO, NO_2, O_3 and PM_{10}) of the previous day collected in an urban site with traffic influences.

The contents of this chapter were adapted from: (i) Pires, J.C.M., Martins, F.G., Sousa, S.I.V., Alvim-Ferraz, M.C.M., Pereira, M.C., **2008**. Prediction of the Daily Mean PM_{10} Concentrations Using Linear Models. *American Journal of Environmental Sciences* 4 (5), 445-453; and (ii) Pires, J.C.M., Martins, F.G., Alvim-Ferraz, M.C.M., Pereira, M.C., **2009**. Comparison of several statistical models to predict O_3 concentrations. *Submitted for publication.*

6.1. Multiple linear regression

Multiple linear regression (MLR) is an extension of the simple linear regression model for data with multiple predictor variables and one outcome. Thus, this statistical model assumes that the best approach to estimate the dependent variable **y** from the explanatory variables **X** is to find the linear combination of these variables that minimizes the errors in reproducing **y**. This relationship is given by:

$$\mathbf{y} = \mathbf{Xb} + \mathbf{e} \tag{6.1}$$

where **b** is the vector of the regression parameters and **e** is the vector of the errors associated to MLR model, which are normally distributed with zero mean and constant variance σ^2 (Agirre-Basurko et al., 2006; Pires et al, 2008c). A common method for estimating the regression parameters is the ordinary least squares. This method obtains the parameters' estimates by minimizing the sum of the squared errors (SSE). The least squares estimate of **b** is given by:

$$\mathbf{b} = \left(\mathbf{X}^{\mathrm{T}}\mathbf{X}\right)^{-1}\mathbf{X}^{\mathrm{T}}\mathbf{y} \tag{6.2}$$

where the superscripts $^{\mathrm{T}}$ and $^{-1}$ refer to the transpose and inverse matrix operations, respectively.

Collinearity is a serious problem of MLR, which means the redundancy in the set of the variables, i.e., the predictors are correlated to each other. It has several consequences: (i) problems in the determination of the regression parameters; and (ii) wrong interpretations of the achieved models (Pires et al., 2008c). The regression parameters are obtained through the Equation 6.2, depending on the inverse of the matrix product. If a strong collinearity exists, this product is singular (Sundberg, 2000). Thus, it does not have a unique inverse and, consequently, there is infinity of solutions for the regression parameters. Moreover, in the presence of collinearity, the standard errors of the regression parameters tend to be large and, consequently, their confidence intervals tend to be very wide. In that case, the test of the hypothesis that the regression parameter is equal to zero against the alternative that it is not equal to zero leads to a failure to reject the null hypothesis (Eberly, 2007). Thus, this regression parameter is considered statistically insignificant and no linear relationship is established between the dependent and the independent variable. Additionally, as the confidence intervals are so wide, excluding a variable (or adding a new one) can change the regression parameters dramatically. Thus, magnitudes and possible directions (signs) of the regression parameters may change depending on which predictors are included in the model.

For this reason, it is always good to verify if the magnitude and a direction of the regression parameter has meaning in the context of the study (Pires et al., 2008c).

In this study, two statistical methods were applied to remove the collinearity between the explanatory variables: (i) principal component analysis (PCA); and (ii) independent component analysis (ICA). The variables created by these linear transformations, called principal components (PCs) and independent components (ICs), are uncorrelated to each other.

6.2. Principal component regression

Principal component analysis (PCA) is mathematically defined as an orthogonal linear transformation that modifies the original data to a new coordinate system such that the greatest variance by any projection of the data comes to lie on the first coordinate (called the first principal component), the second greatest variance on the second coordinate, and so on (Pires et al., 2008a, 2008b). Thus, the PCs are orthogonal and uncorrelated to each other, being determined by linear combinations of the original variables. The directions of the new coordinate axes are given by the eigenvectors of the covariance matrix of the original variables. The magnitude of the eigenvalues corresponds to the variance of the data along the eigenvector direction.

PCs are dependent on the units used to measure the original variables as well as on the range of values they assume. Thus, the data should be standardized before applying PCA. A common standardization method is to transform all the data to have zero mean and unit standard deviation. After the standardization of the original data, the covariance matrix is determined. The eigenvalues are calculated from the following equation (Çamdevýren et al., 2005, Sousa et al., 2007):

$$\left|\mathbf{Cov} - \lambda\mathbf{I}\right| = \mathbf{0} \tag{6.3}$$

where **Cov** is the covariance matrix, λ are the eigenvalues, **I** the identity matrix and **|…|** is the matrix determinant operator. The eigenvectors are calculated by:

$$(\mathbf{C} - \lambda\mathbf{I})\mathbf{V} = \mathbf{0} \tag{6.4}$$

where **V** is the matrix of the weights (or eigenvectors). The PCs are then obtained, multiplying the original data set by the weights.

Varimax rotation is the most widely employed orthogonal rotation in PCA, because it tends to produce simplification of the unrotated loadings to easier interpretation of the results. It simplifies the loadings by rigidly rotating the PC axes such that the variable projections (loadings) on each PC tend to be high or low. The interpretation simplicity of a specific PC is defined as the variance of its squared loadings (Harman, 1976):

$$s_p^2 = \frac{1}{n}\sum_{j=1}^{n}\left(b_{jp}^2\right)^2 - \frac{1}{n^2}\left(\sum_{j=1}^{n} b_{jp}^2\right)^2 \tag{6.5}$$

where n is the number of original variables and b_{jp} is the loading of the original variable j in the principal component p. If the variance is at maximum, the PC has the greatest interpretability. In this case, the loadings tend toward unit and zero. To rotate the loadings of all PCs, the sum of the variances of the squared loadings must be maximized:

$$s^2 = \sum_{p=1}^{m} s_p^2 = \frac{1}{n}\sum_{p=1}^{m}\sum_{j=1}^{n} b_{jp}^4 - \frac{1}{n^2}\sum_{p=1}^{m}\left(\sum_{j=1}^{n} b_{jp}^2\right)^2 \tag{6.6}$$

where m is the number of PCs. The procedure to maximize the variance is described in more detail by Harman (1976). After the rotation, the loadings show the relative contributions of the original variables on each PC.

The principal component regression (PCR) is a regression model that combines linear regression and PCA (Pires et al., 2008c). In the Equations 6.1 and 6.2, the matrix of the original variables **X** is replaced by the matrix of their PCs. Moreover, in the Equation 6.2, the inverse of the matrix product should cause no problem since the PCs are orthogonal. Therefore, PCR solves the inverse matrix problem: the collinearity.

6.3. Independent component regression

Independent component analysis (ICA) is a variant of PCA in which the components are assumed to be mutually statistically independent instead of merely uncorrelated. The uncorrelation is a weaker form of independence (Hyvärinen and Oja, 2000). For example, two random variables z_1 and z_2 are uncorrelated if their covariance is zero:

$$E\{z_1 z_2\} - E\{z_1\}E\{z_2\} = 0 \tag{6.7}$$

where *E{}* is the expectation function. Two variables are considered statistically independent if the value of one of them does not give any information on the value of the other variable. Moreover, the most important property of the independent random variables is given by:

$$E\{h_1(z_1)h_2(z_2)\} - E\{h_1(z_1)\}E\{h_2(z_2)\} = 0 \tag{6.8}$$

where $h_1()$ and $h_2()$ are two functions. Considering the Equations 6.7 and 6.8, the independent variables are always uncorrelated. On the other hand, the uncorrelation does not imply independence.

In the ICA model, the original variables are assumed to be linear combinations of latent variables. The aim of this procedure is to find these variables and how they are linearly mixed. Assuming a non-Gaussian distribution and mutual statistical independence, these latent variables are the ICs. ICA can be mathematically described as (Hyvärinen and Oja, 2000):

$$\mathbf{X} = \mathbf{AS} \tag{6.9}$$

where **X** is the matrix of the original variables, **S** is the matrix of the ICs and **A** is the unknown mixing matrix. The matrix of the ICs can be achieved by determining a matrix **M**, called unmixing matrix, such as:

$$\mathbf{S} = \mathbf{MX} \tag{6.10}$$

FastICA is a popular algorithm for ICA developed by Hyvärinen and Oja (2000). The algorithm is based on a fixed point iteration scheme maximizing non-Gaussianity as a measure of statistical independence. The FastICA procedure is described in detail by Hyvärinen and Oja (2000).

Independent component regression (ICR) is a method that combines linear regression and ICA. In the Equations 6.1 and 6.2, the matrix of the original variables **X** is replaced by the matrix of their ICs.

6.4. Partial least squares regression

Partial least squares regression (PLSR) is a statistical tool that has been designed to deal with MLR problems: (i) limited number of observations; (ii) missing data; and (iii) collinearity. This model can be used in situations where the use of traditional multivariate methods is severely limited, such as when there are fewer observations than predictor variables (Abdi, 2003; Wold et al., 2001). Moreover, it can be used to select suitable predictor variables and to identify outliers before the application of the classical linear regression. PCR is another method that can eliminate some predictor variables. For instance, this regression can be done using only the PCs having the corresponding eigenvalue greater than one (Kaiser criterion). The PCs are uncorrelated (that solves the multicollinearity problem), but the problem of choosing an optimum subset of predictors remains. Nothing guarantees that the PCs which represent the greatest variability of the original data **X** are also relevant for **y**. PLSR searches a set of orthogonal components, called latent vectors, that performs a simultaneous decomposition of **X** and **y** with the constraint that these components explain as much as possible the covariance between **X** and **y** (Abdi, 2003; Wold et al., 2001). The complete procedure is as follows (Abdi, 2003):

Step 1. Normalization of **X** and **y**: $\mathbf{X_0} = \mathbf{X}/\|\mathbf{X}\|$ and $\mathbf{y_0} = \mathbf{y}/\|\mathbf{y}\|$;

Step 2. Definition of the vector **u** with random values;

Step 3. Estimation of the **X** weights: $\mathbf{w} = \frac{\mathbf{X_k}^T\mathbf{u}}{\left\|\mathbf{X_k}^T\mathbf{u}\right\|}$;

Step 4. Estimation of the **X** factor scores: $\mathbf{t} = \frac{\mathbf{X_k}\mathbf{w}}{\left\|\mathbf{X_k}\mathbf{w}\right\|}$;

Step 5. Estimation of the **y** weights: $\mathbf{c} = \frac{\mathbf{y_k}^T\mathbf{t}}{\left\|\mathbf{y_k}^T\mathbf{t}\right\|}$;

Step 6. Estimation of the **y** factor scores: $\mathbf{u} = \mathbf{y_k}\mathbf{c}$;

Step 7. Repetition of the steps 3 to 6 until the convergence of **t**;

Step 8. Determination of the value of **b** used to predict **y** from **t**: $\mathbf{b} = \mathbf{t}^T\mathbf{u}$;

Step 9. Determination of the **X** factor loadings: $\mathbf{p} = \mathbf{X_k}^T\mathbf{t}$;

Step 10. Elimination of the effect of **t** from **X** and **y**: $\mathbf{X_{k+1}} = \mathbf{X_k} - \mathbf{tp}^T$ and $\mathbf{y_{k+1}} = \mathbf{y_k} - \mathbf{btc}^T$;

Step 11. Repetition of the steps 2 to 10 until the determination of a selected number of latent vectors.

All vectors **t**, **u**, **w**, **c** and **p** are stored in the columns of the correspondent matrices **T**, **U**, **W**, **C** and **P** and the scalar *b* is stored in the diagonal matrix **B**. The procedure is repeated till $\mathbf{X_k}$ become a null matrix which correspond that all latent variables were determined.

The prediction of the dependent variable is done by $\hat{\mathbf{y}} = \mathbf{TBC}^T = \mathbf{XB_{PLS}}$. If all latent variables are used, the results of PLSR are similar to that obtained by PCR.

6.5. Quantile regression

Quantile regression (QR) was introduced by Koenker and Bassett (1978) and can be seen as a natural extension of the least squares estimation of conditional mean models. This method presents some advantages when compared with ordinary least squares regression. For example, it allows the examination of the entire distribution of the variable of interest rather than a single measure of the central

tendency of its distribution. It can also provide information about any linear or nonlinear relationships between the dependent variable and the explanatory variables without an a priori knowledge of the type of (potential) non-linearities. Thus, it is more flexible to model data with heterogeneous conditional distribution. To describe the quantile function, a random variable *Y* with the distribution function *F(y)=p(Y≤y)* is considered. The quantile function *Q(τ)* with τ ∈ [0, 1] is defined as follows:

$$Q(\tau) = \inf\{y : F(y) \geq \tau\} \tag{6.11}$$

The median is *Q*(1/2), the first quartile is *Q*(1/4) and the first decile is *Q*(1/10). The median regression minimizes a sum of absolute errors. The remaining conditional quantile functions are estimated by minimizing an asymmetrically weighted sum of absolute errors:

$$\hat{Q}(\tau) = \arg\min_{a}\left\{\sum_{i:yi\geq a}\tau|y_i - a| + \sum_{i:yi<a}(1-\tau)|y_i - a|\right\} \tag{6.12}$$

Equation 6.13 presents a way to estimate the model parameters, considering quantile approach and the regression given by Equation 6.1:

$$\hat{b}(\tau) = \arg\min_{b(\tau)}\left\{\sum_{i:yi\geq \hat{y}_i}\tau|y_i - \hat{y}_i| + \sum_{i:yi<\hat{y}_i}(1-\tau)|y_i - \hat{y}_i|\right\} \tag{6.13}$$

6.6. Statistical significance of regression parameters

It is important to know which explanatory variables are relevant to predict the dependent variable. For the studied models, PLSR is the only one that includes this step in its procedure. For MLR, PCR and ICR, the significance of each regression parameter in the models was evaluated through the calculation of their confidence interval. The parameter $\hat{\beta}_i$ is valid if (Hayter et al. 2006; Pires et al., 2008c):

$$\left|\hat{\beta}_i\right| > \frac{t_{n-k-1}^{\alpha/2}\hat{\sigma}}{\sqrt{Sxx_i}} \tag{6.14}$$

where t is the Student t distribution, n is the number of points, k is the number of parameters, α is the significance level, $\hat{\sigma}$ is the standard deviation given by $\sqrt{SSE/(n-k-1)}$ and Sxx_i is the sum of squares related to x_i given by $\sum_{j=1}^{n}\left(x_{i,j}-\bar{x}_i\right)^2$.

For QR model, bootstrap estimates of standard error (significance level of 0.05) were calculated by randomly sampling each dataset with replacement (1000 times).

6.7. Performance indexes

The linear models were compared through the calculation of the following statistical parameters: mean bias error (MBE), mean absolute error (MAE), root mean squared error (RMSE), Pearson correlation coefficient (R) and index of agreement of second order (d_2), that are commonly referred in literature (Chaloulakou et al., 2003; Gardner and Dorling, 2000).

$$MBE = \frac{1}{n}\sum_{i=1}^{n}\left(\hat{Y}_i - Y_i\right) \tag{6.15}$$

$$MAE = \frac{1}{n}\sum_{i=1}^{n}\left|\hat{Y}_i - Y_i\right| \tag{6.16}$$

$$RMSE = \sqrt{\frac{1}{n}\sum_{i=1}^{n}\left(Y_i - \hat{Y}_i\right)^2} \tag{6.17}$$

$$R^2 = \frac{\sum_{i=1}^{n}\left(Y_i - \bar{Y}_i\right)^2 - \sum_{i=1}^{n}\left(Y_i - \hat{Y}_i\right)^2}{\sum_{i=1}^{n}\left(Y_i - \bar{Y}_i\right)^2} \tag{6.18}$$

$$d_2 = 1 - \frac{\sum_{i=1}^{n} \left(\hat{Y}_i - Y_i\right)^2}{\sum_{i=1}^{n} \left(\left|\hat{Y}_i - \overline{Y}\right| + \left|Y_i - \overline{Y}\right|\right)^2} \tag{6.19}$$

MBE indicates if the observed values are over or under estimated, with values closest to zero being desirable. MAE and RMSE measure residual errors, which give a global idea of the difference between the observed and the modelled values. Due to the power term, RMSE is more sensitive to extreme values than MAE. The lower values of these parameters reflect a better model in terms of its absolute deviation. These three performance indexes (MBE, MAE and RMSE) have the same units of the output variable Y_i. However, R and d_2 are dimensionless. R is a value that gives the quality of a least squares fitting to the original data. Its values are in the interval [0, 1], where values near 1 correspond to better models. The values of d_2 compare the difference between the mean, the predicted and the observed variables, indicating the degree of error free for the predictions. Higher values correspond to better models (Chaloulakou et al., 2003; Gardner and Dorling, 2000).

6.8. Data

This study aims to evaluate the performance of the five statistical models described above for predicting the next day hourly average O_3 concentrations and the daily average concentrations of PM_{10}. In both cases, meteorological and environmental variables were considered as predictors. The environmental data was collected in an urban site (*Matosinhos*) with traffic influences. The meteorological data was measured at *Serra do Pilar* on the left edge of Douro River at an altitude of 90 m approximately. These values are representative for all Oporto Metropolitan Area.

Considering the prediction of O_3 concentrations, the predictors were: (i) the hourly average concentrations of SO_2, CO, NO, NO_2 and O_3 of the previous day; and (ii)

hourly averages of air temperature (T), relative humidity (RH) and wind speed (WS) of the previous day. The analysed period was May and June 2003. The training period was May 2003 (403 data points); first two fortnights of June 2003 was the validation period (306 data points); and last two fortnights of June 2003 was the test period (340 data points).

Considering the prediction of PM_{10} concentrations, the predictors were: (i) the daily average concentrations of SO_2, CO, NO, NO_2 and PM_{10} of the previous day; and (ii) daily average of T, RH and WS of the previous day. Daily average values for these variables were calculated and used if more than 75% of hourly values were available. The analysed period was from January 2003 to December 2005. The training period was 2003 and the first three annual quarters of 2004 and 2005 (826 data points); the last annual quarter of 2004 was the validation period (88 data points); and the last annual quarter of 2005 was the test period (76 data points).

The training period was used to determine the model parameters. The PLSR and QR models are the only ones that required a validation period. In PLSR model, the validation period was used to calculate the number of latent variables. On the other hand, QR model need a validation period to apply the *k*-nearest neighbours (*k*-NN) algorithm. This algorithm was used to determine the number of *k*-NN needed to predict the percentile of the dependent variable in the test period. The test period was used to evaluate the performance of the achieved models when applied to new dataset. The explanatory variables were Z standardized to have zero mean and unit standard deviation.

6.9. Results and discussion

The MLR, PCR and ICR models were determined through subroutines in Visual Basic for Applications developed for Microsoft Excel, while PLSR and QR were achieved using Matlab 7.0 (MathWorks Inc., Natick, MA, USA). The statistical significance of regression parameters in MLR, PCR and ICR models was

evaluated through a t-test with significance level of 0.05. The final models were obtained evaluating all combinations of input variables and selecting the best one (corresponding to the lowest RMSE value) with the constraint that all regression parameters must be statistically significant (Pires et al., 2008c). On the other hand, for QR parameters, the bootstrap technique (with 1000 replacements) was applied to define the parameters' confidence intervals with the significance level of 0.05. As PLSR model considered only the latent variables important in the prediction of the dependent variable, no procedure was applied to evaluate the statistical significance of the regression parameters. Table 6.1 and 6.2 show the statistical significant regression parameters obtained for all linear models for O_3 and PM_{10}, respectively. The regression parameters **b** (i=1, 8) corresponded to SO_2, CO, NO, NO_2, T, RH, WS and O_3/PM_{10}, respectively, in MLR, PLSR and QR models. In PCR and ICR models, these regression parameters corresponded to PCi (i=1, 8) and ICi (i=1, 8). In these models, to be possible the interpretation in terms of the original variables their relationship with PCs and ICs must be also analysed. Table 6.3 presents the varimax rotated factor loadings that result from the application of PCA to the original data. Values in bold correspond to the main contributions of original variables on each PC. For O_3, PCi (i=1, 8) were heavily loaded by CO, WS, SO_2, T, O_3, RH, NO and NO_2, respectively. For PM_{10}, PC1 is heavily loaded by CO, NO and NO_2 and PC2 to PC6 had greater contributions of T, WS, SO_2, RH

Table 6.1 Regression parameters for all statistical models for O_3 concentrations prediction

	b(0)	**b(1)**	**b(2)**	**b(3)**	**b(4)**	**b(5)**	**b(6)**	**b(7)**	**b(8)**
MLR	51.35	2.05			-3.30	8.16		3.49	4.19
PCR	51.35		8.00			-3.67	4.29		
ICR	51.35	-4.22	3.90	-2.45	-5.87	-4.26	-8.91	3.29	2.21
PLSR		0.07	-0.08	0.01	-0.07	0.17	-0.14	0.14	0.20
QR (τ=0.1)	32.10			9.21	-14.69	24.41	7.07	5.35	
QR (τ=0.3)	49.15			5.55	-15.85	18.31		2.84	
QR (τ=0.5)	60.94		-5.73	8.14	-12.29	20.29	5.82	2.95	
QR (τ=0.7)	69.80		-9.40			12.84	1.50		
QR (τ=0.9)	80.33		-0.18						8.63

Table 6.2 Regression parameters for all statistical models for PM_{10} concentrations prediction

	b(0)	b(1)	b(2)	b(3)	b(4)	b(5)	b(6)	b(7)	b(8)
MLR	42.12		2.36		2.88	1.98	-2.74		10.82
PCR	42.12	7.35	4.35	1.41	4.82	4.87	5.19		
ICR	26.39	7.57		3.14		-2.95	1.65	2.49	3.19
PLSR		0.03	0.12	0.04	0.17	0.15	-0.18	0.01	0.33
QR (τ=0.1)	23.7		5.39			3.72	-3.50		4.6
QR (τ=0.3)	33.6					0.64	-2.73		12.3
QR (τ=0.5)	40.8					0.47	-2.41		15.7
QR (τ=0.7)	49.0				2.25		-2.32		16.3
QR (τ=0.9)	62.3				7.33				16.7

Table 6.3 Varimax rotated factor loadings

		PC1	PC2	PC3	PC4	PC5	PC6	PC7	PC8
O_3	**SO_2**	-0.060	0.003	**-0.971**	-0.149	-0.058	-0.114	0.076	-0.094
	CO	**-0.877**	-0.074	-0.064	-0.146	0.180	-0.037	0.327	-0.244
	NO	-0.415	0.027	-0.111	-0.120	0.227	-0.119	**0.827**	-0.225
	NO_2	-0.403	-0.131	-0.175	-0.190	0.231	-0.187	0.289	**-0.763**
	T	-0.149	0.066	-0.185	**-0.897**	-0.152	-0.293	0.102	-0.126
	RH	0.054	-0.241	0.157	0.347	0.191	**0.852**	-0.110	0.139
	WS	0.059	**0.966**	-0.001	-0.058	-0.168	-0.165	0.010	0.072
	O_3	0.194	0.221	-0.079	-0.169	**-0.884**	-0.181	-0.197	0.158
PM_{10}	**SO_2**	-0.171	0.159	-0.061	**0.960**	0.065	-0.121	-0.035	0.002
	CO	**-0.842**	-0.277	-0.176	0.020	0.050	-0.318	-0.008	-0.280
	NO	**-0.952**	-0.090	-0.132	0.162	-0.003	-0.144	0.034	0.139
	NO_2	**-0.742**	-0.014	-0.129	0.234	0.223	-0.355	-0.449	-0.004
	T	0.177	**0.957**	-0.033	0.160	0.132	-0.088	0.000	0.010
	RH	0.076	-0.127	-0.160	-0.065	**-0.967**	0.106	0.033	0.004
	WS	0.194	-0.031	**0.962**	-0.062	0.161	0.077	0.021	0.008
	PM_{10}	-0.440	0.129	-0.094	0.161	0.141	**-0.855**	-0.053	-0.011

Values in bold indicate the original variables that most influence each principal component.

and PM_{10}, respectively. Concerning the relation between the original variables and the ICs, Table 6.4 presents the correlation matrix between these variables for O_3 and PM_{10}. According to the information presented in the first four tables, all statistical models can be interpreted. Considering the prediction of O_3 concentrations, MLR considered that the variables that most influence the predicted O_3 concentrations were SO_2, NO_2, T, WS and O_3 of the previous day.

Table 6.4 Correlation matrix between the original variables and the IC for O_3 and PM_{10}

		IC1	IC2	IC3	IC4	IC5	IC6	IC7	IC8
O_3	**SO_2**	**-0.955**	-0.093	-0.007	-0.249	-0.011	0.020	0.117	-0.010
	CO	-0.010	-0.301	**0.753**	-0.458	-0.022	0.247	0.165	0.234
	NO	0.004	**-0.793**	0.299	-0.380	-0.137	0.193	0.305	0.230
	NO_2	-0.123	-0.266	0.162	**-0.696**	-0.027	**0.653**	0.250	0.157
	T	-0.175	-0.012	-0.071	**-0.703**	-0.028	-0.281	0.296	0.427
	RH	0.147	-0.013	0.184	0.469	0.291	0.185	**-0.728**	0.168
	WS	0.030	0.143	-0.120	0.108	**-0.922**	-0.278	0.149	0.099
	O_3	-0.134	0.280	-0.280	-0.266	-0.289	**-0.659**	-0.193	-0.414
PM_{10}	**SO_2**	0.329	0.038	0.012	-0.129	0.014	**0.923**	0.107	0.096
	CO	0.410	0.203	0.005	0.486	-0.244	0.003	0.288	**0.642**
	NO	0.428	0.146	0.041	0.195	0.138	0.110	0.235	**0.818**
	NO_2	**0.807**	0.170	0.167	0.228	0.027	0.128	0.323	0.346
	T	0.291	0.040	-0.053	**-0.901**	-0.235	0.120	-0.081	-0.152
	RH	**-0.521**	**0.776**	-0.011	0.102	0.212	0.010	-0.256	0.071
	WS	0.133	-0.543	-0.018	0.127	0.037	-0.065	**-0.798**	-0.172
	PM_{10}	**0.526**	0.141	**0.582**	0.010	-0.426	0.152	0.163	0.364

Values in bold correspond to significant correlation coefficients (absolute value greater than 0.5).

PCR selected RH, WS and O_3 concentrations as the important variables. ICR considered important all the predictive variables. QR is the model able to evaluate the influence of original variables in different ranges of O_3 concentration. Accordingly, the results showed that: (i) CO presented negative correlation for percentiles higher than 0.5; (ii) NO and WS presented positive correlation for percentiles lower than 0.5; (iii) NO_2 presented negative correlation percentiles lower than 0.5; (iv) T presented positive correlation for percentiles lower than 0.7; (v) RH presented positive correlation for percentiles 0.1, 0.5 and 0.7; and (vi) O_3 concentrations of the previous day was only statistically significant in the prediction of high O_3 concentrations. Considering the prediction of PM_{10} concentrations, MLR considered CO, NO_2, T, RH and PM_{10} of the previous day. PCR selected PC1 to PC6, which have important contributions of all original variables. ICR considered statistically significant the regression parameters corresponding to IC1, IC3 and IC5 to IC8. Thus, the original variables relevant for prediction of PM_{10} concentrations were: SO_2, CO, NO, NO_2, RH, WS and PM_{10}. QR considered RH and PM_{10} concentration as the most important explanatory

variables. CO concentration and T were important only in low values of τ, while NO_2 concentration was relevant in high values of τ.

The performance of the statistical models in the training and test periods was evaluated through the determination of the performance indexes referred above. Table 6.5 presents the performance indexes obtained in the training period. QR model presented better performances than the other statistical models, as it was the only one that analyse the entire distribution of predicted O_3 and PM_{10} concentrations. PLSR and QR models require a validation period to determine parameters needed for the test period. In PLSR model, the optimum number of latent variables corresponded to the minimum value of sum of squared errors in the validation dataset. Thus, the results showed that only one latent variable for O_3 and two for PM_{10} were needed. In QR model, a procedure must be applied to determine the percentile of a given test point using only the information available: the explanatory variables. The percentile was determined applying the *k*-nearest neighbour (*k*-NN) algorithm. This algorithm was used for classifying objects based on closest examples in the training data. It was based on the Euclidean distance between the correspondent validation point and the training points. The evaluation of the optimal value of *k* nearest training samples depends of the dataset. A good value of *k* can be achieved using cross-validation. The *k*-NN algorithm is as follows:

Step 1. Selection of the *k* value;

Step 2. Determination of *k* nearest training points from the validation point;

Step 3. Determination of percentile of O_3 concentration values correspondent to these training points;

Step 4. Application of the QR equations correspondent to these percentiles using the validation point; $\hat{y}_i = \hat{\beta}_0 + \sum_{i=1}^{k} \hat{\beta}_i x_i$

Step 5. Determination of the average of the *k* values of $\hat{y}_i$;

Step 6. Repetition of the steps 2 to 5 for all validation points;

Step 7. Determination of the error associated to the value of *k*, based on the difference of the average of the *k* values calculated above and the true values;

Step 8. Repetition of the steps 1 to 7 for different values of *k*;

Step 9. Determination of the lowest value of error associated to the optimal value of *k*.

For the test step, it was necessary 27 and 23 nearest points for prediction of the percentile of the test data for O_3 and PM_{10}, respectively.

Table 6.6 presents the performance indexes of the statistical models in the test period. PLSR presented better results, while QR failure the prediction of O_3 and PM_{10} concentrations.

Table 6.5 Performance indexes of the different statistical models for the training period

	Model	**R**	**MBE**	**MAE**	**RMSE**	**d_2**
O_3	**MLR**	0.49	0.00	18.0	22.2	0.62
	PCR	0.49	0.00	17.9	22.3	0.61
	ICR	0.50	0.00	17.9	22.1	0.62
	PLSR	0.48	1.22	18.0	22.4	0.63
	QR	0.56	5.08	15.7	21.1	0.82
PM_{10}	**MLR**	0.71	0.00	12.0	15.9	0.81
	PCR	0.71	0.00	12.0	15.9	0.81
	ICR	0.43	0.00	15.6	20.5	0.55
	PLSR	0.70	0.00	12.5	16.4	0.81
	QR	0.79	2.60	9.9	14.2	0.92

Table 6.6 Performance indexes of the different statistical models for the test period

	Model	**R**	**MBE**	**MAE**	**RMSE**	**d_2**
O_3	**MLR**	0.43	9.41	19.2	23.9	0.64
	PCR	0.41	1.21	19.2	24.1	0.62
	ICR	0.44	2.06	19.0	23.7	0.65
	PLSR	0.45	-10.48	18.7	23.7	0.65
	QR	-	1.76	25.2	30.1	0.60
PM_{10}	**MLR**	0.74	-1.12	12.7	18.4	0.83
	PCR	0.74	-0.90	12.7	18.4	0.84
	ICR	0.68	-1.90	14.0	20.2	0.71
	PLSR	0.75	-2.07	12.2	18.1	0.83
	QR	0.60	2.16	15.2	22.0	0.86

6.10. Conclusions

Five linear models were applied to predict the next day hourly average O_3 concentrations and the daily average PM_{10} concentrations, using as predictors environmental and meteorological data. At same time, the importance of each predictor in the air pollutants formation was analysed based on the statistically significant regression parameters for each model. QR model presented better performance in the training period, because it tries to model the entire distribution of the output value. However, it presented worst predictions in the test period. This means that a new procedure should be found better than *k*-NN algorithm to estimate the percentiles of the output variable in the test dataset with more precision. Concluding, the PLSR presented better predictive performance than the other linear models.

Chapter 7

Stepwise artificial neural networks

This chapter shows the comparison of two systematic methodologies to build artificial neural network models for predicting the hourly average of O_3 concentrations and the daily average of PM_{10} concentrations of the next day. They consist in: (i) adding hidden neurons one by one and (ii) adding input-to-hidden layer synapses one by one. Different types of input variables were tested: original variables, principal components and independent components. In addition, several activation functions were used for the hidden nodes: sigmoid, hyperbolic tangent and sine functions.

The contents of this chapter were adapted from: Pires, J.C.M., Martins, F.G., Alvim-Ferraz, M.C.M., Pereira, M.C., **2009**. Stepwise artificial neural networks for predicting tropospheric ozone and PM_{10} concentrations. *Submitted for publication*.

7.1. Introduction

The artificial neural networks (ANNs) are one of the most used nonlinear models for the prediction of O_3 (Heo and Kim, 2004; Sousa et al., 2006, 2007) and PM_{10} concentrations (Grivas and Chaloulakou, 2006; Perez and Reyes, 2002, 2006). ANN are adaptive statistical models inspired in the biological neural processing system (Tang et al., 2001; Tawadrous and Katsabanis, 2006). The artificial neurons of the networks are modelled attempting to mimic the performances of neural cells in the brain. The first mathematical approach of this method was done with the introduction of simplified neurons by McCulloch and Pitts in 1943 (Montague and Quartz, 1999; Tang et al., 2001; Tawadrous and Katsabanis, 2006). After a period of few applicability of these models, ANN only acquired great

importance in the field of statistical models with: (i) the introduction of the backpropagation algorithm in the learning step, and (ii) the development of new hardware which increased the processing capacities (Tawadrous and Katsabanis, 2006), really important for their application.

ANN can perform several functions such as classification, regression, association and mapping tasks (Corne, 1998; Perez and Reyes, 2002, 2006; Sousa et al., 2006, 2007). They are applied to a wide variety of problems including adaptive control, optimization, medical diagnosis, decision making, as well as in information, signal and speech processing (Gupta and Achenie, 2007; Nagy, 2007; Uncini, 2003). ANN models are characterized by: (i) a set of processing neurons (also designated by nodes); (ii) a pattern of connectivity among neurons; (iii) an activation function for each neuron; and (iv) a learning rule. The processing neurons are distributed in layers (Qingbin et al., 1996): (i) input layer (first layer); (ii) output layer (last layer); and (iii) hidden layers (layers between the input and the output layers). The neurons in different layers are linked by synapses (each one storing a weight value) and the way which these linkages are done defines the structure of the network. There are two main network topologies (Chiang et al., 2004; Pacella and Semeraro, 2007): (i) feedforward networks; and (ii) recurrent networks. In the first one, the information flows only feedforward, from input to output neurons. These networks do not present connections starting in outputs of neurons and ending in inputs of neurons in the same layer or previous layers (feedback connections). Recurrent networks derived from feedforward networks, presenting the two types of connections, the feedforward and the feedback (Arsie et al., 2006; Hu et al., 2007; Yang and Ni, 2005).

The neuron processes the information received by the inputs and calculates an output. An activation function is generally used in which the common functions are: (i) the pure linear; (ii) the sigmoid; and (iii) the hyperbolic tangent (Hernández-Caraballo and Marcó-Parra, 2003). However, many others can be also applied. Besides the inputs, a bias is also used in each processing neuron. Biases

are constant terms that are adapted by the learning rule (like the weight values). The output value of a neuron is given by:

$$y = f\left(\sum_{i=1}^{N} w_i x_i + \theta\right) \tag{7.1}$$

where y is the output value, $f()$ is the activation function, x_i is the input value, w_i is the weight value and θ is the bias.

The adaptation of the ANN weights to minimize the output error is called the training step. In this step, a learning rule must be implemented and the commonly used in ANN is the backpropagation algorithm (Chiang et al., 2004; Yamada et al., 2005). The errors for the neurons of the hidden layers are determined by backpropagating the errors of the output neurons. However, there are alternative algorithms which can be used in the training step. In this study, the modified Marquardt method (Edgar and Himmelblau, 1988) was used to evaluate the weight and bias values that correspond to the minimum value of error between the predicted and the observed output values. The performance of ANN models depends on several factors such as: (i) the learning rule and the number of iterations that influence the minimization of the error on the training step; (ii) the number of learning samples (important for the generalization of the ANN); and (iii) the number of hidden neurons which is influenced by the activation function associated to them.

One of the most important problems to overcome in the training step is the overfitting (Mi et al., 2005). During this step, the error is reduced due to the high number of iterations, but the obtained network usually presents a large error when applied to a new set. In this case, the network has not learned to generalize for new situations (Mi et al., 2005). A method commonly used to improve the generalization of a network is called early stopping (Nguyen et al., 2005; Özesmi et al., 2006). Using this technique, the available data should be divided into three sets (Chiang et al., 2004): (i) the training set, used for determining the network

weights and biases; (ii) the validation set, used to evaluate the performance of ANN during the training step (the increase of validation error stops the training process); and (iii) the test set, used to evaluate the ANN performance.

As it happens in the linear models, ANN is also influenced by the collinearity of the input variables. In this study, two different methods were used to remove the correlation between the original variables (OVs): (i) principal component analysis (PCA) and (ii) independent component analysis (ICA). These statistical methods were described in Chapter 6.

An additional problem to build ANN models is to achieve the adequate network complexity which includes the determination of the significance of each weight value in the network, as it is done for coefficients of linear regressions (Pires et al., 2008c), and the definition of the number of hidden neurons. In general there are two fundamentals to build ANN models (Ghiassi and Saidane, 2005; Medeiros et al., 2006; Rivals and Personnaz, 2003). The first one is called growing approach that begins with a simple network and iteratively adds hidden nodes and hidden layers. The second one is called pruning approach that begins with a large network with low training error and prunes the weights and biases whose removal increase the training error at least. After the removal, the network must be retrained to enhance its performance. Besides the weights, this method can prune also the neurons. The pruning of all input or output weights of a neuron is equivalent to prune the neuron itself.

7.2. Stepwise artificial neural networks

Stepwise artificial neural networks (SWANNs) are systematic methodologies to build ANN models in which it is not needed to define the structure in advance. The size of the ANN structures is determined during the training step. The two SWANNs here reported are based on feedforward neural networks with a single hidden layer. The first SWANN, designated by $SWANN_1$, corresponds to the addition of hidden neurons one by one. The second SWANN ($SWANN_2$) is based

in addition of input-to-hidden layer (IHL) synapses one by one. For both methodologies, the initial values of the weights and biases are selected in such a way that the initial network gives as output the average value of the training data (that corresponds to the simplest model), i.e., the bias linked to the output neuron has the output average of the training data as the initial value, the other biases were equal to one and the weight values were equal to zero.

Figure 7.1 (a to d) shows, as an example, the first three steps of $SWANN_1$ methodology and its final result (assuming the best model with three hidden neurons) for the case of three input neurons. The grey lines correspond to the parameters that are modified in the procedure. The black lines correspond to the final parameters. Using this methodology, the models with different number of hidden neurons are initialized with the same output value (the output average of the training set). Thus, all of these models present the same error values at the beginning. The iterative procedure starts with a network with single hidden neuron (Figure 7.1a). Then, the values of weights and bias were calculated. To obtain a generalized network, the increase of the validation error stops the training process (early stopping method). After, the Akaike Information Criterion (AIC) is determined based on the training set. This parameter is a measure of goodness of fit of a statistical model. The models can be ranked according their AIC. The one having the lowest AIC represents the best model. AIC is given by (Al-Rubaie et al., 2007):

$$AIC = (n)\ln\left(\frac{SSE}{n}\right) + 2k \tag{7.2}$$

where n is the number of data points, SSE is the sum of squared errors and k is the number of parameters (weight and bias values). The procedure is repeated adding hidden neurons one by one (Figure 7.1b-c). The optimal number of hidden neurons corresponds to the minimum value of AIC in the training set (Figure 7.1d). The procedure stops when the minimum value of AIC do not correspond to the last five added hidden neurons.

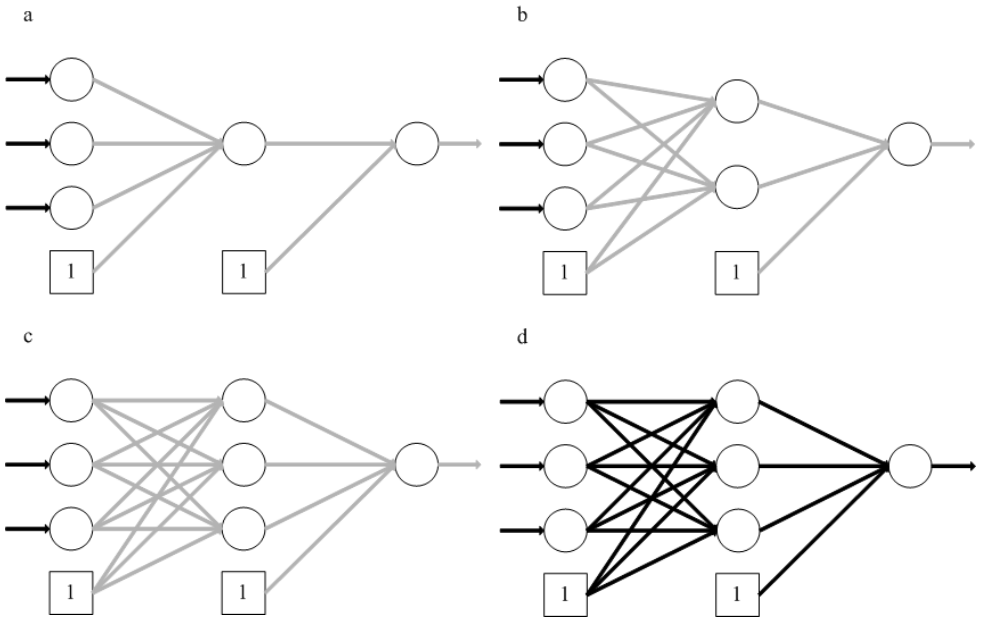

Figure 7.1 Example of the first three steps of $SWANN_1$ methodology (a-c) and its final result (d) for the case of three input neurons.

Figure 7.2 (a to f) shows, as an example, the first five steps of the $SWANN_2$ methodology and its final result (assuming the best model with five IHL synapses) for the case of three input neurons. In this methodology, the initial network (Figure 7.2a) contains a single hidden neuron and all weight values stored in the synapses linked to this neuron are equal to zero (designated here as the free hidden neuron). Thus, these synapses are considered inactive. Moreover, in each step, the $SWANN_2$ models must have always one free hidden neuron. In the initial network, the bias linked to the output neuron has the output average of the training set as the initial value, while the other biases are equal to one and the synapse weights are equal to zero (grey lines in Figure 7.2). The iterative procedure starts with the training of the weight values stored in an inactive IHL synapse and in the correspondent hidden-to-output layer (HOL) synapse. The two biases, one linked to the hidden neuron and other to the output neuron, are also trained. The training of only four parameters in each step is the main advantage of the $SWANN_2$

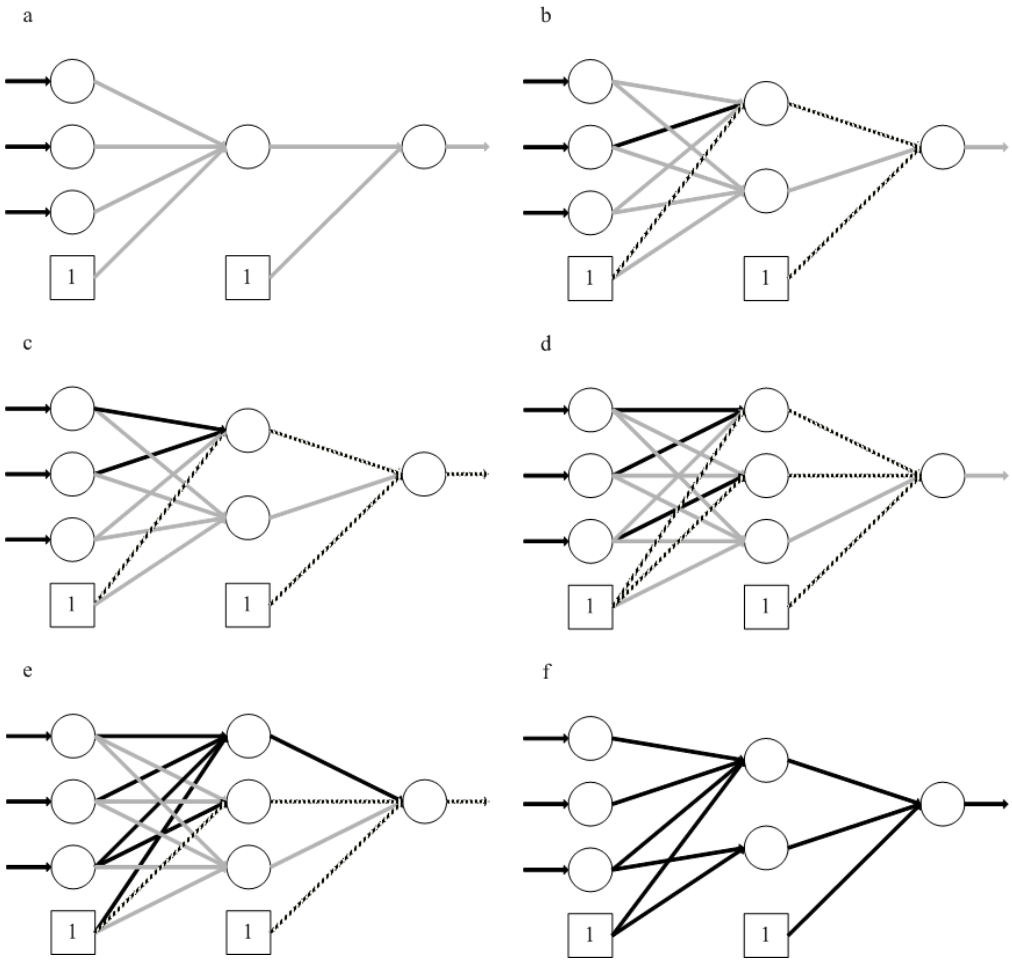

Figure 7.2 Example of the result of five steps of $SWANN_2$ methodology (a-e) and its final result (f) for the case of three input neurons.

methodology comparing to the previous one, which represents a significant reduction in computation time. The training step ends when the validation error starts to increase (early stopping method). This procedure is repeated for all inactive IHL synapses. The IHL synapse corresponding to the least validation error is then selected. The correspondent weight value is fixed for the following steps (black solid lines in Figure 7.2b-e). The calculated values of the HOL synapse weight and the biases are considered initial estimates for the following

steps (black dashed lines in Figures 7.2b-e). Moreover, if the selected synapse links an input neuron and the free hidden neuron, then one hidden neuron must be added (Figure 7.2b and 7.2d). The procedure is repeated, adding IHL synapses one by one. The optimal number of synapses corresponded to the minimum value of AIC in the training set. The procedure stops when the minimum value of AIC do not correspond to the last five IHL synapses.

The study reported in this chapter aims to compare the two systematic methodologies presented early to build ANN models for predicting the concentrations of two pollutants (O_3 and PM_{10}), using as inputs the OVs, the PCs and the ICs.

7.3. Data

The study aimed to predict the next day hourly average of O_3 concentrations and the daily average of PM_{10} concentrations with SWANN using environmental and meteorological data as inputs. The concentrations of pollutants (SO_2, CO, NO, NO_2, PM_{10} and O_3) were recorded in an urban site (*Matosinhos*). The meteorological data were the hourly averages of air temperature (T), relative humidity (RH) and wind speed (WS). For prediction of PM_{10} concentrations, daily averages for these variables were calculated only when at least 75% of hourly averages were available.

In the evaluation of the ANN models, the input variables were SO_2, CO, NO, NO_2, T, HR and WS. Additionally for prediction of O_3 and PM_{10} concentrations of the next day, the O_3 and PM_{10} concentrations were used as inputs, respectively. The period of measurements was from January 2003 to December 2005. Two different periods were studied for O_3 and PM_{10}, due to the different type of variables (hourly and daily average values, respectively) and the seasonal variations for both pollutants (O_3 usually presents high concentrations in summer). Thus, for O_3 concentrations, the training period was from May 2003 to August 2003 (2389 data points), the validation period was May 2004 (740 data points) and the test period

was June 2004 (periods when high O_3 concentrations are frequently measured; 715 data points). For PM_{10} concentrations, the forth quarter of 2004 was considered as validation period (88 data points), the corresponding period of 2005 (76 data points) as test period and the remained data from 2003 to 2005 as training period (826 data points). The explanatory variables were Z standardized to have zero mean and unit standard deviation.

7.4. Results and discussion

$SWANN_1$ and $SWANN_2$ were applied to predict O_3 and PM_{10} concentrations, using OVs, PCs and ICs as input variables. The PCs were determined using a subroutine developed in Microsoft Visual Basic Applications for Microsoft Excel created by the author of this thesis. The ICs were obtained using the FastICA package (available in http://www.cis.hut.fi/projects/ica/fastica/) for Matlab. The author of this thesis also developed the code in Matlab to achieve the $SWANN_1$ and $SWANN_2$ models. Different activation functions were also used: (i) sigmoid function (sig); (ii) hyperbolic tangent function (tgh); and (iii) sine function (sin). Figure 7.3 shows, as an example, the variation of AIC value in the training set with the increase of number of IHL synapses in $SWANN_2$ models, using OVs as inputs and the activation function sine. In this case, the minimum value of AIC

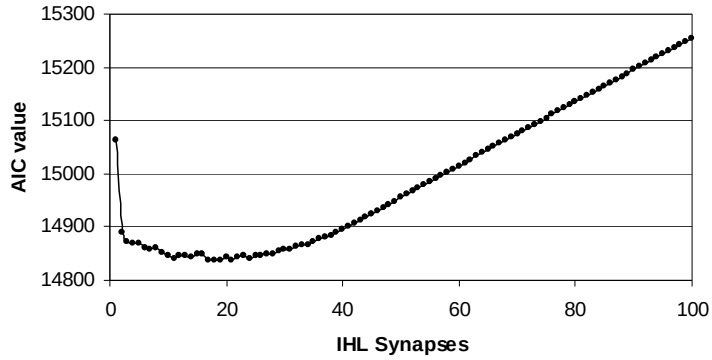

Figure 7.3 Variation of AIC value in the training set with the increase of the number of IHL synapses in $SWANN_2$ models using OVs as inputs and the activation function sine.

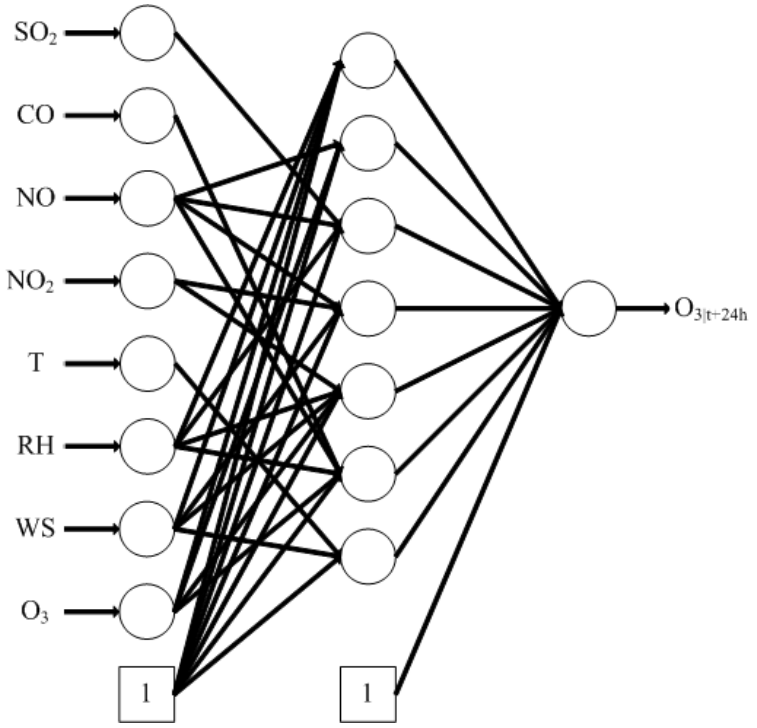

Figure 7.4 $SWANN_2$ model using OVs as inputs and the activation function sine.

corresponded to the addition of 21 IHL synapses. Figure 7.4 presents the final structure of the correspondent model. For this model, all input variables were considered important in the prediction of O_3 concentrations. Table 7.1 shows the number of hidden synapses, hidden neurons and parameters of the $SWANN_1$ and $SWANN_2$ models obtained for the different activation functions and type of input variables. The $SWANN_2$ models presented a significant reduction of the number of parameters, when compared with ANN models with the same number of hidden neurons. For example, an ANN model with 8 inputs and 11 hidden neurons have 111 parameters, while the $SWANN_2$ model using ICs as inputs and the activation function sigmoid only had 52 (less than 50% of the parameters).

The models determined in the training step were then applied to predict hourly average O_3 concentrations and daily average PM_{10} concentrations of the next day in their correspondent test sets. Table 7.2, 7.3 and 7.4 present the performance

indexes of the $SWANN_1$ and $SWANN_2$ models obtained in the training, validation and test periods, respectively (these performance indexes are described in Chapter 6). From the two methodologies here presented, no one overcame the other in both predictions of O_3 and PM_{10} concentrations. In the prediction of O_3 concentrations, $SWANN_2$ models presented, in general, better performances than $SWANN_1$

Table 7.1 Number of IHL synapses, hidden neurons and parameters presented by $SWANN_1$ and $SWANN_2$ models obtained for the different activation functions and type of input variables.

		O_3			**PM_{10}**		
		OVs	**PCs**	**ICs**	**OVs**	**PCs**	**ICs**
$SWANN_1$	sig	(32,4,41)	(8,1,11)	(8,1,11)	(48,6,61)	(56,7,71)	(8,1,11)
	tgh	(16,2,21)	(8,1,11)	(16,2,21)	(32,4,41)	(8,1,11)	(24,3,31)
	sin	(16,2,21)	(40,5,51)	(8,1,11)	(24,3,31)	(16,2,21)	(8,1,11)
$SWANN_2$	sig	(12,4,21)	(22,9,41)	(29,11,52)	(4,2,9)	(17,8,34)	(10,5,21)
	tgh	(18,7,33)	(19,5,30)	(24,8,41)	(6,3,13)	(12,8,29)	(4,3,11)
	sin	(21,7,36)	(35,9,54)	(23,9,42)	(4,2,9)	(5,2,10)	(8,3,15)

Table 7.2 Performance indexes of the $SWANN_1$ and $SWANN_2$ models in the training set for predicting O_3 and PM_{10} concentrations

		$SWANN_1$				**$SWANN_2$**			
		MBE	**MAE**	**RMSE**	**d_2**	**MBE**	**MAE**	**RMSE**	**d_2**
O_3	(OVs, sig)	0.12	17.6	21.9	0.69	0	17.8	22.1	0.68
	(OVs, tgh)	0.30	17.7	22.1	0.67	0.03	17.7	21.9	0.69
	(OVs, sin)	-0.01	17.8	22.1	0.68	-0.11	17.6	22.0	0.69
	(PCs, sig)	0.03	17.9	22.2	0.67	0.03	17.4	21.8	0.69
	(PCs, tgh)	0.02	17.9	22.3	0.67	0.04	17.5	21.9	0.70
	(PCs, sin)	0.29	17.3	21.7	0.69	0.00	17.2	21.6	0.71
	(ICs, sig)	-0.07	17.9	22.3	0.67	0.07	17.4	21.7	0.71
	(ICs, tgh)	-0.13	17.7	22.2	0.68	0.02	17.5	21.9	0.71
	(ICs, sin)	0	17.9	22.2	0.67	0	17.3	21.6	0.71
PM_{10}	(OVs, sig)	-0.28	11.8	15.7	0.82	-0.01	12.5	16.7	0.80
	(OVs, tgh)	-0.95	12.1	16.3	0.81	-0.31	12.4	16.4	0.81
	(OVs, sin)	-0.62	12.6	16.6	0.77	-0.03	12.0	16.1	0.82
	(PCs, sig)	0.42	11.7	15.4	0.84	-0.51	12.6	16.6	0.80
	(PCs, tgh)	0.15	12.2	16.1	0.81	3.33	13.7	17.5	0.78
	(PCs, sin)	0.01	11.9	15.8	0.83	-0.01	12.8	16.9	0.78
	(ICs, sig)	0	16.3	21.3	0.51	0.10	16.8	21.7	0.41
	(ICs, tgh)	-1.10	17.0	22.0	0.27	-0.02	17.1	22.0	0.32
	(ICs, sin)	-0.79	17.2	22.2	0.20	0	17.2	22.2	0.38

Table 7.3 Performance indexes of the $SWANN_1$ and $SWANN_2$ models in the validation set for predicting O_3 and PM_{10} concentrations

		$SWANN_1$				**$SWANN_2$**			
		MBE	**MAE**	**RMSE**	**d_2**	**MBE**	**MAE**	**RMSE**	**d_2**
O_3	(OVs, sig)	0.36	19.6	24.4	0.67	-0.54	19.1	24.0	0.70
	(OVs, tgh)	-0.58	19.8	24.8	0.67	-0.25	19.0	23.8	0.70
	(OVs, sin)	-0.88	19.3	24.3	0.68	-0.15	19.1	23.8	0.70
	(PCs, sig)	-0.59	19.5	24.5	0.68	-1.21	18.9	23.7	0.71
	(PCs, tgh)	-0.57	19.5	24.5	0.68	-0.91	18.8	23.8	0.71
	(PCs, sin)	0.55	20.1	24.9	0.65	-0.52	18.9	23.7	0.72
	(ICs, sig)	-0.72	19.5	24.5	0.68	-0.46	18.7	23.3	0.72
	(ICs, tgh)	-0.64	19.7	24.6	0.66	-0.38	19.0	23.8	0.71
	(ICs, sin)	-0.58	19.5	24.5	0.68	-0.04	18.8	23.3	0.73
PM_{10}	(OVs, sig)	0.53	11.2	13.7	0.77	0.55	11.0	14.0	0.79
	(OVs, tgh)	0.91	11.4	14.4	0.78	0.31	11.0	13.8	0.80
	(OVs, sin)	-0.40	11.3	14.0	0.75	0.28	11.1	14.1	0.77
	(PCs, sig)	0.68	10.9	13.7	0.80	0.19	10.6	13.1	0.80
	(PCs, tgh)	0.18	11.4	14.1	0.76	3.86	11.5	14.0	0.79
	(PCs, sin)	0.34	11.1	13.9	0.78	0.29	10.9	13.6	0.79
	(ICs, sig)	3.08	15.6	19.2	0.48	2.54	13.7	16.5	0.54
	(ICs, tgh)	1.57	14.9	18.2	0.31	1.85	14.4	17.2	0.38
	(ICs, sin)	2.27	15.4	18.4	0.21	2.89	13.6	16.3	0.54

Table 7.4 Performance indexes of the $SWANN_1$ and $SWANN_2$ models in the test set for predicting O_3 and PM_{10} concentrations

		$SWANN_1$				**$SWANN_2$**			
		MBE	**MAE**	**RMSE**	**d_2**	**MBE**	**MAE**	**RMSE**	**d_2**
O_3	(OVs, sig)	-0.11	17.6	22.0	0.73	-1.07	17.6	22.2	0.72
	(OVs, tgh)	0.17	18.4	22.6	0.69	-1.70	18.1	22.5	0.71
	(OVs, sin)	-0.66	18.0	22.2	0.71	-1.49	17.6	22.0	0.73
	(PCs, sig)	-0.23	17.7	22.0	0.72	-1.45	18.2	22.9	0.71
	(PCs, tgh)	-0.21	17.7	22.0	0.72	-1.23	18.1	22.6	0.71
	(PCs, sin)	-0.84	17.6	22.1	0.72	-2.00	17.9	22.6	0.73
	(ICs, sig)	-0.31	17.7	22.0	0.72	-1.72	17.5	22.1	0.74
	(ICs, tgh)	-0.22	17.6	21.9	0.73	-1.94	18.4	23.1	0.70
	(ICs, sin)	-0.31	17.7	22.0	0.72	-2.38	18.1	22.6	0.72
PM_{10}	(OVs, sig)	-1.94	13.7	20.1	0.75	-1.55	14.3	21.3	0.74
	(OVs, tgh)	-2.77	14.3	21.7	0.72	-2.26	13.9	20.9	0.75
	(OVs, sin)	-4.36	14.7	23.6	0.62	-2.00	13.7	21.2	0.74
	(PCs, sig)	-1.93	13.3	19.5	0.79	-2.77	13.5	20.6	0.74
	(PCs, tgh)	-2.15	13.4	20.5	0.74	0.21	13.1	19.9	0.77
	(PCs, sin)	-2.16	13.4	19.9	0.78	-3.00	14.5	22.4	0.68
	(ICs, sig)	-0.97	16.2	24.2	0.50	0.58	16.8	24.7	0.49
	(ICs, tgh)	-4.31	17.2	26.0	0.28	-0.94	17.1	25.2	0.37
	(ICs, sin)	-3.20	17.8	26.6	0.21	0.08	17.2	26.8	0.36

models. No significant differences were verified using the different input variables and activation functions. The sine function presented slightly better results in all sets comparing with the performance of the other activation functions. However, in the prediction of PM_{10} concentrations, $SWANN_1$ models generally presented better results than $SWANN_2$ models. The models using PCs as inputs and the activation function sigmoid obtained the best predictions. The artificial neural networks obtained using ICs as inputs presented the worst results for all sets. Figure 7.5 (a and b) shows, as an example, the predictions of O_3 and PM_{10} concentrations, respectively, using both methodologies (PCs and sine function for O_3; PCs and sigmoid function for PM_{10}). The models presented similar performances in the prediction of the air pollutants concentrations.

7.5. Conclusions

This study aims to predict O_3 and PM_{10} concentrations applying two systematic methodologies to build ANN models. Several input variables and activation functions were used. From the two methodologies here presented, no one overcame the other in both predictions of O_3 and PM_{10} concentrations. In the prediction of O_3 concentrations, the models achieved by $SWANN_2$ methodology presented better performances than the ones achieved by $SWANN_1$ methodology. The use of different input variables or activation functions did not present significant differences in the model performances. However, the application of the activation function sine presented slightly better results than the use of the other functions. In the prediction of PM_{10} concentrations, $SWANN_1$ models using PCs as inputs and the activation function sigmoid presented the best results. Moreover, the models that used ICs as inputs presented the worst results in all sets.

Although the models obtained with $SWANN_2$ methodology did not always present the best performances, this methodology should be used instead of $SWANN_1$. The ANN models obtained through this methodology were achieved in less time (due

to the optimization of few variables on each step) and consider only the important parameters in the prediction of the dependent variable.

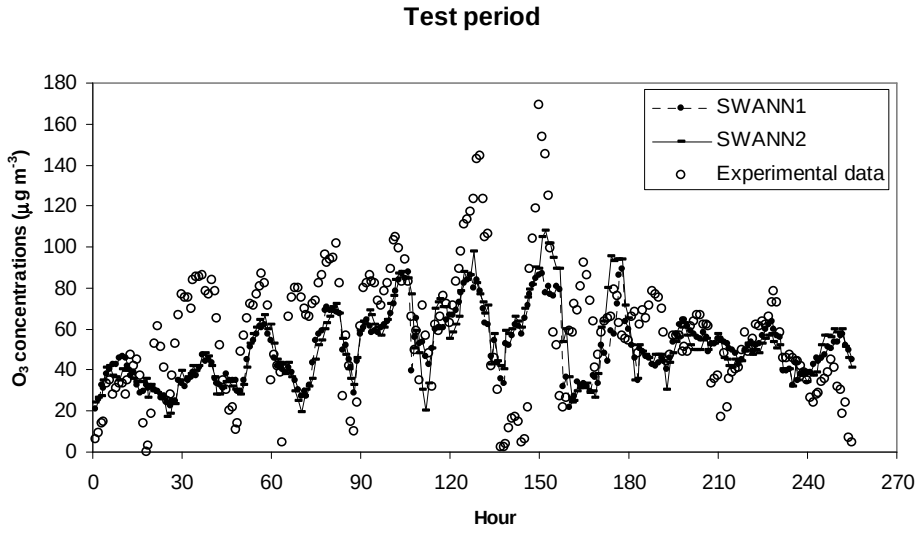

a

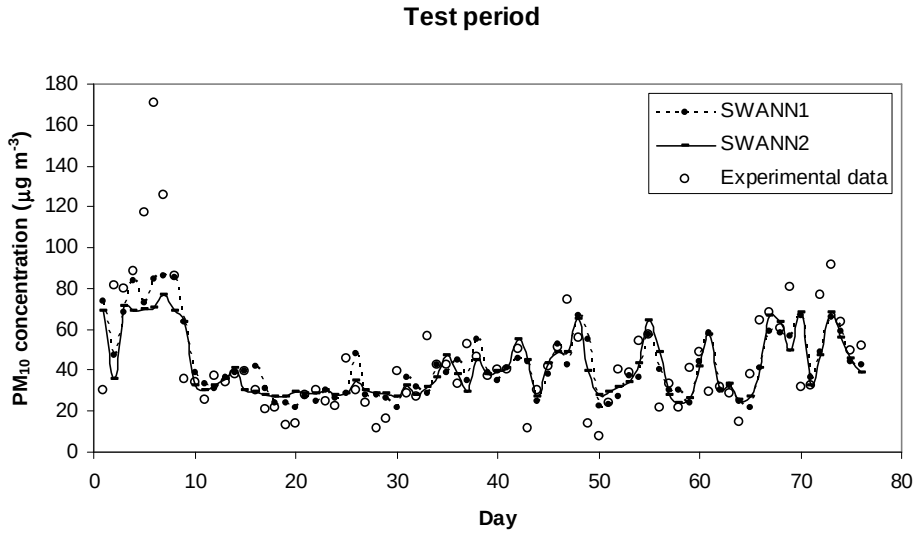

b

Figure 7.5 Example of the predictions of: (a) O_3 concentrations (with PCs and sine function); and (b) PM_{10} concentrations (with PCs and sigmoid function).

Chapter 8

Threshold regression models

This chapter proposes a new technique based on genetic algorithms to define threshold regression models (TR-GA). The threshold regression assumes that the behaviour of the dependent variable changes when it enters in a different regime. The change from one regime to another depends of a specific value (threshold value) of an explanatory variable (threshold variable). In this study, the threshold regression models were composed by two linear equations. The application of genetic algorithms allows evaluating, at the same time: (i) the threshold variable; (ii) the threshold value; and (iii) the statistically significant regression parameters in each regime. The aim of this study was to evaluate the performance of TR-GA models in the prediction of next day hourly average O_3 concentrations.

The contents of this chapter were adapted from: Pires, J.C.M., Martins, F.G., Alvim-Ferraz, M.C.M., Pereira, M.C., **2008**. Genetic Algorithm Based Technique for Defining Threshold Regression Models, *Proceedings of iEMSs 2008: International Congress on Environmental Modelling and Software*, 303-311.

8.1. Introduction

The threshold regression assumes that the behaviour of the dependent variable changes when it enters in a different regime (Terui and Dijk, 2002). The change from one regime to another depends of a specific value (threshold value) of an explanatory variable (threshold variable) (Fouquau et al., 2007). The dependent variable is given by:

$$y_i = \begin{cases} \hat{\alpha}_0 + \sum_{i=1}^{k} \hat{\alpha}_i x_i + \varepsilon_1, \; if \; x_d \leq r \\ \hat{\beta}_0 + \sum_{i=1}^{k} \hat{\beta}_i x_i + \varepsilon_2, \; if \; x_d > r \end{cases} \quad (8.1)$$

where x_i (i=1,…,k) are the explanatory variables, $\hat{\alpha}_i$ and $\hat{\beta}_i$ (i=0,…,k) are the regression parameters, ε_1 and ε_2 are the errors associated with the regressions, r is the threshold value and x_d is the threshold variable (one of the explanatory variables) that determines the division of the original data in two parts (Terui and Dijk, 2002). Multiple linear regression (MLR) was then applied to each part of the data and the regression parameters were determined through the minimization of the sum of squared errors (Pires et al., 2008c). In both regression equations, only the statistically significant regression parameters should be considered. The evaluation of statistical significance of the regression parameters was described in Chapter 6.

Genetic algorithms (GAs) were applied to the threshold regression model (TR-GA model), aiming to optimize the values of r (threshold value) and d (index of threshold variable) with the constraint of all regression parameters must be statistically significant. The main objective of this study was to evaluate the performance of TR-GA models in the prediction of the next day hourly average ozone ($O_{3|t+24h}$) concentrations.

8.2. Genetic algorithms and TR-GA procedure

GA is a search methodology based on the mechanics of natural selection and population genetics (Goldberg, 1989; Holland, 1975). This method starts with a set of individuals (the population) chosen randomly. These individuals (also called chromosomes) have genes that represent a solution of a given problem. GA generates a sequence of populations (the generations) by applying the genetic operators (selection, crossover and mutation) to the individuals. GA presents the following advantages: (i) optimization with continuous or discrete variables; (ii)

derivative function not necessary; (iii) dealing with a large number of variables; (iv) optimization of variables with extremely complex cost surfaces; and (v) providing a list of optimal solutions (not just a single solution). Even that, GA is not the best method to solve all the problems. For example, traditional methods quickly find the solution of a well behave convex analytical function with few variables, while GA is still evaluating the initial population (Haupt and Haupt, 2004). The optimizer should select the best method to solve the problem that has in hands. In this study, GA was selected due to the different type of parameters to optimize and the complexity of the constraints (ensure that all regression parameters are statistically significant).

The population size is the number of individual chromosomes that is presented in a population. A large number of chromosomes increases the population diversity, but it also increases the computation time due to the fitness evaluation step. Goldberg (1989) reported that the population size selected by many GA researchers usually ranges from 30 to 200. In this study, the population size was fixed to 100 chromosomes. Preliminary simulations showed that for this population size the number of generations should be high to achieve convergence. Thus, the number of generations was 500. Figure 8.1 shows the codification of chromosomes. Each chromosome was divided in four sub-strings that correspond to: (i) the value of d; (ii) the value of r; (iii) the explanatory variables used in the first regression (1 – consider the correspondent explanatory variable); and (iv) the explanatory variables used in the second regression (for $x_d > r$).

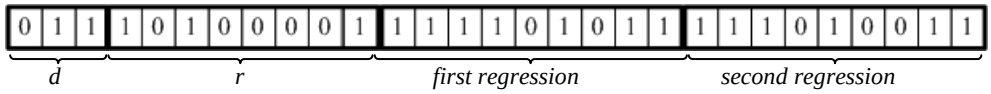

Figure 8.1 Codification of chromosomes.

The selection operator determines which chromosomes are used to generate the next population based on their fitness in the current generation (survival of the

fittest). The fitness function measures the performance of the individual with respect to the particular search problem. The fitness function was defined as:

$$\arg\min f = \sqrt{\frac{SSE_1 \times 10^{ip1} + SSE_2 \times 10^{ip2}}{nl}} \tag{8.2}$$

where *ip* is the number of statistically insignificant regression parameters and *nl* is the number of the training points. The indexes *1* and *2* correspond to the first and second regressions, respectively. In many selection methods, the best solutions can be not selected to reproduce. Therefore, these solutions can be lost after the application of crossover and mutation. To avoid this situation, the best elements were copied to the next generation (elitism). However, this procedure decreases the population diversity in the next generations. To reduce this effect, all the chromosomes in the current generation had equal probability to be chosen by crossover and mutation procedures.

The crossover operator consists in exchanging genetic material (binary substrings) of two parents (two chromosomes of the current generation), creating two new individuals. High crossover rates increase the population diversity, promoting the mixing of chromosomes (Siriwardene and Perera, 2006). The used crossover rate was 0.7.

The mutation operator consists in modifying the chromosomes at random. In bit string representation, the mutation is done by changing 0 to 1 and vice versa in one or more bits. High mutation rates increase the probability of destruction of the best chromosomes (Siriwardene and Perera, 2006). The used mutation rate was 0.1.

Figure 8.2 shows how GA is applied for defining threshold regression models. First, the initial population is randomly created. Then, for each individual in the population, the values of *r* and *d* must be calculated to divide the initial data in two parts. Applying MLR to each part (taking into account only the explanatory variables selected by the chromosome), the regression parameters are determined and also their statistical significance. After, the individual fitness is evaluated.

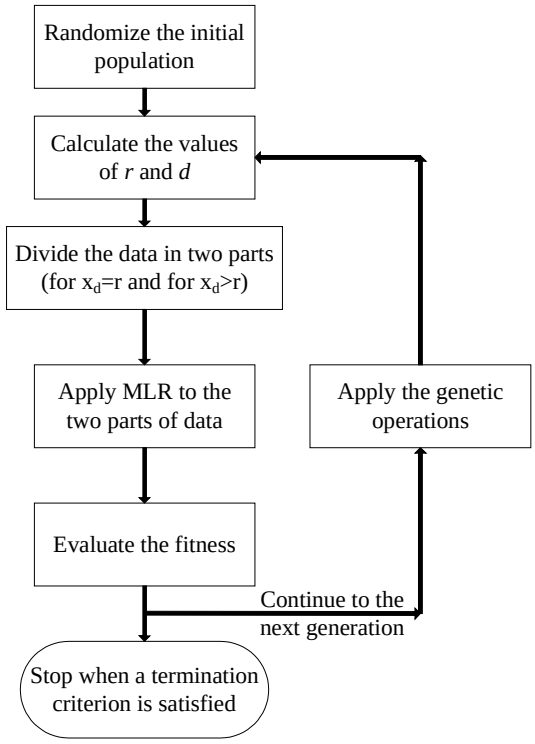

Figure 8.2 Procedure to apply GA for defining threshold regression models.

Finally, the genetic operators are applied to create new individuals in the next generation. This procedure stops when a stopping criterion is achieved (achievement of the maximum number of generations or a desired training error).

8.3. Data

MLR and TR-GA models developed to predict O_3 concentrations considered environmental and meteorological variables as inputs. The environmental data, hourly average concentrations of carbon monoxide (CO), nitrogen oxide (NO), nitrogen dioxide (NO_2) and O_3, were collected in an urban site (*Antas*) with traffic influences. The meteorological variables were temperature (T), solar radiation (SR), relative humidity (RH) and wind speed (WS). The analysed period was from May to July 2004. It was divided in the training (1 May 2004 to 15 July 2004) and test (16 to 31 July 2004) periods.

8.4. Results and discussion

Different TR-GA models were obtained corresponding to different threshold variables. As MLR was the model selected for each regression in TR-GA models, it was considered the basis for comparison for the achieved models. For all models, a t-test (with α=0.05) was performed to evaluate the statistical significance of the regression parameters. Table 8.1 presents the statistically significant regression parameters for TR-GA (M1 to M6) and MLR models and corresponding root mean squared error (RMSE) values in the training period. The regression parameters $\hat{\nu}_i$ (i=1 to 8) correspond to CO, NO, NO_2, T, SR, RH, WS and O_3, respectively ($\hat{\nu}_0$ is the Y intercept value). As all regression parameters were considered statistically significant, the fitness value (calculated in GA procedure) corresponded to the RMSE value in the training data. Therefore, all TR-GA models presented slightly better performances than MLR approach in the given period.

In almost TR-GA models, the MLR parameters were very similar (when validated at same time) to the parameters of the first regression of TR-GA models. Thus, the improvement of the achieved models was expected in the prediction of O_3 concentrations corresponding to their second regression.

For test period, the regression equations obtained in the training step were applied to predict the $O_{3|t+24h}$ concentrations. The performance of the models was evaluated through the calculation of the commonly used statistical indexes: mean bias error (MBE), mean absolute error (MAE), RMSE, Pearson correlation coefficient (R) and index of agreement of second order (d_2) (see Chapter 6). Table 8.2 shows the performance indexes presented by TR-GA and MLR models. MBE was always positive, showing that, in average, the predicted ozone concentrations were overestimated. The MAE, RMSE (absolute error measures), R and d_2 give a global idea of the difference between the observed and modelled values. Thus, slightly better model predictions were obtained in four TR-GA models when compared to

Table 8.1 Statistically significant regression parameters for TR-GA (M1 to M6) and MLR models and correspondent RMSE value in the training data

	$\hat{v}_0$	$\hat{v}_1$	$\hat{v}_2$	$\hat{v}_3$	$\hat{v}_4$	$\hat{v}_5$	$\hat{v}_6$	$\hat{v}_7$	$\hat{v}_8$		**RMSE**
M1	42.1	1.7	-4.1	8.5		3.6		3.2	17.8	$if\ T \leq 23.0$	19.9
	22.6	-8.3	8.5		22.4			5.3	9.0	$if\ T > 23.0$	
M2	43.5	2.1			4.5	2.4		4.5	15.1	$if\ RH \leq 82.0$	20.0
	26.8		-5.4	14.5		3.7	13.7		17.2	$if\ RH > 82.0$	
M3	41.2		-3.9	7.3		6.1		5.4	12.5	$if\ O_3 \leq 75.0$	20.0
	77.2		16.4		10.6					$if\ O_3 > 75.0$	
M4	43.7	2.6	-5.1	8.2		3.5	-5.3	3.0	14.2	$if\ NO_2 \leq 72.3$	20.1
	40.2	-6.9		6.9		5.1		8.4	6.0	$if\ NO_2 > 72.3$	
M5	12.5				8.4	5.3	-15.6	4.6	10.0	$if\ RH \leq 55.7$	20.1
	43.3	1.7	-3.8	7.0		3.3	-3.9	3.4	14.9	$if\ RH > 55.7$	
M6	57.5	23.9		5.4	4.9	2.2	-4.0	4.3	15.7	$if\ CO \leq 304.4$	20.1
	44.7		-2.8	4.3		3.1	-2.2	3.8	14.4	$if\ CO > 304.4$	
MLR	42.6		-2.2	5.3		3.9	-3.7	3.5	13.9		20.7

Table 8.2 Performance indexes of the TR-GA and MLR models in the test period

Model	**MBE**	**MAE**	**RMSE**	**R**	**d_2**
M1	0.31	15.42	19.66	0.74	0.83
M2	1.61	15.63	19.77	0.74	0.83
M3	0.81	15.92	20.68	0.71	0.81
M4	0.14	16.01	20.94	0.70	0.80
M5	0.43	15.51	19.98	0.73	0.81
M6	1.66	15.45	19.80	0.74	0.83
MLR	0.25	15.59	20.29	0.73	0.81

MLR. The TR-GA1 model presented the best results in both training and test periods. Figure 8.1 shows the codification of the correspondent chromosome. This model assumed that the $O_{3|t+24h}$ behaviour changed at the temperature of 23 ºC. For temperatures below 23 ºC, $O_{3|t+24h}$ depended on CO, NO, NO_2, SR, WS and O_3, while for higher values, it depended on CO, NO, T, WS and O_3.

The main differences of the regressions in M1 model were the incorporation of NO_2 concentrations and SR as important variables in O_3 formation for

temperatures below 23 ºC, being T only important for temperatures above this threshold value. These observations could be explained by the relative influence of volatile organic compounds (VOC) and nitrogen oxides (NO_x) in O_3 formation. Seinfeld and Pandis (1998) presented the complex chemical reactions involved in this system and showed that there is a competition between VOC and NO_x for the hydroxyl radical (OH), very important in the O_3 formation. At high VOC to NO_x ratio, OH reacts with VOC; otherwise, the NO_x reaction predominates. In general, increasing VOC concentrations means the appearance of more ozone. The effect of NO_x concentration increase depends on the VOC to NO_x ratio (positive correlation for high ratios and negative correlation for low ratios) (Seinfeld and Pandis, 1998). The temperature has a great influence on O_3 formation. High temperatures favour VOC to NO_x ratio because VOC concentrations increase more with temperature than NO_x concentrations. Accordingly, the results showed that temperature increase lead to higher O_3 concentrations (positive correlation between O_3 concentrations and temperature was observed in the second regression of M1). Simultaneously, as expected, a positive correlation between NO and O_3 concentrations was also observed. At lower temperatures, VOC to NO_x ratio decrease and O_3 concentrations are greatly dependent on NO_x concentrations. As the correspondent chemical reactions are catalysed by solar radiation (Seinfeld and Pandis, 1998), this variable was considered statistically significant in the first regression of M1, presenting a positive correlation with O_3 concentrations. Furthermore, as expected for lower VOC to NO_x ratio, a negative correlation between NO and O_3 concentrations was observed.

8.5. Conclusions

GA was applied to define threshold regression models for prediction of the next day hourly average O_3 concentrations. These models assume that the dependent variable changes its behaviour when an explanatory variable takes a specific value. Applying the procedure presented in this study, different TR-GA models were obtained corresponding to different threshold variables and threshold values. In

both training and test periods, four of these models presented slightly better results than MLR approach. Additionally, the best model showed that $O_{3|t+24h}$ changed its behaviour at the temperature of 23 ºC. For temperatures below that value, $O_{3|t+24h}$ depended of CO, NO, NO_2, SR, WS and O_3, while for higher temperatures, it depended of CO, NO, T, WS and O_3.

Chapter 9

Genetic Programming

This chapter shows how genetic programming can be applied to predict the next day hourly average O_3 concentrations. Due to the complexity of this problem, genetic programming is an adequate methodology as it can optimize, simultaneously, the structure of the model and its parameters. It is an artificial intelligence methodology that uses the same principles of the Darwinian Theory of Evolution. Genetic programming enables the automatic generation of mathematical expressions that are modified following an iterative process applying genetic operations.

The contents of this chapter were adapted from: Pires, J.C.M., Alvim-Ferraz, M.C.M., Pereira, M.C., Martins, F.G., **2009**. Prediction of Tropospheric Ozone Concentrations: Application of a Methodology Based on the Darwin's Theory of Evolution. *Submitted for publication.*

9.1. Introduction

The formation of O_3 is a complex, nonlinear, time and space varying process. Accordingly, several studies presented different statistical approaches to predict O_3 concentrations (Al-Alawi et al., 2008; Coman et al., 2008; Omidvari et al., 2008; Pires et al., 2008c; Sousa et al., 2006, 2007, 2009), including linear and nonlinear models. The applied linear models found in the literature were: (i) multiple linear regression; (ii) principal component regression; (iii) quantile regression; and (iv) time series. On the other hand, the most common nonlinear model was the artificial neural network. The selection of a model must consider some features, such as, complexity, flexibility, accuracy and speed of computation (Pires et al., 2008d). Artificial neural network models usually presented better

performance than the linear ones (Al-Alawi et al., 2008; Sousa et al., 2006, 2007) due to the nonlinearity behaviour associated to the O_3 formation. However, they are included in a group called black box models, having limited interpretation. Moreover, the selection of the optimal network architecture and the computation time are the main disadvantages of these models.

Besides the structure, the success of a statistical model depends of several factors: (i) the data size; (ii) the method to optimize their parameters; (iii) the input variables; and (iv) the collinearity between the input variables. The collinearity between the input variables can be eliminated through the application of principal component analysis (see Chapter 6).

As many factors could influence the performance of models, their development should have more degrees of freedom. For the models referred above, their structure is fixed in advance and only the parameters are optimized. In stochastic processes, such as the prediction of O_3 concentrations, the structure of the models should be more flexible. In this context, genetic programming (GP) could be a successful methodology, as it does not assume in advance any structure for the model. GP can optimize both the structure of the model and its parameters, simultaneously. As far as it is known, no study was published applying GP for predicting air pollutant concentrations. This study aims to predict the next day hourly average O_3 concentrations applying GP to the original input variables and their correspondent principal components.

9.2. Genetic programming

Genetic programming is an artificial intelligence methodology that uses principles of the Darwin's Theory of Evolution. Its search strategy is based on genetic algorithms (GAs) introduced by John Holland in the 1960s (Goldberg, 1989). GAs use bit strings as chromosomes and are commonly applied in function optimization. This algorithm has several disadvantages, for example, the length of the strings is static (Koza, 1992). Additionally, the size and the shape of the

model, solution of a given problem, are generally not known in advance. Similar to the GAs, the GP, introduced by John Koza in 1990s (Koza, 1992), is based on simple rules that imitate biological evolution. It is a good alternative for GA due to its valuable characteristics, such as the flexible variable-length solution representation. Moreover, GP enables the automatic generation of mathematical expressions. The expressions are represented as trees structures (see Figure 9.1), which contains functions as nodes and terminals as leafs. The terminals are the input variables and constants and the functions are all operators that are available to solve the problem (Grosman and Lewin, 2004; Koza, 1992; Tsakonas, 2006). There is specific syntax to create solutions in GP. For example, the addition operator must have at least two inputs and the exponential operator must have only one input. On the other hand, GAs have no grammar (Parkins and Nandi, 2004). Both methods (GAs and GP) use the genetic operations (selection, crossover and mutation). In selection, part of population (the fittest individuals) is retained and the remainder new generation is the result of crossover and mutation operations on the individuals of the actual population. In crossover, represented in Figure 9.2, two individuals are selected, their tree structures are divided at a randomly selected crossover point, and the resulting sub-trees are recombined to form two new individuals. In mutation, a random change is performed on a selected individual by substitution (Chen et al., 2008; Grosman and Lewin, 2004).

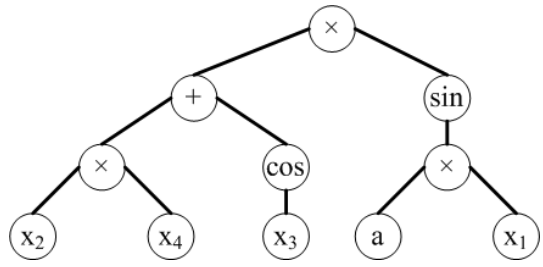

$$(x_2 \times x_4 + \cos(x_3)) \times \sin(a \times x_1)$$

Figure 9.1 Example of tree representation of expressions used in GP and respective formula.

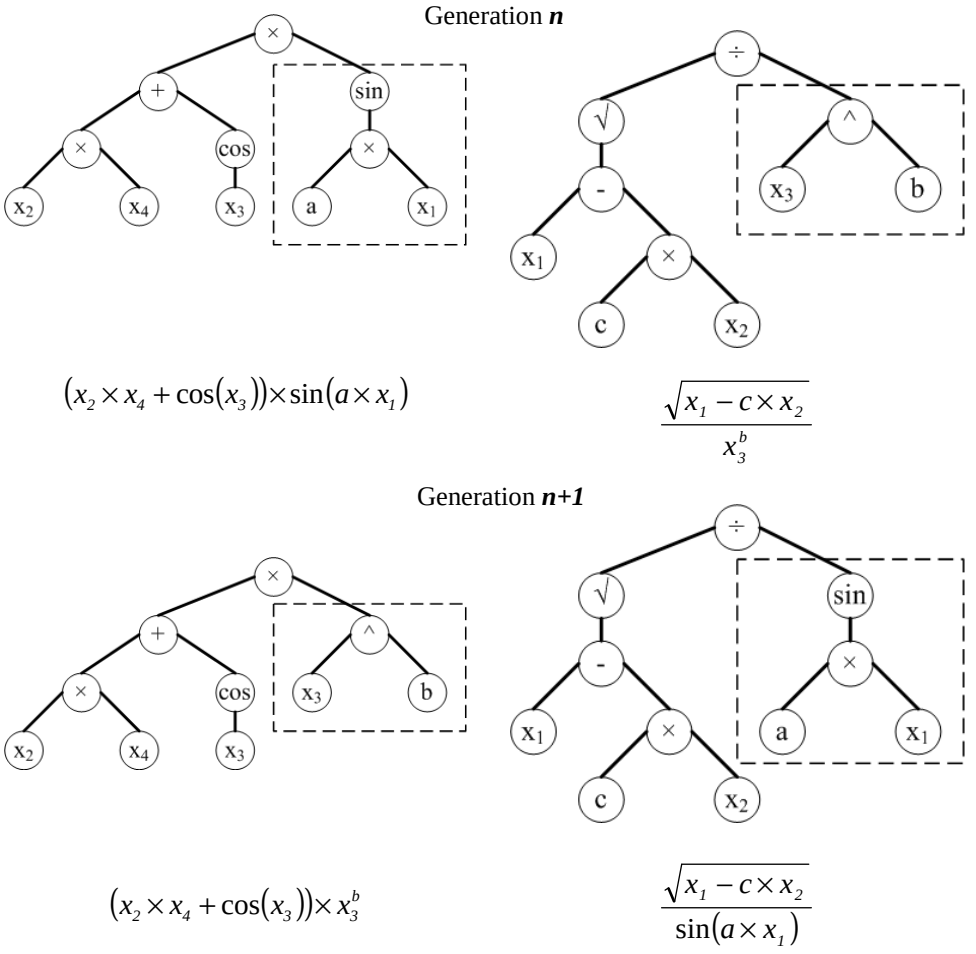

Figure 9.2 Example of crossover operation between two trees.

Figure 9.3 shows two examples of mutation operation. This genetic operation can change a functional group or a terminal.

In this study, several populations were considered at the same time. After the application of genetic operations to each population, migration of individuals between the populations was allowed. Populations which do not normally interact will have different combinations. Through this procedure, the migration will delay the individual convergence (Oussaidène et al., 1997). The constant creation of new combinations of individuals from different populations will have an important role

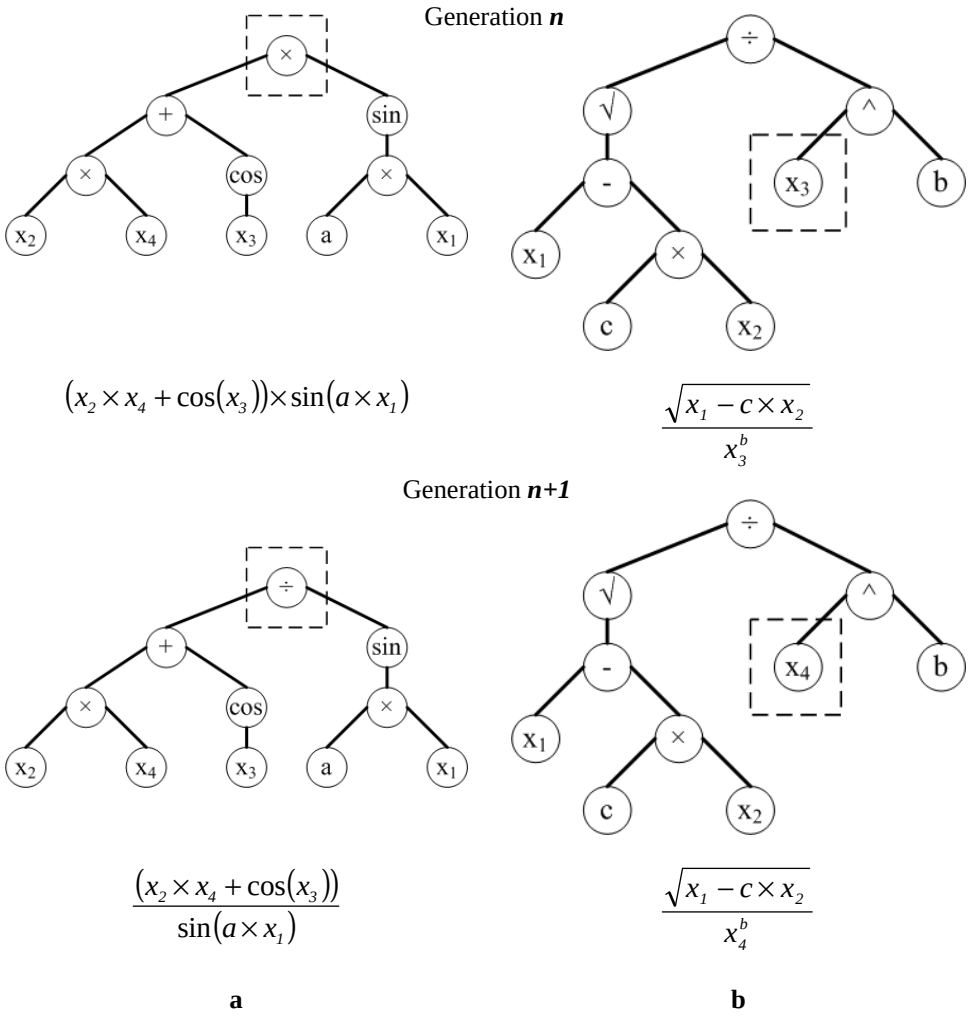

Figure 9.3 Examples of mutation operation in: (a) a function; and (b) a terminal.

for the achievement of the best solutions. For each population, it must be chosen different data to avoid premature convergence. The original data was resampled to create different data for each population. As a result of migration, the best individual could go to another population and it is possible that this individual will not be the best in the new population. In this case, the former population lost the best individual. To avoid this possibility in this study, the migration was not applied to the best individuals in each population, but to the other individuals that were randomly selected.

Figure 9.4 summarizes the GP procedure. The initial functions are created randomly. Then, each individual is evaluated through a fitness function, using the data set created for the correspondent population. The genetic operations are applied to all individuals and then the migration is applied. This iterative procedure finishes when a termination criterion (achievement of the maximum number of generations or a determined error defined in advance) is satisfied.

9.3. Data

The inputs of GP models were the hourly averages of air pollutant concentrations and meteorological variables measured 24 hours before. The atmospheric concentrations of carbon monoxide (CO), nitrogen oxide (NO), nitrogen dioxide

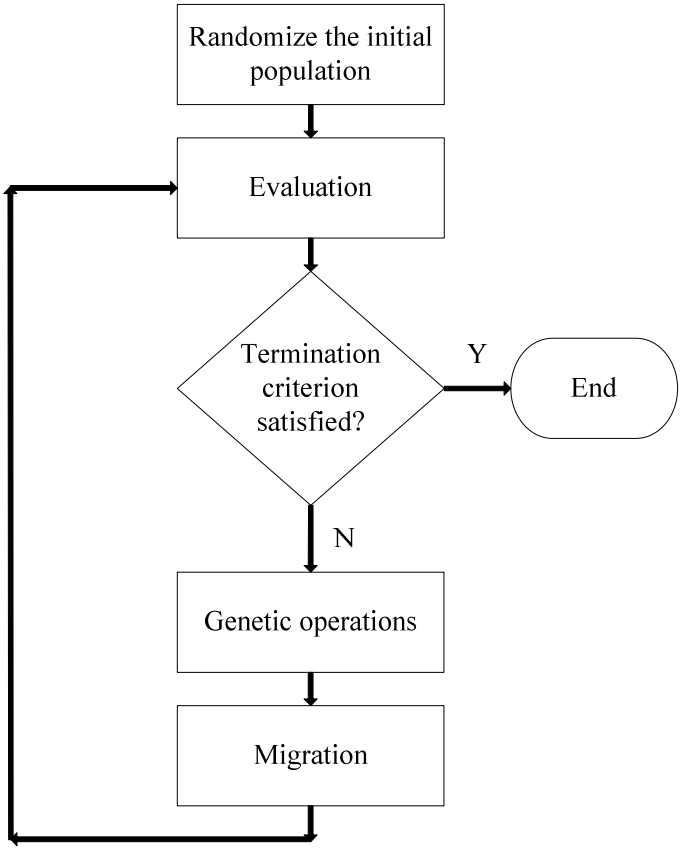

Figure 9.4 GP procedure.

(NO_2) and O_3, were collected in an urban site (*Antas*) with traffic influences. The meteorological variables were the hourly averages of air temperature (T), solar radiation (SR), relative humidity (RH) and wind speed (WS).

The analysed period was from May to July 2004. It was divided in the training (1 May 2004 to 15 July 2004 – 1443 data points) and test (16 to 31 July 2004 – 369 data points) periods. The data was Z standardized to have zero mean and unit standard variance.

9.4. Results and discussion

GP procedure was coded by the author of this thesis using Matlab 7.0 (MathWorks Inc., Natick, MA, USA). Table 9.1 shows the main control parameters of GP. The tree size is defined as the number of levels in the tree. For example, in Figure 9.1, the tree size is 4. The fittest individuals correspond to the ones that presented the lowest errors in the training step. As the results obtained by GP method are probabilistic, several runs should be made before taking conclusions. In this study, four different runs were done using 3, 4 and 5 populations at same time. GP models were determined using as inputs the original variables (OVs) and PCs.

Table 9.1 Values of GP control parameters

Parameter	Value
Population size	100
Number of populations	{3, 4, 5}
Maximum number of generations	100
Maximum initial tree size	7
Function set	+, -, ×, /, ^, √, sin, cos, tan, exp, log, sinh, cosh, tanh, sign
Terminal set	Input variables (OVs or PCs) and constants (0 to 9.9 with step of 0.1)
Selection method	Elitism
Crossover method	Random single point
Crossover rate	0.7
Mutation method	Random node or terminal replacement
Mutation rate	0.1
Migration method	Random selection of individuals
Migration rate	0.1

Table 9.2 shows the results of the varimax rotation on the eight PCs and the cumulative variance (in percentage). Values in bold correspond to the main contributions of the explanatory variables on each PC. Additionally, the loadings having an absolute value greater than 0.4, were also considered important (values in italic). Accordingly, the first PC (PC1) had important contributions of two meteorological variables (T and RH); PC2, PC3, PC4, PC5, PC6, PC7 and PC8 were heavily loaded by NO_2, SR, WS, O_3, CO, NO and RH, respectively.

Besides the ability of construction of a functional relationship between the output and the input variables, GP can also detect relevant input variables. Figure 9.5 shows the percentage of the occurrences of each input for the 4 GP runs in the best 20 individuals of the last generation using 3, 4 and 5 populations. Considering the occurrences greater than 50%, using OVs, the inputs considered relevant were T, RH and O_3. Using PC, the inputs most important were PC1, PC2 and PC5. The OV that have important contributions on the selected PC were T, RH, NO_2 and O_3. The importance of these variables can be justified by the photochemical formation of O_3 involving NO_x and VOC in which T and RH have important roles (Zolghadri et al., 2004). The presence in the models of O_3 concentrations measured on the previous day represents the accumulation from one day to another.

Table 9.2 Principal components varimax rotated loadings

	PC1	**PC2**	**PC3**	**PC4**	**PC5**	**PC6**	**PC7**	**PC8**
CO	-0.041	0.294	-0.016	0.134	0.113	**0.891**	0.292	0.031
NO	-0.100	0.278	0.086	0.102	0.183	0.315	**0.873**	0.029
NO_2	0.102	**0.896**	-0.043	0.150	0.096	0.291	0.256	-0.045
T	**0.948**	0.073	0.212	-0.099	-0.129	-0.031	-0.079	-0.132
SR	0.224	-0.036	**0.950**	-0.084	-0.154	-0.010	0.067	-0.099
RH	*-0.516*	-0.094	-0.250	0.281	0.371	0.053	0.048	**0.663**
WS	0.124	-0.141	0.087	**-0.937**	-0.208	-0.122	-0.090	-0.113
O_3	0.170	-0.111	0.178	-0.232	**-0.898**	-0.119	-0.177	-0.149
% Cumulative Variance	41.2	66.5	75.7	84.5	90.6	94.8	97.9	100.0

Values in bold indicate the variables that mostly influence the correspondent principal component.

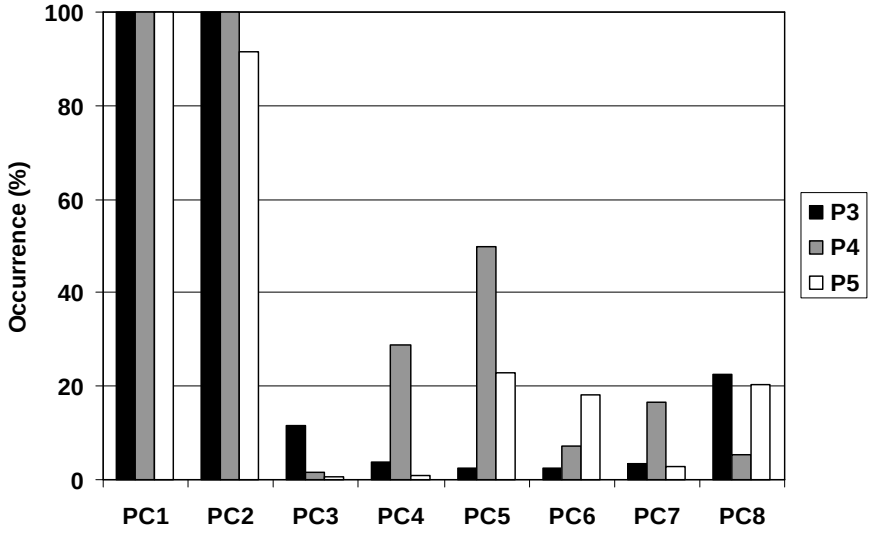

a

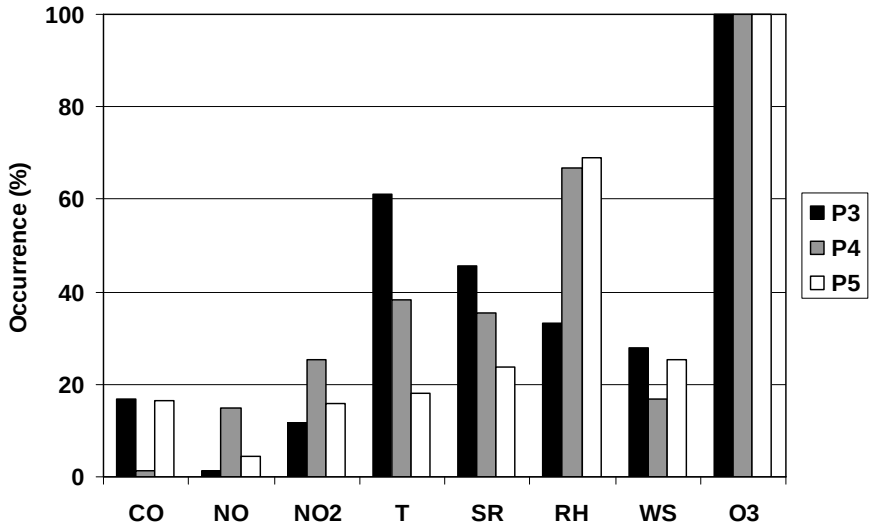

b

Figure 9.5 Occurrence (in percentage) of each input for the 4 GP runs in the 20 best solutions of the last generation using 3, 4 and 5 populations (P3, P4 and P5): (a) OV and (b) PC.

The GP models were obtained using the training set and their predictive performances were evaluated using a different set (test set). The selected

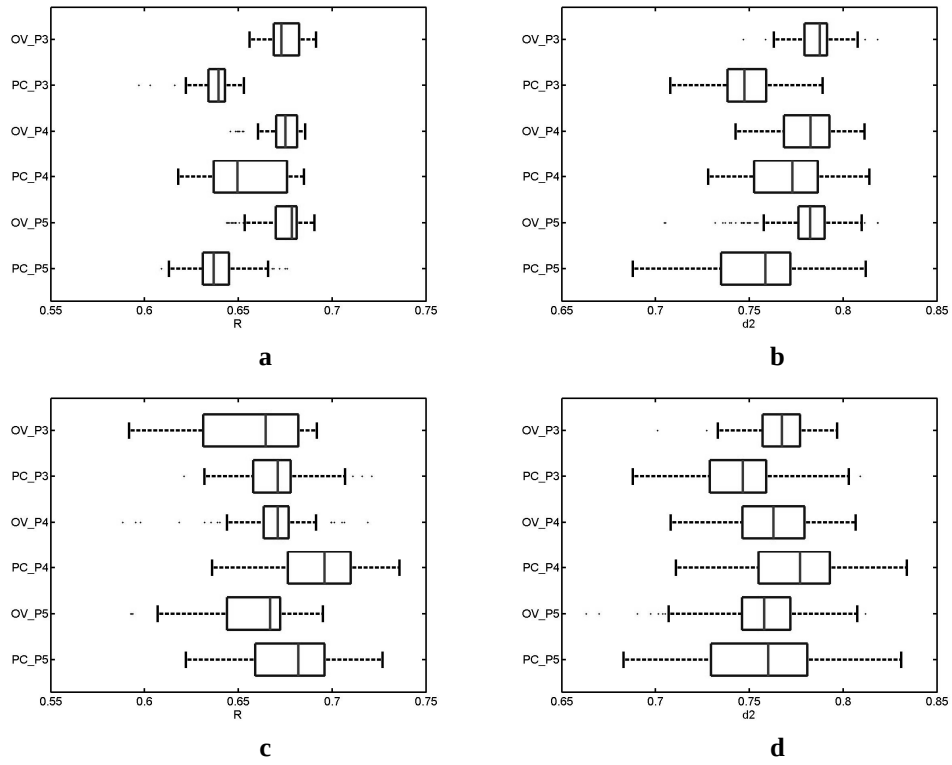

Figure 9.6 Box and whisker diagrams with the performance indexes of GP models in training (a and b) and test (c and d) periods.

performance indexes were the Pearson correlation coefficient (R) and index of agreement of the second order (d_2) (see Chapter 6). Figure 9.6 shows the box and whisker diagrams with performance indexes (in the training and test periods) of the GP models using 3, 4 and 5 populations (P3, P4 and P5) for OVs and PCs. In the training period, the GP models that used OVs as inputs presented good performances. However, their predictive performances were worse when compared with the models using PC. Additionally, the best GP models were obtained using 4 populations. Equations 9.1 and 9.2 represent the GP model with best predictive performance using PCs and OVs, respectively:

$$O_{3,t+24h} = 35.53 + 9.60 \times PC_1 + 5.70 \times PC_2 - 10.60 \times PC_5 + PC_1 \times PC_2 - \\ - 2 \times PC_1 \times PC_5 - PC_2 \times PC_5 + PC_1^{\,2} + PC_5^{\,2} \qquad (9.1)$$

$$O_{3,t+24h} = 38.95 + 9.50 \times O_{3,t} - RH_t \times \left(8.90 + e^{T_t} + T_t - RH_t\right) \quad (9.2)$$

Figure 9.7 shows the performance of these GP models in the test period. Comparing the two GP models, the one using PC showed better performance in the prediction of the next day hourly average O_3 concentrations. Taking into account the flexibility for creation the models and the results obtained from them, GP showed to be a very useful methodology to provide early warnings to the population about high O_3 concentrations episodes.

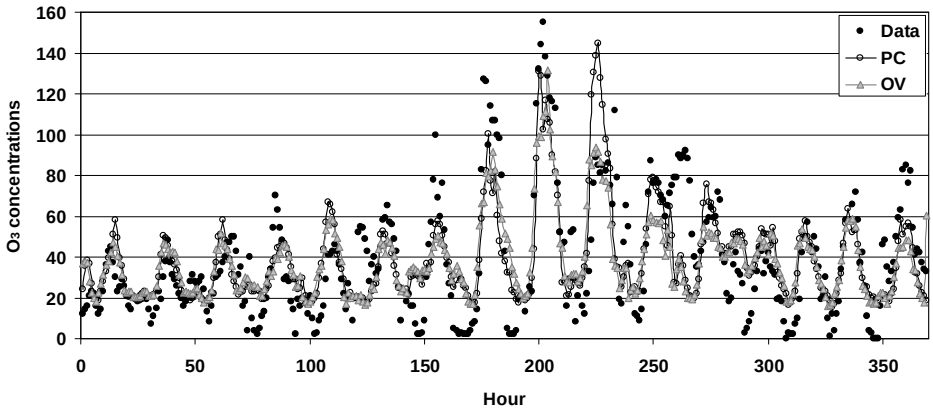

Figure 9.7 Performance of the best GP model in all test period.

9.5. Conclusions

Aiming the prediction of the next day hourly average of O_3 concentrations, GP was applied using as inputs the OVs and their PCs. This methodology was able to select the relevant variables. Applying GP with original variables, T, RH and O_3 were considered significant inputs for prediction. On the other hand, when applied to PCs, the selected ones had important contributions of the same variables and also of NO_2. GP models using the OVs presented better performance in training period but worse performance in test period, when compared with the models obtained using the PCs. Additionally, the best predictive models were obtained using 4 populations at the same time. The good performance of the models

associated to the facility to achieve them showed that GP can be very useful to solve several environmental complex problems.

Chapter 10

Multi-gene Genetic Programming

This chapter aims to apply a multi-gene genetic programming methodology for predicting the daily average of PM_{10} concentrations on the next day. This methodology is based on the principles of the simple genetic programming algorithm. The models are also encoded in tree structures that are modified following an iterative process; the model structure and parameters are optimized at same time. The main differences between the simple and the multi-gene genetic programming methodologies are: (i) an individual is composed by several tree structures, called genes, and not a single one; and (ii) the output value is calculated through the linear combination of the outputs of the different genes belonging to the same individual.

The contents of this chapter were adapted from: Pires, J.C.M., Alvim-Ferraz, M.C.M., Pereira, M.C., Martins, F.G., 2009. A Multi-Gene Genetic Programming Methodology to Generate Models for Predicting the Daily Average of PM_{10} Concentrations, *submitted for publication.*

10.1. Introduction

The choice of a model for any case study occurs in different steps in which the first one is the selection between the two main classes: mechanistic and phenomenological models. The mechanistic models are more concerned with the underlying processes (physical, chemical and biological processes), using functions based on theoretical expectations (Bolker, 2008). On the other hand, phenomenological models are concentrated on observed patterns in the data, using functions that organize the experimental observations within a formal structure. The use of phenomenological models has become increasingly recommended for applications where the mechanistic description of the interdependence between

variables is either unknown or very complex. The prediction of air pollutant concentrations is a complex problem and, specifically for PM_{10}, phenomenological models are particularly attractive, due to the complexity of the involved processes (Corani, 2005; Perez and Reyes, 2002; Fuller et al., 2002; Pires et al., 2008d).

The studies presented in Chapter 5 showed that the structure definition is an important step for the model success, being followed by the optimization of its parameters. In all studies aiming the prediction of PM_{10} concentrations, the structures of the models were defined in advance and after the parameters were determined minimizing an objective function. As PM_{10} concentrations are highly influenced by stochastic processes (such as meteorological effects, dry deposition and chemical reaction), the determination of the model should be done optimizing the model structure and parameters simultaneously. Thus, this study aims to predict the daily average of PM_{10} concentrations optimizing the model structure and parameters simultaneously, using multi-gene genetic programming (MGP). As far it is known, no study was presented applying MGP for the prediction of PM_{10} concentrations.

MGP follows the same principles of genetic programming described in Chapter 9. It is a method that predicts the output variable through the weighted linear combination of the outputs from several symbolic tree structures that correspond to the different genes. The weights are determined by minimizing the sum of squared errors of the predicted values.

10.2. Data

The variables selected as PM_{10} predictors were the concentrations of several air pollutants (SO_2, CO, NO, NO_2 and PM_{10}) and meteorological variables (air temperature - T; relative humidity – RH; and wind speed - WS). The concentrations of pollutants were recorded in an urban site (*Matosinhos*) with traffic influences. Daily average values for these variables were calculated and used if more than 75% of hourly averages were available.

The period of measurement (from January 2003 to December 2005) was divided in training and test periods. The training data were used to determine the MGP models and the test data were used to evaluate the performance of application to a new set. The test data corresponded to the last quarter of 2005 (76 data points), considering training data the remaining period (914 data points). The explanatory variables were Z standardized to have zero mean and unit standard deviation.

10.3. Results and discussion

The MGP algorithm was coded in Matlab 7.0 (MathWorks Inc., Natick, MA, USA) by the author of this thesis. Several parameters must be defined for the MGP approach. In this study, the population size was fixed to 200. The maximum number of generations was 100. The crossover and mutation rates define the probability that an individual is selected for the crossover or mutation operation, respectively; their values were 0.8 and 0.1. The 10% of the best individuals (20 individuals) were selected for the next generation (elitism). The fittest individuals were the ones presenting the lowest root mean squared error (RMSE) in the training period. To avoid early convergence, a new dataset for the evaluation of individuals was created, by random sampling the original data, with replacement when the 20 best individuals of the actual generation were the same of the previous one. However, in the last 10 generations the individuals were evaluated using the original data. Since the MGP results are probabilistic, several MGP runs of the algorithm must be performed and their results analysed before taking conclusions. Ten MGP runs were done with the individuals composed by five genes. The predicted PM_{10} concentrations were calculated through the linear combination of the outputs from the five correspondent tree expressions.

Besides the ability of construction of a functional relationship between the output and the input variables, MGP also detects the relevant inputs. Figure 10.1 shows

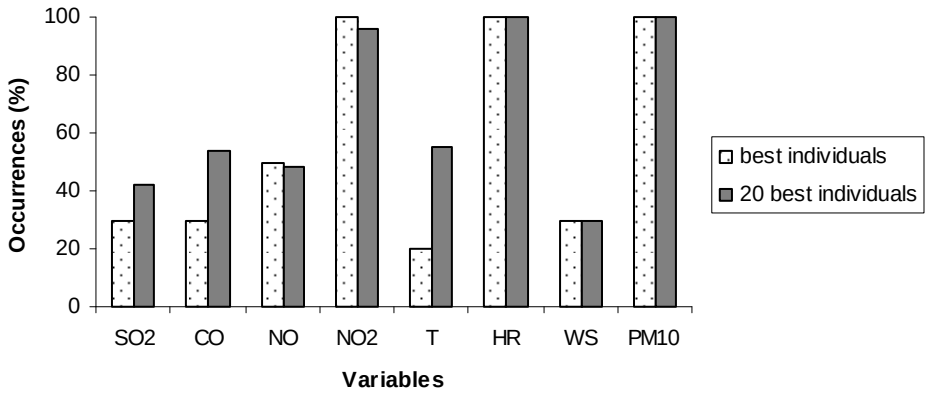

Figure 10.1 Occurrence of each input for the 10 MGP runs in the best solutions (10 individuals) and in the 20 best solutions of the last generation (200 individuals).

the occurrences of each input in the best solution in each of the 10 runs (10 individuals) and in the 20 best individuals in the last generation (20×10=200 individuals). According to the results, NO_2, HR and PM_{10} were the inputs that were selected in almost all solutions presented in the 10 MGP runs. The monitoring site is highly influenced by traffic emissions, which is, in this environment, the main source of PM_{10} and nitrogen oxides (Pereira et al., 2005); thus, the concentrations of these two air pollutants should be correlated and this justifies the importance of NO_2 concentrations in the prediction of PM_{10} concentrations. Also important is the PM_{10} concentration of the previous day since it represents the accumulation of PM_{10} from one day to another. The relative humidity is determinant for PM_{10} prediction, since wet and dry deposition has an important role on the removal of PM_{10} from the air. The results showed that SO_2, T and WS presented less relevance in the prediction of PM_{10} concentrations.

Table 10.1 presents the best solutions obtained in the 10 MGP runs and the correspondent value of RMSE in the training data; to test these models, the inputs were Z standardized. The performances of the ten models in the training period were very similar, being evaluated through the application to a new data (test

Table 10.1 Best solutions of the 10 MGP runs and correspondent RMSE in the training period

Model	Solution	RMSE
M1	$y = 37.05 + 2.87\times[\tan(PM_{10}) - RH + 1.54] + 1.54\times[\log(\lvert NO_2\rvert)] + 7.89\times[0.40 + PM_{10}] + 0.42\times[CO - 3.20^{\text{sign}(PM_{10})+RH}] + 4.15\times\left[\sin\left(\frac{NO_2}{\lvert 10.41 - CO\rvert^{1.65}}\right) + PM_{10}\right]$	15.91
M2	$y = 43.21 - 2.57\times[\text{sign}(\cos(0.70 - NO_2 - \cosh(\text{sign}(SO_2)))) - NO_2] - 2.46\times[RH] + 3.33\times[\sin(PM_{10})] + 10.92\times[PM_{10}] + 0.78\times[1 - PM_{10} - \tanh(RH + NO_2)]$	15.89
M3	$y = 42.53 + 11.84\times[PM_{10}] - 0.38\times[\cos(WS) + NO] + 4.29\times[NO_2] - 0.53\times\left[-\frac{0.18}{SO_2}\right] - 2.70\times[RH]$	15.89
M4	$y = 40.61 + 2.61\times[NO_2^{\cos(PM_{10})}] - 0.16\times[\log(\lvert\tanh(RH)\rvert)\times CO] - 2.72\times[RH] + 3.94\times[NO_2 + \sin(PM_{10})] + 9.40\times[PM_{10}]$	15.88
M5	$y = 42.27 + 11.68\times[PM_{10}] + 0.67\times[\text{sign}(NO_2)] + 3.45\times[NO_2] - 0.26\times\left[\frac{\sin(\log(\lvert\sin(\cos(RH\times PM_{10}))\rvert))}{SO_2}\right] - 2.80\times[RH]$	15.88
M6	$y = 32.46 + 10.68\times[1 + PM_{10}] - 4.11\times\left[\sqrt{\exp(\sin(\cos(RH)))}\times 1.29 - 2.15\right] - 1.57\times\left[\exp\left(\text{sign}\left(\log\left(\left\lvert\tanh\left(\cosh\left(\sqrt{\lvert NO\rvert}\right)\right)\right\rvert\right)\times PM_{10}\right)\right)\right] - 2.13\times[RH] + 3.66\times[NO_2]$	15.93
M7	$y = 41.02 - 2.83\times[RH] - 0.08\times[NO] + 7.59\times[\tanh(PM_{10}) + PM_{10}] + 1.30\times\left[-1.18 - NO + \exp\left(\frac{\exp(\sin(NO))}{1.40}\right)\right] + 3.47\times[NO_2]$	15.88

Table 10.1 Best solutions of the 10 MGP runs and correspondent RMSE in the training period (continued)

Model	Solution	RMSE
M8	$y = 41.48 + 11.12 \times [PM_{10}] - 2.66 \times \left\lfloor \sin\left(\tanh\left(\left\lvert RH \right\rvert^{8.7 \times PM_{10}} + WS\right)\right) + RH \right\rfloor + 4.22 \times \left[\tanh\left(\sin\left(\sqrt{\lvert NO_2 \rvert}^{\sqrt{\lvert 0.76 - \tanh(NO) \rvert}} \right) \right) + NO_2 \right] + 1.29 \times [T] - 0.37 \times [RH + \cosh(PM_{10})]$	15.86
M9	$y = 41.65 + 1.20 \times [\cos(\log(\lvert \sin(NO) \rvert))] + 1.43 \times [NO_2 + WS \times \log(\lvert NO_2 \rvert)] - 3.31 \times [RH] + 3.81 \times [\sin(NO_2)] + 11.99 \times [PM_{10}]$	15.91
M10	$y = 44.37 + 5.10 \times [\tanh(NO_2)] + 2.13 \times [CO - 0.98] + 10.86 \times [PM_{10}] - 2.68 \times [RH] + 1.96 \times [T]$	15.91

Table 10.2 Performance indexes of the best solutions of the 10 MGP runs in the test period

Model	MBE	MAE	RMSE	R	d_2
M1	-0.32	13.31	19.07	0.72	0.82
M2	-0.53	12.89	18.83	0.73	0.82
M3	-0.34	12.81	18.58	0.74	0.83
M4	-0.42	12.76	18.94	0.73	0.82
M5	-0.35	12.71	18.70	0.73	0.83
M6	-0.46	12.77	18.53	0.74	0.83
M7	-0.48	12.99	18.82	0.73	0.82
M8	-1.61	13.24	19.39	0.71	0.79
M9	-0.50	12.91	18.90	0.73	0.82
M10	-1.20	12.66	18.66	0.74	0.82

data). The selected performance indexes were the mean bias error (MBE), mean absolute error (MAE), RMSE, Person correlation coefficient (R) and index of agreement of second order (d_2) (see Chapter 6). Table 10.2 shows the performance indexes of the MGP models in the test period; MBE was negative in all models, meaning that, in average, the PM_{10} concentrations were underestimated; moreover, the performances achieved by the models in the test period were also very similar. One of the several advantages of MGP is the achievement of a list of optimal solutions (not just a single one). Consequently, the other solutions were also applied to the test period. Besides presenting a worst performance in the training

period (RMSE=15.95) when compared to the best solution in the correspondent run (RMSE=15.89), the solution represented by the Equation 10.1 was the model with best predictions of PM_{10} concentrations (RMSE=17.92).

$$y = 42.01 + 0.06 \times \left[\frac{T - NO}{3.10^{RH} - \tanh(PM_{10})} \right] + 3.80 \times [NO_2] - 2.78 \times [RH] + 12.10 \times [PM_{10}] - 0.30 \times \left[\frac{\sin(CO + 10.60)}{\sin\left(\tanh\left(\sqrt{\left| \frac{2.90 \times \tanh(RH)}{\cos(\log(|SO2|)) \times PM_{10}} \right|} - NO_2 \right) \right)} \right] \quad (10.1)$$

Figure 10.2 shows the performance of the best MGP model (represented by the Equation 10.1) in the whole test period. Although the model underestimated the highest PM_{10} concentrations, the model had in general good estimations. The difficulty of predicting the extreme values could be solved applying the quantile regression to this methodology. QR model has the advantage of allowing the

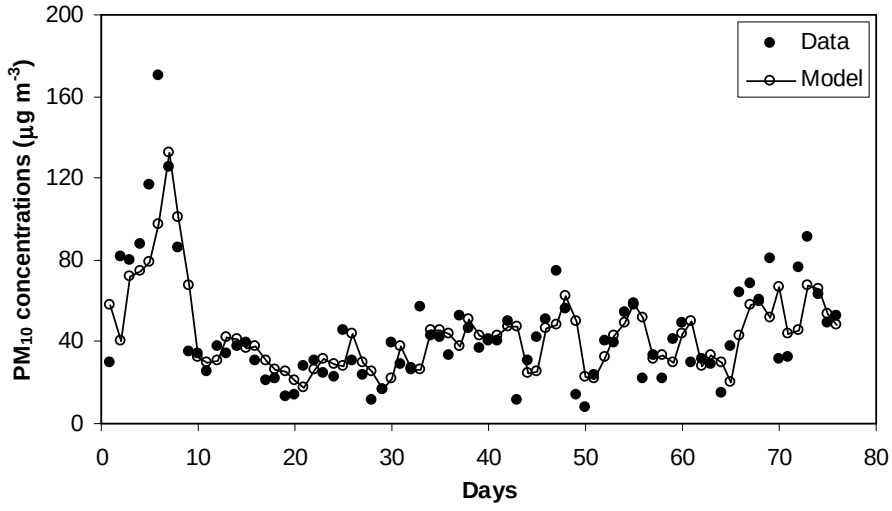

Figure 10.2 Performance of the MGP model in the test period.

examination of the entire distribution of the variable of interest rather than measuring the central tendency of its distribution. For example, Sousa et al. (2009) compared the performance of MLR and QR in the prediction of tropospheric ozone concentrations and concluded that QR presented better performance than MLR especially in the extreme values.

Considering the flexibility for creating the predictive models, MGP is a promising methodology to estimate environmental complex air pollution problems.

10.4. Conclusions

Aiming the prediction of the daily average of PM_{10} concentrations on the next day, MGP was applied. The results showed two important features of MGP: the selection of the relevant inputs and the construction of the predictive model. The variables considered important for PM_{10} concentrations prediction were NO_2 concentrations, RH and PM_{10} concentrations measured in the previous day. MGP provided several models that presented similar performances indexes. The good performances of the models showed that MGP is a useful tool to public health protection as it can provide early warnings to the population about high PM_{10} concentrations episodes.

Chapter 11

Final Words

In this thesis, two important issues in the field of air quality management were approached. First, statistical methods were applied to characterize the air pollution behaviours in Oporto-MA, which was followed by the determination of redundant measurements in the air quality monitoring network. Second, the statistical models were developed and applied to predict the O_3 and PM_{10} concentrations. This chapter also proposes future work concerning these two issues.

11.1. General conclusions

The characterization of the air pollution behaviours in Oporto-MA was an important step to determine redundant measurements in the local air quality monitoring network. If two different monitoring sites present similar air pollution behaviour, only one should operate, since the measured values at this monitoring site are representative for the two regions. With the actual distribution of monitoring sites, several redundant measurements were identified. The applied statistical methods were able to determine the patterns on air quality data and to evaluate the minimum number of monitoring sites that should operate for each air pollutant. For principal component analysis, two different criteria were applied to select the number of principal components. Using Kaiser criterion (which is often applied), the principal components selected did not represent sufficient variance of the original data. Other criterion, which selects the number of principal components representing at least 90% of the original data variance, presented better results, when the concentrations of air pollutants at the removed monitoring sites were predicted. This means that this method or one that selects principal

components with more information about the original variables should be applied for these studies. Accordingly, the number of monitoring sites could be reduced more than 50% in some of the analysed air pollutants.

The air pollution behaviours are greatly influenced by the relative location of emission point sources. This was observed for SO_2, for which the principal component analysis determined the existence of at least six monitoring sites (the highest number selected with Kaiser criterion). The location of emission sources was determined analysing the variation of air pollutant concentrations with the wind direction. For SO_2, an emission source was identified inside the area defined by the air quality monitoring network. Thus, for each wind direction, different places will be affected by the emissions from that source and, for that reason, they presented different air pollution behaviour.

The statistical methods should be applied using data corresponding to smaller periods. Longer periods hide seasonal differences in air pollution behaviours between monitoring sites. In this case, a wrong decision (remove or displace a monitoring site) can be taken. For example, applying principal component analysis (using the Kaiser criterion) to the PM_{10} data of three years, the *Vila do Conde* site was grouped with other sites, when this site presented higher concentrations and different daily profiles of PM_{10} concentrations. This happens in several periods from 17 h to 22 h. In the remaining periods, *Vila do Conde* site had similar PM_{10} behaviour. The emission source responsible of this difference was identified at N-NW direction sector. However, this source took less relevance in the last year of study. Despite this different behaviour, the site was grouped with other sites by the principal component analysis using Kaiser criterion. Using other criterion for selection of the number of principal components and analysing smaller periods (annual quarters), *Vila do Conde* site belonged to a different group.

In the second part of the thesis, statistical models were developed to predict O_3 and PM_{10} concentrations. The linear models had an advantage of taking less computational time than the other models. Taking into account the performance of

these models, quantile regression was the best model in the training period, as it tries to model the entire distribution of the dependent variable. However, this method presented bad predictive performance. Partial least squares regression was the linear model with best predictive performance for both air pollutant concentrations.

Until now, no study was presented aiming the prediction of air pollutant concentrations through statistical models using independent components. Independent component regression and stepwise artificial neural networks (using independent components as inputs) were applied. However, both models presented bad performances.

The recommended statistical approaches to solve stochastic problems, such as prediction of air pollutant concentrations, were the ones using the evolutionary procedure. They presented the best predictive performances for both air pollutants: (i) threshold regression using genetic algorithms and genetic programming for O_3; and (ii) multi-gene genetic programming for PM_{10}. They have the advantage of not defining the model structure in advance. The model structure and parameters were optimized simultaneously. The threshold regression, which was applied to predict O_3 concentrations, assumed different relationships between the O_3 concentrations and their precursors. This is important for this air pollutant, as it is formed by chemical reactions that are influenced by different regimes. In this study, only two regression equations were applied (assuming two regimes). This method is also similar to quantile regression with the advantage that it is not needed to predict the percentile of the output variable.

The accuracy of the predictions from statistical models is a function of the quality of the data in the various databases. The lack of adequate data on air pollutant concentrations is a major limitation of the statistical methods. When the data needed to drive the models are available, the models provide policy makers with useful information on the exposure of the population to air pollutants.

11.2. Future work

Concerning the management of the equipment of the air quality monitoring networks, the method to evaluate redundant measurements was tested and presented adequate results. After the selection of redundant monitoring sites, the correspondent equipment can be displaced to other regions increasing the monitored area. The location of new monitoring sites can be determined using a mobile air quality monitoring equipment. Using this equipment, the air pollutant concentrations should be measured in a determined place during sufficient large period. Principal component analysis should be applied to data of the fixed and mobile monitoring sites. If the place presents different air pollution behaviour from other regions, it should have a monitoring site.

Concerning the prediction of air pollutant concentrations, the data size should be reduced. It was observed that the models have difficulties to predict extreme values, tending for the average value of the training data. The data corresponding a large period contain different relationships between variables, which is difficult to model in only one equation. The reduction of the data size also decreases the computation time to achieve the statistical models. Additionally, it is important to explore the potentialities of the threshold regression. This model could be applied assuming more than two equations and also non-linear relationships between input and output variables in each regime. In this case, the codification of chromosomes in GA should be modified.

To improve the results of these models in the air quality modelling, the objective function could also be changed. In air quality modelling, it is not important to know the exact concentrations of the air pollutant, but to predict the range of values that will limit these concentrations. An example of an objective function that can be applied in this field is the minimization of the sum of absolute errors, when the absolute error is greater than a defined value.

References

Abdi, H., **2003**. *Partial Least Squares (PLS) Regression*. In: Encyclopedia of Social Sciences Research Methods (eds. M. Lewis-Beck, A. Bryman and T. Futing), 1-7. Thousand Oaks: Sage.

Abdul-Wahab, S.A., Bakheit, C.S., Al-Alawi, S.M., **2005**. Principal component and multiple regression analysis in modelling of ground-level ozone and factors affecting its concentrations. *Environmental Modelling & Software* 20 (10), 1263-1271.

Agirre-Basurko, E., Ibarra-Berastegi, G., Madariaga, I., **2006**. Regression and multilayer perceptron-based models to forecast hourly O_3 and NO_2 levels in the Bilbao area. *Environmental Modelling & Software* 21, 430-446.

Al-Alawi, S.M., Abdul-Wahab, S.A., Bakheit, C.S., **2008**. Combining principal component regression and artificial neural networks for more accurate predictions of ground-level ozone. *Environmental Modelling & Software* 23(4), 396-403.

Al-Rubaie, K.S., Godefroid, L.B., Lopes, J.A.M., **2007**. Statistical modeling of fatigue crack growth rate in Inconel alloy 600. *International Journal of Fatigue* 29 (5), 931-940.

Alvim-Ferraz, M.C., Pereira, M.C., Ferraz, J.M., Almeida e Mello, A.M.C., Martins, F.G., **2005**. European Directives for Air Quality: Analysis of the New Limits in Comparison with Asthmatic Symptoms in Children Living in the Oporto Metropolitan Area, Portugal. *Human and Ecological Risk Assessment* 11 (3), 607-616.

Alvim-Ferraz, M.C.M., Sousa, S.I.V., Pereira, M.C., Martins, F.G., **2006**. Contribution of anthropogenic pollutants to the increase of tropospheric ozone levels in Oporto Metropolitan Area, Portugal since the 19th century. *Environmental Pollution* 140, 516-524.

ApSimon, H.M., Warren, R.F., **1996**. Transboundary air pollution in Europe. *Energy Policy* 24 (7), 631-640.

Arsie, I., Pianese, C., Sorrentino, M., **2006**. A procedure to enhance identification of recurrent neural networks for simulating air–fuel ratio dynamics in SI engines. *Engineering Applications of Artificial Intelligence* 19 (1), 65-77.

Barros, N., Toll, I., Soriano, C., Jiménez, P., Borrego, C., Baldasano, J.M., **2003**. Urban photochemical pollution in the Iberian Peninsula: the Lisbon and Barcelona airsheds. *Journal of the Air and Waste Management Association* 53, 347–359.

Baur, D., Saisana, M., Schulze, N., **2004**. Modelling the effects of meteorological variables on ozone concentration – a quantile regression approach. *Atmospheric Environment* 38, 4689-4699.

Bolker, B., **2008**. Ecological Models and Data in R. Princeton University Press, Princeton.

Brunekreef, B., Holgate, S.T., **2002**. Air pollution and health. *The Lancet* 360 (9341), 1233-1242.

Bytnerowicz, A., Omasa, K., Paoletti, E., **2006**. Integrated effects of air pollution and climate change on forests: A northern hemisphere perspective. *Environmental Pollution* 147 (3), 438-445.

Çamdevýren, H., Demýr, N., Kanik, A., Keskýn, S., **2005**. Use of principal component scores in multiple linear regression models for prediction of *Chlorophyll*-a in reservoirs. *Ecological Modelling* 181 (4), 581-589.

Carlson, R.W., **1979**. Reduction in the photosynthetic rate of *Acer, quercus* and *Fraxinus* species caused by sulphur dioxide and ozone. *Environmental Pollution* (1970) 18 (2), 159-170.

Carmichael, G.R., Streets, D.G., Calori, G., Amann, M., Jacobson, M.Z., Hansen, J., Ueda, H., **2002**. Changing trends in sulfur emissions in Asia: Implications for acid deposition, air pollution and climate. *Environmental Science & Technology* 36 (22), 4707-4713.

Chaloulakou, A., Saisana, M., Spyrellis, N., **2003**. Comparative assessment of neural networks and regression models for forecasting summertime ozone in Athens. *Science of the Total Environment* 313, 1-13.

Chan, L.Y., Liu, H.Y., Lam, S., Wang, T., Oltmans, S.J., Harris, J.M., **1998**. Analysis of the seasonal behavior of tropospheric ozone at Hong Kong. *Atmospheric Environment* 32 (2), 159-168.

Chen, J.S., Chang, C.L., Hou, J.L., Lin, Y.T., **2008**. Dynamic proportion portfolio insurance using genetic programming with principal component analysis. *Expert Systems with Applications* 35(1-2), 273-278.

Chiang, Y.M., Chang, L.C., Chang, F.J., **2004**. Comparison of static-feedforward and dynamic-feedback neural networks for rainfall–runoff modelling. *Journal of Hydrology* 290 (3-4), 297-311.

Coman, A., Ionescu, A., Candau, Y., **2008**. Hourly ozone prediction for a 24-h horizon using neural networks. *Environmental Modelling & Software* 23(12), 1407-1421.

Corani, G., **2005**. Air quality prediction in Milan: feed-forward neural networks, pruned neural networks and lazy learning. *Ecological Modelling* 185, 513-529.

Corne, S.A., **1998**. Artificial neural networks for pattern recognition. *Concepts in Magnetic Resonance* 8 (5), 303-324.

Dockery, D.W., Pope, C.A., **1994**. Acute Respiratory Effects of Particulate Air Pollution. *Annual Review of Public Health* 15, 107-132.

Dueñas, C., Fernández, M. C., Cañete, S., Carretero, J., Liger, E., **2002**. Assessment of ozone variations and meteorological effects in an urban area in the Mediterranean Coast. *Science of the Total Environment* 299 (1-3), 97-113.

Dueñas, C., Fernández, M.C., Cañete, S., Carretero, J., Liger, E., **2005**. Stochastic model to forecast ground-level ozone concentration at urban and rural areas. *Chemosphere* 601, 1379-1389.

Eberly, L.E., **2007**. *Multiple linear regression*. In: Methods in Molecular Biology (ed W.T. Ambrosius), Volume 404, Humana Press, Totowa, 165-187.

EC Directive, **1999**. Council Directive 99/30/EC, relating the limit values for sulphur dioxide, nitrogen dioxide and oxides of nitrogen, particulate matter and lead in ambient air. *Official Journal of the European Communities* L163, 41-60

EC Directive, **2000**. Council Directive 2000/69/EC, relating to limit values for benzene and carbon monoxide in ambient air. *Official Journal of the European Communities* L313, 12-21.

EC Directive, **2002**. Council Directive 2002/3/EC, relating to ozone in ambient air. *Official Journal of the European Communities* L67, 14-30.

EC Directive, **2008**. Council Directive 2008/50/EC, on ambient air quality and cleaner air for Europe. *Official Journal of the European Communities* L151, 1-44.

Edgar, T.F., Himmelblau, D.M., **1988**. *Optimization of Chemical Processes*. McGraw-Hill, New York, 214-215.

Fouquau, J., Hurlin, C., Rabaud, I., **2007**. The Feldstein–Horioka puzzle: A panel smooth transition regression approach. *Economic Modelling* 25 (2), 284-299.

Fuller, G.W., Carslaw, D.C., Lodge, H.W., **2002**. An empirical approach for the prediction of daily mean PM10 concentrations. *Atmospheric Environment* 36, 1431-1441.

Gardner, M.W., Dorling, S.R., **2000**. Statistical surface ozone models: an improved methodology to account for non-linear behaviour. *Atmospheric Environment* 34, 21-34.

Garg, A., Shukla, P.R., Kapshe, M., **2006**. The sectoral trends of multigas emissions inventory of India. *Atmospheric Environment* 40 (24), 4608-4620.

Ghiassi, M., Saidane, H., **2005**. A dynamic architecture for artificial neural networks. *Neurocomputing* 63, 397–413.

Goldberg, D.E, **1989**. *Genetic Algorithms in Search. Optimization and Machine Learning*, Kluwer Academic Publishers, Boston, MA.

Gramsch, E., Cereceda-Balic, F., Oyola, P., Baer, D., **2006**. Examination of pollution trends in Santiago de Chile with cluster analysis of PM_{10} and Ozone data. *Atmospheric Environment* 40 (28), 5464-5475.

Grivas, G., Chaloulakou, A., **2006**. Artificial neural network models for prediction of PM_{10} hourly concentrations, in the Greater Area of Athens, Greece. *Atmospheric Environment* 40 (7), 1216-1229.

Grivas, G., Chaloulakou, A., **2006**. Artificial neural network models for prediction of PM_{10} hourly concentrations, in the Greater Area of Athens, Greece. *Atmospheric Environment* 40 (7), 1216-1229.

Grosman, B., Lewin, D. R., **2004**. Adaptive genetic programming for steady-state process modelling. *Computers & Chemical Engineering* 28(12), 2779-2790.

Guerra, J.-C., Rodríguez, S., Arencibia, M.-T., García, M.-D., **2004**. Study on the formation and transport of ozone in relation to the air quality management and vegetation protection in Tenerife (Canary Islands). *Chemosphere* 56, 1157-1167.

Gupta, R.R., Achenie, L.E.K., **2007**. A network model for gene regulation. *Computers & Chemical Engineering* 31 (8), 950-961.

Harman, H.H., **1976**. *Modern Factor Analysis*, third edition. University of Chicago Press, 290-296.

Hashim, J.H., Pillay, M.S., Hashim, Z., Shamsudin, S.B., Sinha, K., Zulkifli, Z.H., **2004**. *A Study of Health Impact and Risk Assessment of Urban Air Pollution in the Klang Valley, Malaysia*. A research project report provided by WHO - Western Pacific Regional Office. Available in (accessed on December 2006) http://www.airimpacts.org/documents/local/UKMreport.pdf.

Haupt, R.L., Haupt, S.E., **2004**. *Practical Genetic Algorithms*, second edition, John Wiley & Sons, 27-49, New Jersey.

Hayter, A. J., Wynn, H. P., Liu, W., **2006**. Slope modified confidence bands for a simple linear regression model. *Statistical Methodology* 3 (2), 186-192.

Heo, J.S., Kim, D.S., **2004**. A new method of ozone forecasting using fuzzy expert and neural network systems. *Science of the Total Environment* 325 (1-3), 221-237.

Hernández-Caraballo, E.A., Marcó-Parra, L.M., **2003**. Direct analysis of blood serum by total reflection X-ray fluorescence spectrometry and application of an artificial neural network approach for cancer diagnosis. *Spectrochimica Acta Part B: Atomic Spectroscopy* 58 (12), 2205-2213.

Hoek, G., Brunekreef, B., Goldbohm, S., Fischer, P. and van der Brand, P.A., **2002**. Association between mortality and indicators of traffic-related air pollution in the Netherlands: a cohort study. *The Lancet* 360 (9341), 1203-1209.

Holland, J.H., **1975**. *Adaptation in Natural and Artificial Systems*, University of Michigan Press, Ann Arbor.

Hu, Q.P., Xie, M., Ng, S.H., Levitin, G., **2007**. Robust recurrent neural network modelling for software fault detection and correction prediction. *Reliability Engineering & System Safety* 92 (3), 332-340.

Hyvärinen, A., Oja, E., **2000**. Independent component analysis: algorithms and applications. *Neural Networks* 13 (4-5): 411-430.

Jorba, O., Gassó, S., Baldasano, J.M., **2003**. Regional circulations within the Iberian Peninsula east coast. *26th International Technical Meeting of NATO-CCMS on Air Pollution Modelling and its Application*, Istanbul, Turkey, 26–30 May.

Kalabokas, P.D., Bartzis, J.G., Papagiannakopoulos, P., **2002**. Atmospheric levels of nitrogen oxides at a Greek oil refinery compared with the urban measurements in Athens. *Water, Air, and Soil Pollution* 2, 703-716.

Kannel, P.R., Lee, S., Kanel, S.R., Khan, S.P., **2007**. Chemometric application in classification and assessment of monitoring locations of an urban river system. *Analytica Chimica Acta* 582, 390-399.

Kappos, A.D., Bruckmann, P., Eikmann, T., Englert, N., Heinrich, U., Hoppe, P., Koch, E., Krause, G.H.M., Kreyling, W.G., Rauchfuss, K., Rombout, P., Schulz-Klemp, V., Thiel, W.R., Wichmann, H.E., **2004**. Health effects of particles in ambient air. *International Journal of Hygiene and Environmental Health* 207 (4), 399-407.

Kley, D., Kleinmann, M., Sanderman, H., Krupa, S., **1999**. Photochemical oxidants – state of the science. *Environmental Pollution* 100 (1-3), 19-42.

Koelemeijer, R.B.A., Homan, C.D., Matthijsen, J., **2006**. Comparison of spatial and temporal variations of aerosol optical thickness and particulate matter over Europe. *Atmospheric Environment* 40 (27), 5304-5315.

Koenker, R., Basset, G., **1978**. *Regression quantiles*. Econometrica 46, 33–50.

Koza, J.R., **1992**. *Genetic Programming I – On the Programming of Computers be Means of Natural Selection*, MIT Press, Cambridge MA.

Kukkonen, J., Partanen, L., Karppinen, A., Ruuskanen, J., Junninen, H., Kolehmainen, M., Niska, H., Dorling, S., Chatterton, T., Foxall, R., Cawley, G., **2003**. Extensive evaluation of neural network models for the prediction of NO_2 and PM_{10} concentrations, compared with a deterministic modelling system and measurements in central Helsinki. *Atmospheric Environment* 37 (32), 4539-4550.

Lee, E.H., Pausch, R.C., Rowland, R.A., Mulchi, C.L., Rudorff, B.F.T., **1997**. Responses of field-grown soybean (cv. Essex) to elevated SO_2 under two atmospheric CO_2 concentrations. *Environmental and Experimental Botany* 37 (2-3), 85-93.

Leeuw, F.A.A.M., **2000**. Trends in ground level ozone concentrations in the European Union. *Environmental Science & Policy* 3 (4), 189-199.

Liu, C.W., Lin, K.H., Kuo, Y.M., **2003**. Application of factor analysis in the assessment of groundwater quality in a blackfoot disease area in Taiwan. *Science of the Total Environment* 313 (1-3), 77-89.

Manly, B.F.J., **1994**. *Multivariate Statistical Methods – A Primer*, second edition. Chapman and Hall, London, 129-133.

McKenna, J.E., **2003**. An enhanced cluster analysis program with bootstrap significance testing for ecological community analysis. *Environmental Modelling & Software* 18 (3), 205-220.

Medeiros, M.C., Teräsvirta, T., Rech, G., **2006**. Building neural network models for time series: a statistical approach. *Journal of Forecasting* 25 (1), 49-75

Mendiguchía, C., Moreno, C., Galindo-Riaño, M.D., García-Vargas, M., **2004**. Using chemometric tools to assess anthropogenic effects in river water: A case study: Guadalquivir River (Spain). *Analytica Chimica Acta* 515 (1), 143-149.

Mi, X., Zou, Y., Wei, W., Ma, K., **2005**. Testing the generalization of artificial neural networks with cross-validation and independent-validation in modelling rice tillering dynamics. *Ecological Modelling* 181 (4), 493-508.

Millán, M., Salvador, R., Mantilla, E., **1996**. Meteorology and Photochemical Air Pollution in Southern Europe: Experimental Results from EC Research Projects; *Atmospheric Environment* 30, 1909-1924.

Montague, P.R., Quartz, S.R., **1999**. Computational approaches to neural reward and development. *Mental Retardation and Developmental Disabilities Research Reviews* 5 (1), 86-99.

Nagy, Z.K., **2007**. Model based control of a yeast fermentation bioreactor using optimally designed artificial neural networks. *Chemical Engineering Journal* 127 (1-3), 95-109.

Nguyen, M.H., Abbass, H.A., McKay, R.I., **2005**. Stopping criteria for ensemble of evolutionary artificial neural networks. *Applied Soft Computing* 6 (1), 100-107.

Nunnari, G., Dorling, S., Schlink, U., Cawley, G., Foxall, R., Chatterton, T., **2004**. Modelling SO_2 concentration at a point with statistical approaches. *Environmental Modelling & Software* 19 (10), 887-905.

Omidvari, M., Hassanzadeh, S., Hosseinibalam, F., **2008**. Time series analysis of ozone data in Isfahan. *Physica A: Statistical Mechanics and its Applications* 387 (16-17), 4393-4403.

Oussaidène, M., Chopard, B., Pictet, O.V., Tomassini, M., **1997**. Parallel genetic programming and its application to trading model induction. *Parallel Computing* 23 (8), 1183-1198.

Özesmi, S.L., Tan, C.O., Özesmi, U., **2006**. Methodological issues in building, training, and testing artificial neural networks in ecological applications. *Ecological Modelling* 195 (1-2), 83-93.

Pacella, M., Semeraro, Q., **2007**. Using recurrent neural networks to detect changes in autocorrelated processes for quality monitoring. *Computers & Industrial Engineering* 52 (4), 502-520.

Parkins, A.D., Nandi, A.K., **2004**. Genetic programming techniques for hand written digit recognition. *Signal Processing* 84 (12), 2345-2365.

Pereira, M.C., Santos, R.C., Alvim-Ferraz, M.C.M., **2007**. Air quality improvements using European environment policies: a case study of SO_2 in a Coastal region in Portugal. *Journal of Toxicology and Environmental Health, Part A* 70, 1-5.

Pereira, M.C., Alvim-Ferraz, M.C.M., Santos, R.C., **2005**. Relevant aspects of air quality in Oporto (Portugal): PM_{10} and O_3. *Environmental Monitoring and Assessment* 101, 203-221.

Perez, P., Reyes, J., **2002**. Prediction of maximum of 24-h average of PM_{10} concentrations 30 h in advance in Santiago, Chile. *Atmospheric Environment* 36 (28), 4555-4561.

Perez, P., Reyes, J., **2006**. An integrated neural network model for PM_{10} forecasting. *Atmospheric Environment* 40 (16), 2845-2851.

Pires, J.C.M., Martins, F.G., Sousa, S.I.V., Alvim-Ferraz, M.C.M., Pereira, M.C., **2008c**. Selection and Validation of Parameters in Multiple Linear and Principal Component Regressions. *Environmental Modelling & Software* 23 (1), 50-55.

Pires, J.C.M., Martins, F.G., Sousa, S.I.V., Alvim-Ferraz, M.C.M., Pereira, M.C., **2008d**. Prediction of the daily mean PM_{10} concentrations using linear models. *American Journal of Environmental Sciences* 4 (5), 445-453.

Pires, J.C.M., Sousa, S.I.V., Pereira, M.C., Alvim-Ferraz, M.C.M., Martins, F.G., **2008a**. Management of Air Quality Monitoring using Principal Component and Cluster Analysis – Part I: SO_2 and PM_{10}. *Atmospheric Environment* 42 (6), 1249-1260.

Pires, J.C.M., Sousa, S.I.V., Pereira, M.C., Alvim-Ferraz, M.C.M., Martins, F.G., **2008b**. Management of Air Quality Monitoring using Principal Component and Cluster Analysis – Part II: CO, NO_2 and O_3. *Atmospheric Environment* 42 (6), 1261-1274.

Prybutok, V.R., Yi, J., Mitchell, D., **2000**. Comparison of neural network models with ARIMA and regression models for prediction of Houston's daily maximum ozone concentrations. *European Journal of Operational Research* 122 (1), 31-40.

Qingbin, L., Zhong, J., Mabao, L., Shichun, W., **1996**. Acquiring the constitutive relationship for a thermal viscoplastic material using an artificial neural network. *Journal of Materials Processing Technology* 62 (1-3), 206-210.

QualAr, 2006. Environmental Institute database for air quality website (accessed on October 2006): www.qualar.org

Raub, J.A., **1999**. Health effects of exposure to ambient carbon monoxide. *Chemosphere - Global Change Science I* (1-3), 331-351.

Raub, J.A., Mathieu-Nolf, M., Hampson, N.B., Thom, S.R., **2000**. Carbon monoxide poisoning - a public health perspective. *Toxicology* 145 (1), 1-14.

Reddy, M.S., Venkataraman, C., **2002**. Inventory of aerosol and sulphur dioxide emissions from India: I - Fossil fuel combustion. *Atmospheric Environment* 36(4), 677-697.

Rivals, I., Personnaz, L., **2003**. Neural-network construction and selection in nonlinear modeling. *IEEE Transaction on Neural Networks* 14 (4), 804–819.

Schlink, U., Dorling, S., Pelikan, E., Nunnari, G., Cawley, G., Junninen, H., Greig, A., Foxall, R., Eben, K., Chatterton, T., Vondracek, J., Richter, M., Dostal, M., Bertucco, L., Kolehmainen, M., Doyle, M., **2003**. A rigorous inter-comparison of ground-level ozone predictions. *Atmospheric Environment* 37, 3237-3253.

Seinfeld, J.H., Pandis, S.N., **1998**. *Atmospheric Chemistry and Physics – from Air Pollution to Climate Changes*. A Wiley-Interscience Publication, USA.

Shrestha, S., Kazama, F., **2007**. Assessment of surface water quality using multivariate statistical techniques: A case study of the Fuji river basin, Japan. *Environmental Modelling & Software* 22 (4), 464-475.

Singh, K.P., Malik, A., Mohan, D., Sinha, S., **2004**. Multivariate statistical techniques for the evaluation of spatial and temporal variations in water quality of Gomti River (India) - a case study. *Water Research* 38 (18), 3980-3992

Singh, K.P., Malik, A., Sinha, S., **2005**. Water quality assessment and apportionment of pollution sources of Gomti river (India) using multivariate statistical techniques - a case study. *Analytica Chimica Acta* 538 (1-2), 355-374.

Siriwardene, N.R., Perera, B.J.C., **2006**. Selection of genetic algorithm operators for urban drainage model parameter optimisation. *Mathematical and Computer Modelling* 44 (5-6), 415-429.

Slini, T., Kaprara, A., Karatzas, K., Moussiopoulos, N., **2006**. PM_{10} forecasting for Thessaloniki, Greece. *Environmental Modelling & Software* 21 (4), 559-565.

Sousa, S.I.V., Martins, F.G., Alvim-Ferraz, M.C.M., Pereira, M.C., **2007**. Multiple linear regression and artificial neural networks based on principal components to predict ozone concentrations. *Environmental Modelling & Software* 22, 97-103.

Sousa, S.I.V., Martins, F.G., Pereira, M.C., Alvim-Ferraz, M.C.M., **2006**. Prediction of ozone concentrations in Oporto city with statistical approaches. *Chemosphere* 64, 1141-1149.

Sousa, S.I.V., Pires, J.C.M., Martins, F.G., Pereira, M.C., Alvim-Ferraz, M.C.M., **2009**. Potentialities of quantile regression to predict ozone concentrations. *Environmetrics* 20, 147-158.

Strand, A., Hov, O., **1996**. The impact of man-made and natural NO_x emissions on upper tropospheric ozone: a two-dimensional modal study. *Atmospheric Environment* 30, 1291-1303.

Sundberg, R., **2000**. Aspects of statistical regression in sensometrics. *Food Quality and Preference* 11 (1-2): 17-26.

Tang, Z., Tamura, H., Kuratu, M., Ishizuka, O., Tanno, K., **2001**. A Model of the Neuron Based on Dendrite Mechanisms. *Electronics and Communications in Japan (Part III)* 84 (8), 11-24.

Tawadrous, A. S., Katsabanis, P. D., **2006**. Prediction of surface crown pillar stability using artificial neural networks. *International Journal for Numerical and Analytical Methods in Geomechanics* 31 (7), 917-931.

Terui, N., Dijk, H.K., **2002**. Combined forecasts from linear and nonlinear time series models. *International Journal of Forecasting* 18 (3), 421-438.

Tsakonas, A., **2006**. A comparison of classification accuracy of four genetic programming-evolved intelligent structures. *Information Sciences* 176 (6), 691-724.

Uncini, A., **2003**. Audio signal processing by neural networks. *Neurocomputing* 55 (3-4), 593-625.

United States Environmental Protection Agency (USEPA), **1998**. *How nitrogen oxides affect the way we live and breathe*, Office of Air Quality Planning and Standards, Washington DC (Publication EPA-456/F-98-005).

United States Environmental Protection Agency (USEPA), **2000**. *Air quality criteria for carbon monoxide*, Office of Research and Development, Washington DC (Publication EPA 600/P-99/001F).

United States Environmental Protection Agency (USEPA), **2004**. *Final Regulatory Analysis: Control of Emissions from Nonroad Diesel Engines*, Office of Transportation and Air Quality (Publication EPA 420-R-04-007).

Wang, S., Xiao, F., **2004**. AHU sensor fault diagnosis using principal component analysis method. *Energy and Buildings* 36(2), 147-160.

Wang, W., Lu, W., Wang, X., Leung, A., 2003. Prediction of maximum daily ozone level using combined neural network and statistical characteristics. *Environment International* 29, 555-562.

Wold, S., Sjöström, M., Eriksson, L., **2001**. PLS-regression: a basic tool of chemometrics. *Chemometrics and Intelligent Laboratory Systems* 58 (2): 109-130.

World Bank Group (WBG), **1998**. *Pollution Prevention and Abatement Handbook*, Washington DC, 223-226.

World Health Organization (WHO), **2000**. *Air quality Guidelines for Europe*, second edition, WHO Regional Office, Copenhagen.

Yamada, K., Kuroyanagi, S., Iwata, A., **2005**. A supervised learning method using duality in the artificial neuron model. *Systems and Computers in Japan* 36 (9), 34-42.

Yang, H, Ni, J., **2005**. Dynamic neural network modeling for nonlinear, nonstationary machine tool thermally induced error. *International Journal of Machine Tools and Manufacture* 45 (4-5), 455-465.

Yidana, S.M., Ophori, D., Banoeng-Yakubo, B., **2008**. A multivariate statistical analysis of surface water chemistry data—The Ankobra Basin, Ghana. *Journal of Environmental Management* 86, 80-87.

Zolghadri, A., Monsion, M., Henry, D., Marchionini, C., Petrique, O., **2004**. Development of an operational model-based warning system for tropospheric ozone concentrations in Bordeaux, France. *Environmental Modelling & Software* 19(4), 369-382.